

M. Georgiou

Innovative Tidal Inlet Design

Design Methodology for Boughaz 1 inlet, Lake Bardawil



Innovative Tidal Inlet Design

Design Methodology in Boughaz 1 inlet, Lake Bardawil

By

M. Georgiou

in partial fulfilment of the requirements for the degree of

Master of Science

in Civil Engineering

at the Delft University of Technology.

Student number:	4621506	
Thesis committee:	Prof.dr.ir Aarninkhof, S.G.J.,	TU Delft
	Dr. ir. De Vries, S.,	TU Delft
	Dr. ir. Ngan-Tillard, D.J.M.,	TU Delft
	Ir. Van der Hoeven, M.L.E.B.,	The Weather Makers
	Ir. Lanter, M.J.C,	The Weather Makers
	Ir. Mol, A.C.S.,	DEME-Group

This thesis is confidential and cannot be made public.



Table of Contents

LIST OF FIGURES.....	vi
LIST OF TABLES.....	x
1 Introduction	1
1.1 Tidal inlet systems.....	2
1.2 Lake Bardawil	3
1.3 Problem description.....	4
1.4 Research objective and research questions	6
1.5 Thesis outline	7
2 Background	9
2.1 Study area	10
2.1.1 Boughaz 1- West inlet	10
2.1.2 Data review	11
2.2 Stabilization of inlet systems and sediment bypassing.....	17
2.2.1 Stability models.....	17
2.2.2 Stability studies of Boughaz 1 inlet	21
2.2.3 Previous related study	22
3 Methods	25
3.1 Design methodology	26
3.1.1 Design elements.....	27
3.1.2 Design parameters and requirements	28
3.1.3 Followed procedure	32
3.1.3.1 Inlet cross sectional area.....	34
3.1.3.2 Approach channel	35
3.1.3.3 Inlet nourishment design	36
3.2 Design modelling.....	39
3.2.1 Data collection	39
3.2.1.1 Wave data analysis.....	39
3.2.1.2 Tidal data.....	42
3.2.1.3 Sediment data	42
3.2.2 Modelling approach and model set up	44
3.2.2.1 Modelling approach	44
3.2.2.2 Delft3D Flexible Mesh	46
3.2.2.3 Delft3D	47
4 Results	53
4.1 Design elements analysis	54

4.1.1	Initial state	54
4.1.2	Inlet cross sectional area.....	58
4.1.3	Approach channel	62
4.1.4	Inlet nourishment	65
4.1.5	Conclusions and final combined design choice	69
4.2	Final combined design analysis.....	72
4.2.1	Hydrodynamics	73
4.2.2	Morphology.....	74
4.2.3	Sensitivity analysis	76
4.2.4	Stability	80
5	Discussion.....	83
5.1	Available data.....	84
5.2	Methodology.....	84
5.3	Modelling	85
6	Conclusions – Recommendations	87
6.1	Conclusions	88
6.2	Recommendations	93
7	References.....	97
	Appendix A – Background.....	102
	Appendix B - Climate.....	106
	Appendix C - Validation.....	113
	Appendix D – Overview of Results	115

LIST OF FIGURES

Figure 1-1: Morphological features of the tidal inlet system(Bosboom & Stive, 2015).	2
Figure 1-2: The position of the three inlets in Lake Bardawil. On the western side: Boughaz 1 inlet. On the east side: Boughaz 2 and Zaranik inlet respectively,("Lake Bardawil," 2015)	3
Figure 1-3: Current situation of Boughaz 1 inlet. Sediment disruption due to the vicinity of the breakwater and shoreline erosion downstream.	4
Figure 1-4:Cyclic behaviour of the tidal inlet system in the western area of Lake Bardawil.	5
Figure 2-1: Evolution of Boughaz 1 inlet during 1984-2016. 1984: Instable system, 1986-1995: Breakwaters and maintenance dredging works, 2016: Current state("Lake Bardawil," 2015).	10
Figure 2-2: Erosion and deposition patterns along the Port Said and Bardawil Subcells in Lake Bardawil. Deposition is seen at the updrift side of the breakwater and erosion in the lee side (Linnarsund & Mårtensson, 2008).....	11
Figure 2-3: Monthly salinity levels measured in ‰ (El-Bana et al., 2002; Lanfers, 2016).	12
Figure 2-4: Wave rose indicate wave conditions and predominant wave direction (PWD) at a depth of 14 m with situ measurements(Nassar, Mahmood, Masria, Fath, & Nadaoka, 2018).	13
Figure 2-5:Western water arm related to western inlet in Lake Bardawil (Embabi & Moawad, 2014; "Lake Bardawil," 2015).....	14
Figure 2-6: Types of sediment fractions within the lagoon (Piere, 2016).	15
Figure 2-7: Volume and direction of net transport rates [$m^3/year$] along the Sinai northern coast Emanuelsson and Mirchi (2007)	16
Figure 2-8: Morphological evolution of the Boughaz 1 inlet during 1991-1999. Green line:1991, blue line:1994 and red line: 1999 (Linnarsund & Mårtensson, 2008).	17
Figure 2-9: Escoffier's closure curve Lanfers (2016).....	18
Figure 2-10: Models of inlet sediment by-passing Duncan M FitzGerald, Kraus, and Hands (2000).	20
Figure 2-11: Shoreline evolution with two different maintenance works. Scenario 5a: Eight short groins with the inclusion of one-time nourishment. Scenario 5b: Implementation of yearly 100,000 m^3 of nourishment at the east side of the inlet entrance(Nassar et al., 2018).	22
Figure 2-12: Water level variations outside and inside of the Lake Bardawil. Red line: Outside, blue line: Inside.(Lanfers, 2016)	23
Figure 2-13: Water exchange between Mediterranean Sea and Lake Bardawil(Lanfers, 2016).	24
Figure 3-1: Concept of the design methodology.	26
Figure 3-2: Overview of the design parameters of each design element. At the top, the top view graph is presented. The cross sections given in the top view graph are illustrated with further detail at the bottom of the figure.	29
Figure 3-3: Flow chart of the followed design procedure of Boughaz 1 inlet. Within the light blue colour box, indication of the design sequence followed to examine the hydrodynamic response is given. The optimal design is selected. Within the darker blue colour box, the hydrodynamic and morphological response of the selected final combined design choice is examined under three different cases. Case 1: Tide only. Case 2:Tide + sediment. Case 3: Tide + sediment + waves.	33
Figure 3-4: Shape configurations of inlet cross-sectional area. (1) Trapezoidal, (2) Triangular, (3) Trapezoidal with two depths.	35
Figure 3-5: Top view of the designs of approach channel within the model Delft3D FM.	36
Figure 3-6: Location of the wave model point taken from Argoss model ("Lake Bardawil," 2015).	40
Figure 3-7: Wave roses near Lake Bardawil. Left: Wave rose for the offshore point(BMT Argoss). Right: Wave rose for a nearly nearshore point(Nassar et al., 2018).	41
Figure 3-8: Flow chart of the simulation runs based on the design methodology.	44
Figure 3-9: Flow chart of the simulation runs examined with the Delft3D. Simulation 1: Case 1, tide only condition. Simulations 2-3: Case 2, tide with two sediment properties. Simulations 4-11: Case 3, tide, sediment and waves. Simulation 2-7: Simulations with a grain size equal to 180 μm . Simulations 3-11: Simulations with 330 μm grain size.....	45
Figure 3-10: Flow grid within Delft3D FM.....	46

Figure 3-11: Computational flow grid. Higher local refinement along the land boundary and within Boughaz 1 inlet.	48
Figure 3-12: Computational wave grid. Higher local refinement area along Boughaz 1 inlet.	50
Figure 4-1: Locations of consideration. Grey: Offshore. Blue: West inlet. Orange: East inlet. Light blue: Slack point. Light green: Point 1. Green: Point 2.	54
Figure 4-2: Water level variations at offshore and near the inlets. East inlet refers to Boughaz 2 inlet and West inlet refers to Boughaz 1 inlet.	55
Figure 4-3: Water level variations at different locations within the inlets and lake.	56
Figure 4-4: Flood velocity vector plot within the lake.	56
Figure 4-5: Cross sectional velocity of the most efficient design cross-sectional areas in the west inlet.	60
Figure 4-6: Current flows within the west inlet. The velocity magnitude (m/s) is presented during ebb and during flood for the initial state and inlet cross sectional area 9.	60
Figure 4-7: Water level variation during spring of the different cross-sectional areas designs within the west inlet.	61
Figure 4-8: Comparison of the cross-sectional velocity between initial state, base scenario and approach channel designs.	63
Figure 4-9: Current flows within the west inlet. The velocity magnitude (m/s) is presented during ebb and during flood for the approach channel design 2. The upper left and right figure indicates the approach channel with shallow lake and the bottom left and right the approach channel with the deep lake.	64
Figure 4-10: Comparison of current flows between inlet cross section design element and approach channel. The white dashed line is the reference line to indicate the extension of the current flows with and without the approach channel.	64
Figure 4-11: Water level variation during spring of the approach channel, initial state and base scenario.	65
Figure 4-13: Comparison of the current flows between inlet cross section design element, approach channel and inlet nourishment. The white dashed line is the reference line to indicate the extension of the current flows during ebb.	67
Figure 4-12: Comparison of the cross-sectional velocity between initial state, base scenario and inlet nourishment designs.	67
Figure 4-14: Water level variation during spring of the inlet nourishment designs, compared with the initial state and base scenario.	68
Figure 4-15: Comparison of the current flows between the final state and the initial state of Boughaz 1 inlet.	69
Figure 4-16: Velocity variation. Comparison between initial state and final design.	70
Figure 4-17: Water level variation. Comparison between initial state and final design.	70
Figure 4-18: Final combined design approach. Determination of the optimal to the hydrodynamics design. Each design element is depicted with the associated defined parameter values.	71
Figure 4-19: Flow chart of the simulation runs within Delft3D.	72
Figure 4-20: Control areas of the most important features in the tidal inlet system. 1 -2 : Inlet nourishment and approach channel which cover the ebb-delta area, 3: Inlet gorge, 4: Flood delta.	75
Figure 4-21: Morphological changes of the inlet cross-section of simulation 7.	76
Figure 4-22: Morphological changes of the inlet nourishment of simulation 7.	77
Figure 6-1: The most important design elements which can mimic nature with their associated parameters. ...	89
Figure A-1: Nearshore significant wave height time series. The highest 12-hour wave height was used for the determination of DoC.	105
Figure B-1: Monthly salinity levels measured in ‰ (El-Bana et al., 2002; Lanfers, 2016).....	106
Figure B-2: Temperature (Celsius) and evaporation(mm/day) in North Sinai	107
Figure B-3: Mean evaporation (mm/day) on Sinai Peninsula.	107
Figure B-5: Distribution of the wave height, $H_s(m)$, direction $Dir (^{\circ})$ and peak period $T_p(s)$. Figure B-3: Mean evaporation (mm/day) on Sinai Peninsula.....	107
Figure B-4: Offshore wave model point location	108
Figure B-5: Distribution of the wave height, $H_s(m)$, direction $Dir (^{\circ})$ and peak period $T_p(s)$	111
Figure B-6: Depth map used for the nearshore bathymetry.	112

Figure D-1: Water level variations for both models runs. Blue: Marker x, time step 6s. Red: Marker o, time step 4.5 s. 114

Figure D-2: Depth-averaged velocity magnitude within the inlet, at 10 m depth. Blue: Marker x, time step 6s. Red: Marker o, time step 4.5 s. 114

Figure E-1: Residual eddies found while implementing the inlet nourishment design during ebb and flood currents. The blue colour indicates the initial state, thus without the inlet nourishment and the red colour indicates the examination of the inlet nourishment design. 116

Figure E-2: Residual eddies found while implementing the new inlet nourishment design and reshaping the western barrier. The red colour indicates the old inlet nourishment design while the green colour the new design. 117

Figure E-3: Morphological changes of the inlet cross sectional area for all the simulations. The same behavior is observed for all the simulations. 120

Figure E-4: Morphological changes of the inlet nourishment design for all the simulations. 120

Figure E-3: Morphological changes of the inlet cross sectional area for all the simulations. The same behavior is observed for all the simulations. 120

Figure E-4: Morphological changes of the inlet nourishment design for all the simulations. 121

Figure E-5: Bottom depth changes of the inlet nourishment with different values of the wave related transport factor. 123

Figure E-5: Bottom depth changes of the inlet nourishment with different values of the wave related transport factor. 123

LIST OF TABLES

<i>Table 2-1: Longshore transport processes along Lake Bardawil (Linnarsund & Mårtensson, 2008).</i>	16
<i>Table 2-2: Stability and bypassing mode of a tidal inlet system related to the r factor (Bosboom & Stive, 2015; P. Bruun et al., 1978; De Vriend et al., 2002).</i>	19
<i>Table 3-1: Design parameters of the associated design elements.</i>	28
<i>Table 3-2: Range values of each design parameter for the three design elements provided by TWM/DEME.</i>	32
<i>Table 3-3: Different design approaches of the cross-sectional design element.</i>	34
<i>Table 3-4: Different design approaches of the approach channel inlet.</i>	35
<i>Table 3-5: Different design approaches of the inlet nourishment.</i>	38
<i>Table 3-6: Wave conditions implemented within Delft3D model.</i>	41
<i>Table 3-7: Tidal data implemented within the models (Gary D. & Erofeeva Y., 2002).</i>	42
<i>Table 3-8: Sediment grain sizes nearshore of Boughaz 1 inlet (Piere, 2016).</i>	43
<i>Table 4-1: Tidal prism results related to the cross-sectional design element.</i>	58
<i>Table 4-2: Maximum flood and ebb current velocities (m/s) based on cross-section design element.</i>	59
<i>Table 4-3: Tidal prism results related to the approach channel design element.</i>	62
<i>Table 4-4: Maximum flood and ebb current velocities (m/s) based on approach channel design element.</i>	63
<i>Table 4-5: Tidal prism results related to the inlet nourishment design element.</i>	66
<i>Table 4-6: Average tidal prism for all the simulations carried out with the Delft3D software. With grey colour the tide only case is indicated, while with light blue and orange are the simulations of $d_{50}=180\ \mu\text{m}$ and $330\ \mu\text{m}$ respectively.</i>	73
<i>Table 4-7: Control volume changes at the morphodynamic features of the tidal inlet system.</i>	78
<i>Table 4-8: Sensitivity analysis of the tidal prism.</i>	79
<i>Table 4-9: Sensitivity analysis of the morphological features within the west inlet.</i>	79
<i>Table 4-10: Stability factor r. P/M ratio defined for the Boughaz 1 inlet.</i>	80
<i>Table 6-1: The determined parameter values for the final combined design of the initial phase of the design methodology.</i>	91
<i>Table A-1: Combination of the coefficients C and q defined with the O'Brien relationship by Jarrett (1976)(Escoffier, 1977).</i>	102
<i>Table B-1: Scatter plot of significant wave height (m) relative direction and peak period (s) relative to direction.</i>	109
<i>Table B-2: Wave conditions defined from the input reduction method.</i>	111
<i>Table D-1: Model accuracy validation with two different time steps.</i>	113
<i>Table E-1: Tidal prism results for all the designs of the cross-sectional area design.</i>	115
<i>Table E-2: Tidal prism calculations during spring tide. The colour differences illustrate the two different grain sizes. With light blue: $180\ \mu\text{m}$ while with light orange: $330\ \mu\text{m}$.</i>	118
<i>Table E-3: Tidal prism calculations during neap tide. The colour differences illustrate the two different grain sizes. With light blue: $180\ \mu\text{m}$ while with light orange: $330\ \mu\text{m}$.</i>	118
<i>Table E-4: All the combinations and associated results of the tidal prism while applying sensitivity analysis.</i>	119
<i>Table E-5: Morphological changes based on sensitivity analysis.</i>	123

Abstract:

Lagoons are connected to the sea by the presence of openings along their barriers. These openings, also known as tidal inlets, can either be natural or man-made and they highly determine the hydrodynamics within the lagoon system.

Tidal inlet systems are important for commercial shipping, favor for harbor construction in the low energy region, for recreational boating and marinas in back-barrier lagoons and vital for ecology. The functionality of the tidal inlet system is highly determined by its morphology, hydrodynamic conditions and geometrical features. Sufficient water exchange, tidal prism, between the lagoon and sea are essential for the improvement of the water quality in the lagoon. Furthermore, the need to mimic nature is crucial for not deforming the natural behavior of these systems. Such systems are found worldwide, and many of them are difficult to be understood due to their complex processes and lack of data. One of these systems is Lake Bardawil.

Lake Bardawil, is located at the North coast of the Sinai Peninsula in Egypt and its ecological value is of great importance. Its convex shape covers an area of about 600 – 629 km², with a maximum width of 20.5 km and its barriers have a length of approximately 80 km. Its existence mainly depends on the presence of three inlets which connect the lagoon with the Mediterranean Sea. Two of them are man-made, called Boughaz 1 and Boughaz 2, while the third is natural and is called Zaranik. Boughaz 1 is located in the western side of the lake while Boughaz 2 and Zaranik are in the eastern side. It is reported that Zaranik inlet is rarely open due to sedimentation.

Although, Lake Bardawil is considered the least polluted lagoon area in Egypt and in Mediterranean region, it is experiencing many problems which worsen these conditions. Salinity, high temperature and evaporation rates, the limited water exchange in combination with the way of living conditions of thousands of families in the area lead to the collapse of the ecosystem and closure of tidal inlets. For that reason, human interventions took place by constructing hard structures to stabilize the inlet systems and thus allowing the water exchange between sea and lagoon. However, the blockage of the dominant longshore sediment transport at the west side of the inlets, led to the shoreline accretion and erosion updrift and downdrift of the inlets respectively. Subsequently, the functionality of the inlets is weakened, resulting in inlet instability which consequently affects the ecosystem recreation.

Extensive researches have been made to examine several aspects of this system such as geomorphology, morphology, hydrology and ecology of the system but many of them are not accessible nor available which increases the complexity of assessing and examining the system response. One of the recent researches that is carried out by the Dredging, Environmental and Marine Engineering (DEME), The Weather Makers (TWM) and Laniers (2016), studied how the ecosystem and the fish population of Lake Bardawil can be restored by new hydraulic interventions. This thesis is an extension of this work, but current focus is put on the determination of an innovative design and associated methodology which is based on natural design elements and can improve the functionality of Boughaz 1 inlet.

Boughaz 1 was constructed in 1955 to allow the water exchange between the sea and the lagoon. It is reported that its length varies between 600 – 1000 m and its width is 150 – 500 m while a maximum of 6 m depth is reached with dredging operations. Over the passing years, it has been subjected to a reduced tidal prism resulting in poor water quality in the lagoon, limited fish migration from the sea and sedimentation causes the need for dredging maintenance works for improving its functionality. This led to the construction of breakwaters in 1985 until 1995 for the stabilization of the inlet and for the protection of the fish population in the lagoon. However, sedimentation and erosion are observed

along the shoreline which did not only negatively affect the inlet functionality but the natural behaviour as well.

A design methodology is carried out to understand and improve the functionality of the Boughaz 1 inlet. The design methodology is based on the most important natural design elements, namely inlet cross sectional area, approach channel and inlet nourishment. Numerical models (Delft3D and Delft3D FM) are used to assess the influence of the different designs on the functionality of the system. A hydrodynamic analysis is carried out for each design element to define the final combined design of the initial phase of this design process. This final design is examined under hydrodynamics and with the initial deposition and erosion patterns.

The tidal prism, flow velocities and water levels are examined to define the final combined design of the inlet. It is shown that, narrower and deeper inlet cross sectional areas can lead to potential increase of the tidal prism (43- 48 %) in Boughaz 1 inlet. The approach channel and inlet nourishment can extend and concentrate the high flows over the inlet entrance, with the former to increase the tidal prism (>10 %), flow velocities (14 %) and water level conditions (25 %) within the inlet. The reshaping of the barriers is found important for finalizing the design of the west inlet while the depth of the lagoon is found to be a crucial factor to determine the tidal prism and flow velocities in the system. The final combined design improved the hydrodynamic response of the Boughaz 1 inlet, with the tidal prism to exceed the 60 % from the initial state. Furthermore, the flow velocities and the water level within the inlet are increased with the specific design approach. The former is calculated equal to 0.81- 0.80 during flood and ebb respectively, while the latter is found equal to 0.40 m.

The final combined design is further examined with the presence of four different wave conditions and involving morphological changes. The selected wave conditions had a limited effect on the hydrodynamics of this design. The aim to mimic nature is validated with the initial deposition and erosion patterns. The stability of the system with the stability factor is improved with respect to the initial state of the system. The stability of the inlet system is increased from poor to fair to poor conditions and it is found that can even be fair during spring and small littoral drift processes. It is concluded that the functionality of the Boughaz 1 inlet can be optimized with the adapted design methodology, however, further research is needed to understand extensively the detailed morphological behaviour of each element on longer timescales. This will assess the period of the maintenance dredging works as well as the bypassing mode of the system.

Preface:

With this MSc thesis report my academic studies are fulfilled. It was a tough but enjoyable ride and I would have done it all over again if needed.

I would like to thank all the people that were involved in this thesis for the time and effort they spent on helping me produce something that is valuable. To begin with, I would like to thank my professor Dr. Aarninkhof for all the tips and guidelines that he gave me during our thesis meetings. In addition, I want to thank Dr. De Vries for all the help and support that he provided throughout the whole period of my thesis. Also, I would like to thank Dr. Ngan-Tillard who provided me useful information to successfully finish my thesis. It was really helpful and reassuring to know that people from the university do not care only about the content of a thesis but for the students as well.

Furthermore, I would like to thank The Weather Makers and namely Ir. Van der Hoeven and Ir. Lanter for the opportunity that they gave me to contribute on such an interesting topic. I want to also thank them for all the support that they provided whenever it was needed. I would also like to thank Ir. Mol from DEME group for all the help that he gave me with this thesis.

To conclude, I want to thank my family, my boyfriend and my friends for all the support that they gave me throughout the years. I could have never done it otherwise. I owe you for a lifetime.

1 | Introduction

The first chapter of this thesis provides briefly general information about tidal systems, their functionality, and their relevance to society and environment. In relation to that, a general description of the area of interest is given and the problems present in the area are analyzed. Finally, the objective of this thesis is given while a short layout of the thesis is described.

1.1 Tidal inlet systems

Tidal inlet systems are of great importance for society and for the environment. High percentage of human population lives and works near such areas and several species of marine life grow in these regions (Bosboom & Stive, 2015). The main interest in such systems were mainly for commercial and recreational aspects while in the latest stage these systems are found to be ecologically valuable as well.

Over the passing years, extensive researches have been made to understand the response of the tidal inlet systems all over the world. Due to human interventions and/or natural processes, the information flow is everlasting. On the other hand, several features of these systems are still unidentified and difficult to be understood.

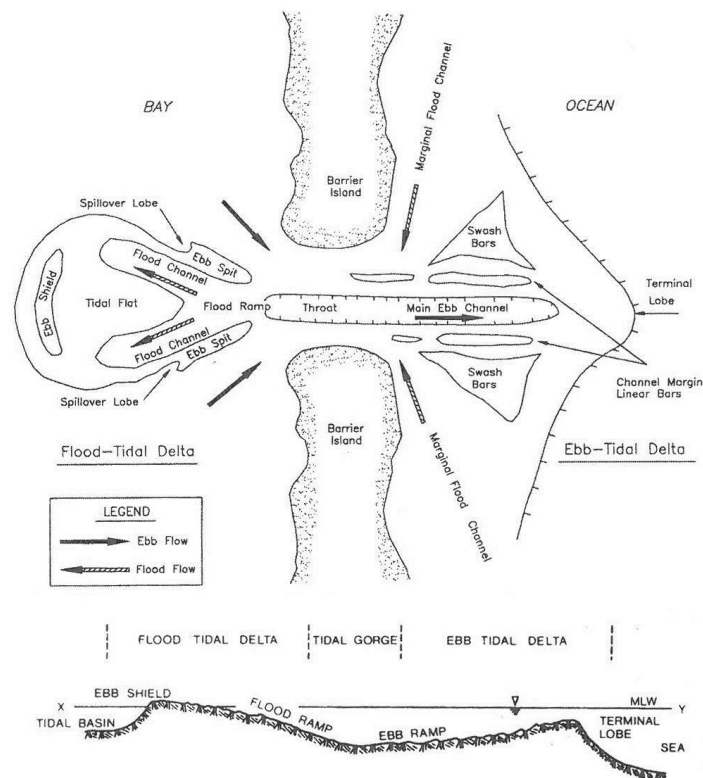


Figure 1-1: Morphological features of the tidal inlet system (Bosboom & Stive, 2015).

Tidal inlets and their associated basins (lagoons) are a common feature of lowland coastal systems all around the world (De Vriend, Dronkers, Stive, Van Dongeren, & Wang, 2002). Some of them are found to be natural while others are man-made and/or modified with hard structure. Tidal inlet system define the entire morphological system which consists the entrance itself, ebb-tidal delta and flood tidal delta, see Figure 1-1 (Bosboom & Stive, 2015). The inlet can be described as the connection point between sea and tidal lagoon. This connection is also called gorge or throat (Bosboom & Stive, 2015).

The tidal inlet system is highly dynamic and is mostly depended on the tide, since the offshore wave energy is relatively low inside the lagoon area. This is due to the presence of long stretches of barriers and the geometry of the outer delta, ebb tidal delta, which dissipate the offshore wave energy before entering the basin. However, wave energy plays a crucial role for the outer delta formation and for sand by-passing systems along the coast, thus should always be taken into consideration. Water flows into the lagoon with the flood currents and out during ebb (De Vriend et al., 2002).

It is reported that tidal inlet systems are important for commercial shipping, favor for harbor construction in the low energy region, for recreational boating and marinas in back-barrier lagoons and vital for ecology. The functionality of the tidal inlet system is highly determined by its morphology, hydrodynamic conditions and geometrical features. Sufficient water exchange, tidal prism, between the lagoon and sea is essential for the improvement of the water quality in the lagoon. Furthermore, high flow velocities through the inlet contribute to the increase of the fish migration and stability of the system while it reduces the sedimentation through the inlet. These conditions, related to the functionality of the system, are greatly determined by the geometrical features of the tidal inlet system.

There are several natural tidal inlets which can mimic nature due to their dynamic functionality while many other inlets have been modified by constructing hard structures such as breakwaters or jetties to improve that. Although breakwaters can minimize the abrupt sedimentation and thus improve the functionality of the inlets, the behaviour of these systems is gradually changing result in different governing physical processes which might worsen these conditions compare the natural system. For that reason, the aim to mimic nature is important for not deforming the natural behaviour of the system and thus providing healthier and functional tidal inlet system.

1.2 Lake Bardawil

Numerous tidal inlet systems present all over the world. One of those systems is Lake Bardawil, which is at the north coast of the Sinai Peninsula in Egypt. Northern Sinai, occupies about 8000 km², or 13% of the area of Sinai Peninsula (Khalil & Shaltout, 2006).

The Bardawil lagoon covers an area of about 600 - 629 km² which is not entirely filled with water during summer season but appears as separate ponds and lakes (El-Bana, Khedr, Van Hecke, & Bogaert, 2002; Embabi & Moawad, 2014; Khalil & Shaltout, 2006). It extends for almost 80 km with the length of the inner shores to be approximately 611 km whilst the maximum width is about 20.5 km (Embabi & Moawad, 2014; Khalil & Shaltout, 2006). The lake is very shallow with a mean depth of 1.2 m (Ellah & Hussein, 2009) and its existence depends on the connection between the Mediterranean Sea through three main inlets. Two of these inlets are artificially constructed (Boughaz 1 and Boughaz 2) and both remain open due to periodic dredging operations. Boughaz 1 is located at the west side of Lake Bardawil and Boughaz 2 inlet is at the east side of the system, see Figure 1-2. The third inlet is natural and located in the eastern side of the Lake Bardawil. Its name is Boughaz El-Zanarik and covers a distance of 2 km in the eastern side of lake Bardawil. This inlet is 20 m wide and 1 m deep. Due to its very shallow configuration the inlet is seasonally closed due to siltation (Khalil & Shaltout, 2006).



Figure 1-2: The position of the three inlets in Lake Bardawil. On the western side: Boughaz 1 inlet. On the east side: Boughaz 2 and Zaranik inlet respectively, ("Lake Bardawil," 2015)

1.3 Problem description

Lake Bardawil is considered as the least polluted lagoon area in Egypt and in the Mediterranean region (El-Bana et al., 2002). However, this does not imply that the lake is not subject to any other problems which can worsen these conditions and subsequently the ecosystem.

Over the passing years, reduction of the water depth has been observed within the inlet entrances due to sedimentation induced by wind-waves, currents and/or aeolian transport through coastal processes after re-opening the inlets. The water exchange between the Mediterranean Sea and Lake Bardawil has been reduced substantially, resulting in limited fresher water and high salinity levels within the system (Lanters, 2016). These consequent processes were a major threat for the ecosystem (Lanters, 2016; Linnarsund & Mårtensson, 2008; Nassar et al., 2018) and for engineering purposes as well since the need for frequent dredging maintenance works increased substantially.

Higher values of water salinity were observed (up to 70-90‰) after the fully closure of both the west and east artificial inlets (Boughaz 1&2) in 1970 (Khalil & Shaltout, 2006). Although, the opening of the inlets with dredging operations resulted in reduction of the water salinity to a percentage 45‰ near the inlets and 65‰ in the fringes, the salinity level is still higher than the salinity of 39‰ in the Mediterranean Sea (Linnarsund & Mårtensson, 2008). This characterised the lake as hyper saline. The salinity levels greatly depend on the local climatic conditions, the evaporation rate and the type of the lagoon (Ellah & Hussein, 2009). Lowest values of salinity present during winter period (Khalil & Shaltout, 2006), when the evaporation rate is less and strong wind forces exist (Ellah & Hussein, 2009) while the opposite happens during dry season, see Appendix B.

Environment degradation and considerable changes in its ecosystem are found to be crucial for the living conditions of the fishermen in Lake Bardawil (Ellah & Hussein, 2009; Lanters, 2016). For these reasons, maintenance dredging operations and breakwater construction were essential to guarantee both artificial inlets remain open for longer period (Abohadima, El-Bagoury, & Rakha).

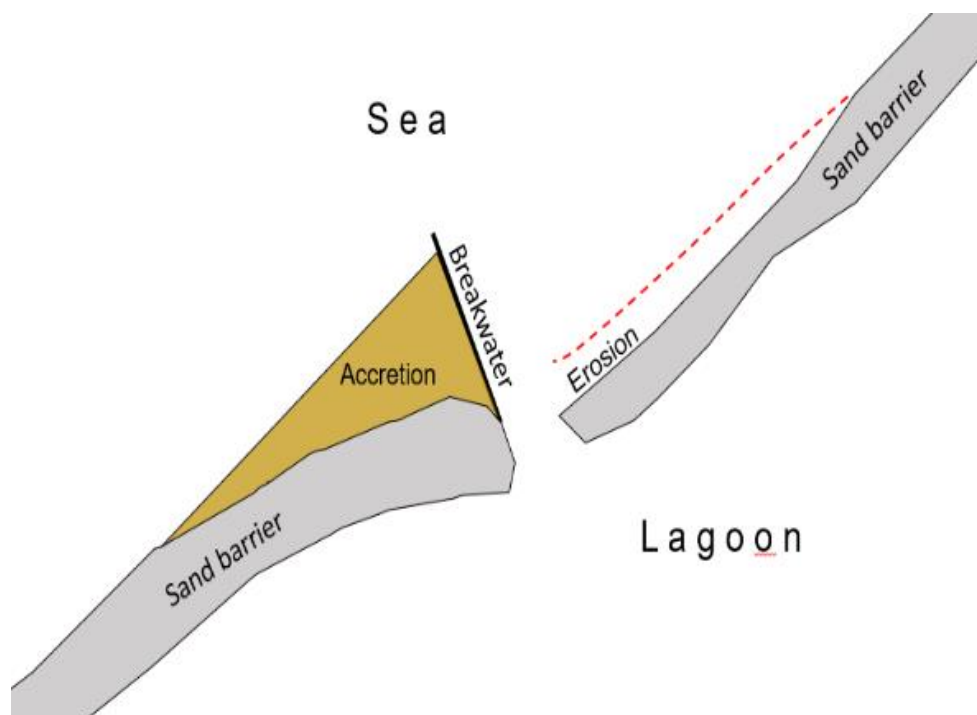


Figure 1-3: Current situation of Boughaz 1 inlet. Sediment disruption due to the vicinity of the breakwater and shoreline erosion downstream.

The construction of breakwaters at both sides of the artificial inlets during 1986 to 1995, was essential for minimizing the abrupt sedimentation within the inlet and thus reducing the need for dredging operations. However, their presence led to unstable processes along the shore. The constructed breakwaters resulted in shoreline erosion in the east side of the inlets while accretion is seen in the updrift side, see Figure 1-3 (Khalil & Shaltout, 2006; Linarsund & Mårtensson, 2008; Nassar et al., 2018). This entails that the natural behaviour of the tidal inlet systems is gradually changed due to the presence of the breakwaters and inlet instability is observed.

The problems affecting the tidal inlet system of Lake Bardawil are for great importance not only for engineering purposes but for the ecosystem as well. The reduction of water exchange between lagoon and the Mediterranean Sea, due to sediment infilling, results in a poorer circulation inside the lagoon area (Abohadima et al.) which can lead to eutrophication (Ellah & Hussein, 2009). Furthermore, limited water exchange with the adjacent sea reduces water quality and thus increases water salinity which this is a threat for the ecosystem (Abohadima et al.).

Problem statement:

Lake Bardawil is an important fish catchment area and thousand families fully depend on this for living (Abohadima et al.). The instability of the tidal inlet system due to human activities affects the physical development of the hydrodynamics and morphodynamic processes of the system and the adjacent coastal areas. These subsequently disturb the evolution of the ecosystem and thus the living conditions of these families. An appropriate research related to the acknowledgement of the hydrodynamics and morphological changes of the inlet system under different design approaches is required such as the problems depicted above to be resolved for healthier conditions. In this thesis project focus will be made to the west artificial inlet, Boughaz 1. A cyclic behaviour of the system is depicted in Figure 1-4.

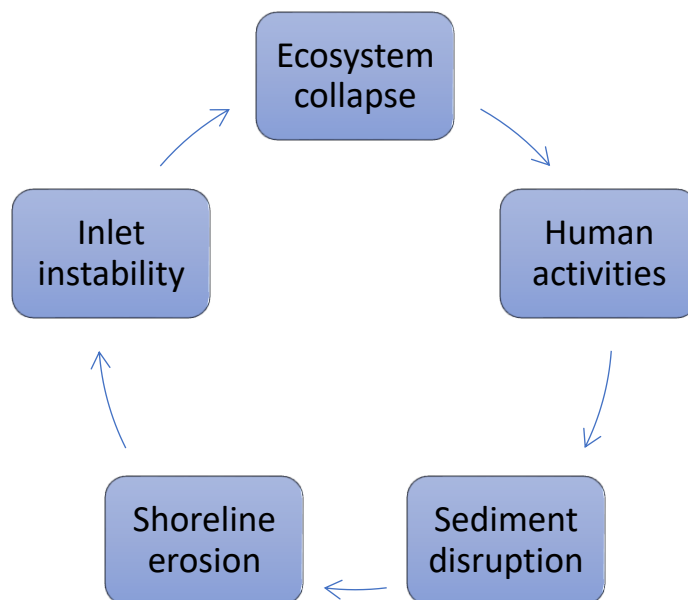


Figure 1-4: Cyclic behaviour of the tidal inlet system in the western area of Lake Bardawil.

1.4 Research objective and research questions

Research Objective:

Healthier functionality of the tidal inlet system does not coincide with the prevention of the natural conditions exist in the area. This can be explained clearer by understanding that the tidal inlet system in Bardawil will always be subjected to sediment infilling, but this should not harm its functionality. Boughaz 1 requires sufficient water exchange between the sea and the lagoon while mimicking its natural behaviour. This will provide more stable conditions in the area. According to that, the acknowledgement of the behaviour of the system under certain design adaptations plays crucial role for the future developments in the area. In case one tries to mimic nature and optimize the morphological stability of the inlet under the prevailing environmental conditions, multiple benefits could be achieved, such as safety, reduction of maintenance costs and a healthy ecosystem.

The bigger goal of the restoration of Lake Bardawil requires a dynamic stable inlet design which not only can reduce the maintenance dredging works but also can be beneficial for the natural capital in the area. The scope of this research is to understand and define a design methodology which is based on natural elements, leads to a new innovative tidal inlet design and improves the functionality of the Boughaz 1 inlet under the optimization of the hydrodynamic and its morphological conditions. The innovative tidal inlet design is based on the initial phase of a design process and not to a detailed final design. Considering this, the innovative design of the inlet will be based on the removal of the breakwaters in Boughaz 1 inlet such as the functionality of the natural system under soft engineering solutions can be observed.

To understand the effectiveness of the selected design adaptations in combination with the response of the tidal inlet system, the following main research question and accordingly the sub-questions should be answered.

Research question:

“Can the functionality of Boughaz 1 inlet be optimized by mimicking nature?”

While the sub-questions are the following:

- **Which are the most important elements that can mimic nature?**
- **Which parameters affect the hydrodynamic response of each design element?**
- **What combination of design element can optimize the functionality of Boughaz 1 inlet and what is the final combined design choice?**
- **How sensitive are the hydrodynamics associated with the selected design of the Boughaz 1 inlet to certain sediment properties and wave conditions?**
- **How sensitive is morphology associated with the selected design of the Boughaz 1 inlet to certain sediment properties and wave conditions?**
- **Is the stability related to the functionality of the Boughaz 1 inlet system, improved in the new design?**

1.5 Thesis outline

The thesis is separated into six chapters. Following the first chapter of the report, a background work is given. In this chapter, a detailed information of the specify area of interest is provided with the associated data. To that, the stability models that are used to define and analyse the design methodology are provided, with the related works that have already be done. The third chapter focuses on the methodology that is followed within the thesis. Specifically, the third chapter illustrates the design methodology and the design modelling approach plan. Based on that, the associated results are given in chapter 4 and discussion is provided in chapter 5. The thesis is finalised with the conclusion and recommendations in chapter 6. Briefly, a description of each chapter is given below.

Chapter 2: Background

- Description of the study area and the data provided from different sources.
- Literature review of the stability models and related examples.
- Related modelling studies.

Chapter 3: Methods

- Description of the design methodology:
 - o Definition of the design elements, parameters.
 - o Description of the design procedure.
- Description of the design modelling:
 - o All the data that is used within the models are provided with the associated analysis.
 - o Description of the model set up and the modelling approach.

Chapter 4: Results

- The results of the Delft3D FM software are given first, related to the hydrodynamics conditions for each design element and the stability models.
- Followed that, the results related to Delft3D software are provided. Specifically, the hydrodynamics and morphological response of the elements is given. The concept of sensitivity analysis is described, and all the results are related to the stability models.

Chapter 5: Discussion

- Remarks, limitations and assumptions that are taken into consideration are illustrated in that chapter.

Chapter 6: Conclusions and recommendations

- Concluding remarks related to the whole system and the specify area of interest are provided while recommendations related to the thesis work and for future research are given.

2 | Background

In this chapter, more detailed description of the study area is provided. This includes the historical background and the data review found from literature. Following that a general description of the methods that are used by several studies to identify the stability of the inlets is given in combination with the models that describe the sediment bypassing processes. Related to that, an information regarding the studies done within the area of interest are provided.

2.1 Study area

2.1.1 Boughaz 1- West inlet

This thesis project will focus on a new innovative design of the west inlet of Lake Bardawil. Boughaz 1 was originally constructed in 1955 to connect Lake Bardawil with the Mediterranean Sea (Khalil & Shaltout, 2006). Its existence depends on the maintenance dredging operations that are carried out over time. It is reported (2006) that the length of inlet had a range between 600 to 1000 m and its width was about 150 m, while the inlet depth was between 4-6 m (Khalil & Shaltout, 2006). The basin area of Boughaz 1 inlet system covers one third of the total lagoon area, thus approximately 200 km², while the width of the basin area varies from 4 to 10 km (Embabi, 2017).



Figure 2-1: Evolution of Boughaz 1 inlet during 1984-2016. 1984: Instable system, 1986-1995: Breakwaters and maintenance dredging works, 2016: Current state("Lake Bardawil," 2015).

Breakwaters and maintenance dredging works were started in 1986 until 1995 to stabilize the inlet system and to protect the fish population in the lagoon, see Figure 2-1 (Khalil & Shaltout, 2006). The inlet size was changed with dredging operations to about 6 m depth and 500 m width, whilst the breakwaters were constructed to the east and west of the inlet. The construction of these structures around the inlet entrance led to deposition of coarser materials in the western side of the inlet while erodible materials were found at the eastern side, see Figure 2-2 (Khalil & Shaltout, 2006).

In general, two Subcells which describe the erosion and deposition patterns have been formed to describe the alongshore sediment transport patterns in the area. The Port Said Subcell which is extended until the east side of the west inlet of the Lake Bardawil, shows the accumulation of sediment along the west side of the inlet while erodible features have been observed downstream of the inlet (Linersund & Mårtensson, 2008). This shows the strong effect of the hard structures in the area.

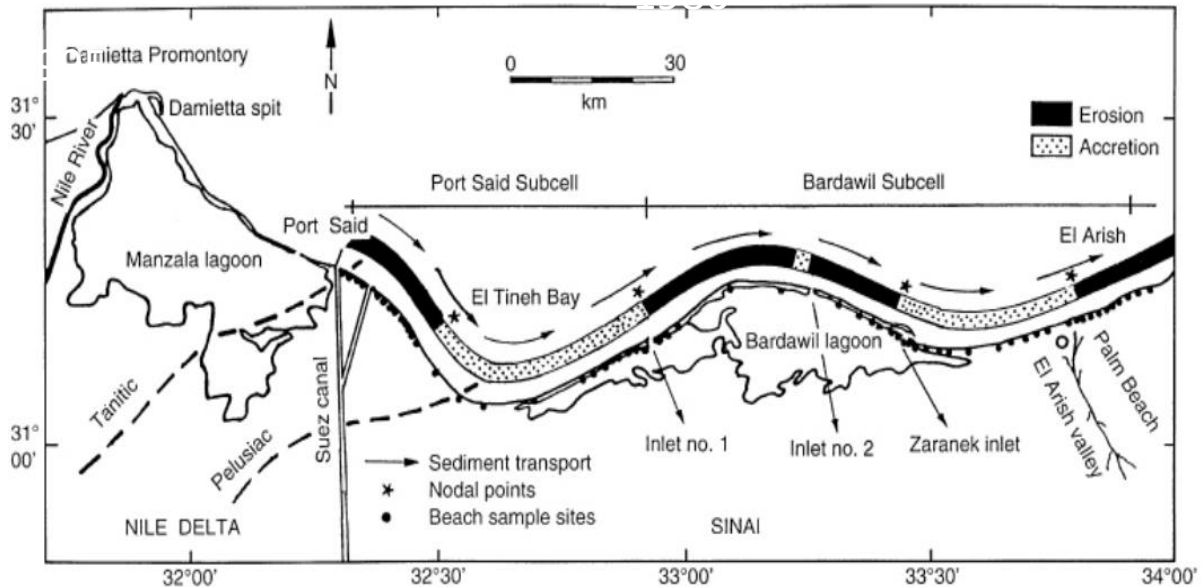


Figure 2-2: Erosion and deposition patterns along the Port Said and Bardawil Subcells in Lake Bardawil. Deposition is seen at the updrift side of the breakwater and erosion in the lee side (Linersund & Mårtensson, 2008).

2.1.2 Data review

To understand the response of the inlet, the main characteristics of the Boughaz 1 inlet should be indicated. These include the metocean conditions (wind, waves, climate), and geomorphological data (sedimentary data, landscape). Although, there is a high lack of data, through the years several studies have been made to gain an inside for the response of the system. According to several studies, the following conditions are presented in Lake Bardawil:

Metocean data

- Salinity and evaporation rates:

Lake Bardawil is considered as hypersaline lake due to the limited water exchange with the Mediterranean Sea. The salinity levels depend on the local climatic conditions and the evaporation rate (Ellah & Hussein, 2009). Lowest values of salinity present during winter period (Khalil & Shaltout, 2006), when the evaporation rate is less and strong wind forces exist (Ellah & Hussein, 2009) while the opposite happens during dry season. These values can be observed in the Figure 2-3. The salinity levels in the western side of the Lake Bardawil, where Boughaz 1 inlet is located, do not fluctuate through the years and almost constant value of 55‰ is observed. The salinity levels are considered higher compared the Mediterranean Sea. Subsequently, the high evaporation rates in Lake Bardawil show significant values compared the nearby areas, see also Appendix B. The evaporation rate exceeds the value of 6 mm/day when the temperature is over 23 C°, which can be considered high enough than

the other locations. However, these values may give inaccurate results since the meteorological stations are situated within the cities (Lanters, 2016).

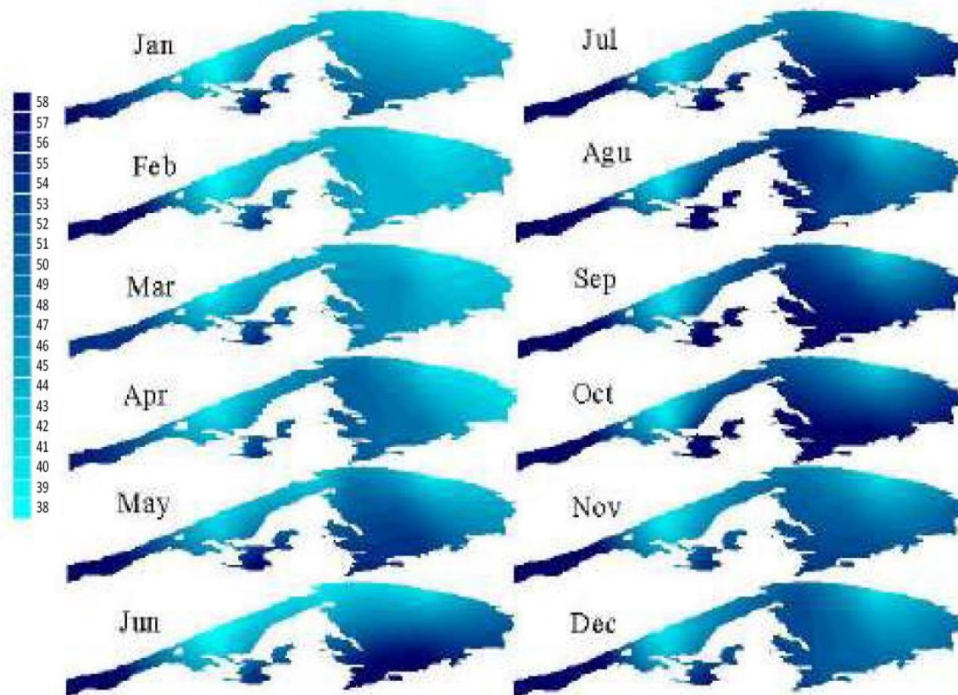


Figure 2-3: Monthly salinity levels measured in ‰ (El-Bana et al., 2002; Lanters, 2016).

- Wind climate:

Wind acts as a surface force in the water and plays crucial role for the circulation motion within the lagoon and thus the water exchange between Mediterranean Sea and Lake Bardawil (Embabi & Moawad, 2014; Lanters, 2016; Linnarsund & Mårtensson, 2008). Seasonality is an important indicator for the wind direction. During winter months, winds approaching the shore from south-west (SW) and west (W) are presented to be the strongest yearlong, whilst during spring south south-west (SSW) and west south-west (WSW) are the most dominant ones (Linnarsund & Mårtensson, 2008). Measurements done from 1999 to 2000 and 2005 showed average wind speed values of about 3.69 m/s and 4.92 m/s respectively, whereas the hourly maximum speed about 13 m/s for the strongest winds (Linnarsund & Mårtensson, 2008). Wind generated waves along the coast are responsible for the generation of longshore currents towards east during summer and winter, whilst during spring the longshore currents are towards the west (Embabi & Moawad, 2014).

- Wave climate:

The dominant wave direction during winter season is from W, north north-west (NNW) to north-west (NW) whereas during summer is NW (Embabi & Moawad, 2014; Klein, 1986; Linnarsund & Mårtensson, 2008). Nassar et al. (2018) with situ measurements showed that for the year 2010 the predominant direction of the waves is from NW and N whilst only 5% approaching from south-east (SE) as indicated in the wave rose. All the studies show good correlation to the NW waves which are important for the easterly directed longshore currents (Embabi & Moawad, 2014; Linnarsund & Mårtensson, 2008; Nassar et al., 2018). Waves during winter are much higher than the waves during summer. Near the area of Lake Bardawil, the wave height was found to be more than 3.66 m for more than 4% of the winter time, while the wave heights more than 3.66 m appear less than 2% of the summer time (Klein, 1986). The average wave height and period during the whole year was found 0.5 m and 6.3 s respectively (Embabi & Moawad, 2014). Nevertheless, the wave climate near the Lake Bardawil is mainly depended on the wind climate and thus wind generated waves act as an important factor in the area (Emanuelsson & Mirchi, 2007).

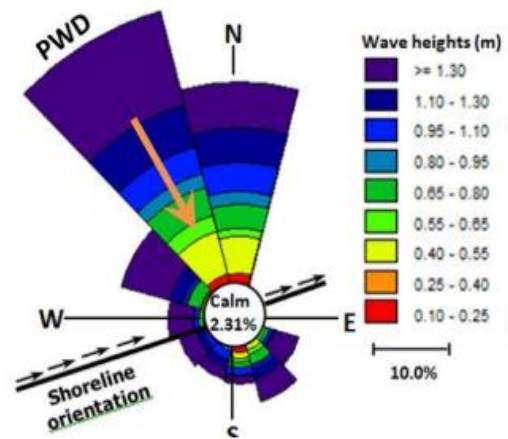


Figure 2-4: Wave rose indicate wave conditions and predominant wave direction (PWD) at a depth of 14 m with situ measurements (Nassar, Mahmood, Masria, Fath, & Nadaoka, 2018).

- Tide – water level fluctuations:

The North Sinai coast is characterized by micro tidal regime (Ellah & Hussein, 2009) which indicates that the mean tidal range is less than 2 m (Bosboom & Stive, 2015). Linnarsund and Mårtensson (2008), found a mean tidal range of about 30 cm along the coast. During neap tide the tidal range was found to be 25 cm whilst during spring 35 cm. However, Nassar et al. (2018) with situ measurements found a tidal range to be approximately equal to 55 cm. The tidal environment is characterized with mixed energy, mainly as semidiurnal (Bosboom & Stive, 2015). According to Linnarsund and Mårtensson (2008), the average tidal level inside Lake Bardawil and especially for Boughaz 1 inlet is less than 16cm. Embabi and Moawad (2014) estimated the inflow and outflow velocities approximately equal to 0.70 m/s during flood and ebb duration respectively.

Geomorphological data

- Basin area landscape:

In the basin area of the Boughaz 1 inlet, two smaller lagoon areas are present namely, El-Rewaqa and El-Marqab. These lagoons are the most noticeable ones, and their dimensions in N-S direction approaches 3.60 to 4.65 km while in the E-W direction is between 3.00 and 4.50 km. These small lagoon areas are inter-connected with a small opening and extend until the main basin area. Furthermore, micro-lagoons are also visible in the basin area which are partially closed by Gazirat Mehaisan and connected with the main basin area with larger opening, Figure 2-5 (Embabi & Moawad, 2014).

- Barriers:

The width of the long stretches of barriers which separate the lagoon from the Mediterranean Sea is about 300-1000 m, whereas the length of the barrier is almost 90 km. Their height varies over the length. According to Embabi and Moawad (2014), the highest point level approaches 56 m above sea level which is in the El-Qals dune, while the average level is in the range of 10-15 m. There are several features presented on the barriers stretch such as active coastal sand dunes, sabkhas, coastal micro-lagoon/barriers, micro-tidal deltas, micro-fans and submerged lee dunes and their presence depends on the sediment transport from the nearshore waves.

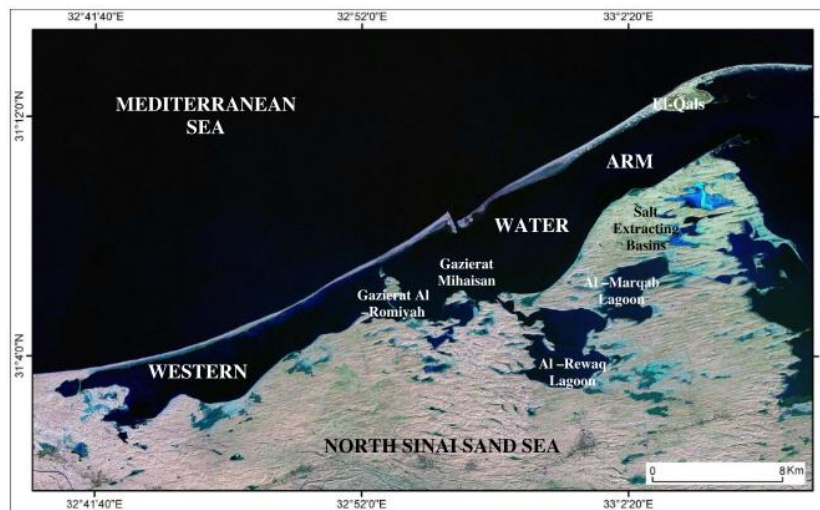


Figure 2-5: Western water arm related to western inlet in Lake Bardawil (Embabi & Moawad, 2014; "Lake Bardawil," 2015)

- Sediment properties in the area:

Near the surf zone, the sediment gets into suspension by waves and tides and are transferred towards the lake by the tidal inflow. Sediment sources are also found to be from the Nile Delta and from aeolian transport and are mostly transported in the eastward direction (Emanuelsson & Mirchi, 2007; Embabi & Moawad, 2014; Nassar et al., 2018). According to Khalil and Shaltout (2006), the lagoon is mostly clayey sand, with sand in the borders of the lagoon area and with silty clay in the deepest parts. The sediment properties within the lagoon have been studied by Frahat (2006) during 2004 and no up to date sediment properties are reported. Most of the lagoon area consists mainly sand sediment (72%), whilst lower fractions of mud and gravel exist in the area, see Figure 2-6.

Within the inlets, mostly two sediment properties are presented. The first one, which consists the highest fraction of sediment (98.1%), is sand, whereas a percentage of 1.9% of gravel was also found at the Boughaz 2 inlet though. Mud fractions were not presented within the inlets (Khalil & Shaltout, 2006).

Studies had showed that in the accreted area, at the west side of Boughaz 1 inlet the sediment is coarser than in the east area due to the presence of the extended breakwaters. At the east side of the inlet erosive features are observed (Emanuelsson & Mirchi, 2007). The average mean grain size is found to be 250 μm and 200 μm in west and east side of the Boughaz 1 inlet respectively. The maximum grain size at the west side of Boughaz 1 inlet is 330 μm while the lowest is found to be 180 μm . In the east side of the inlet a grain size ranges from 160 to 280 μm were found as well (Piere, 2016).

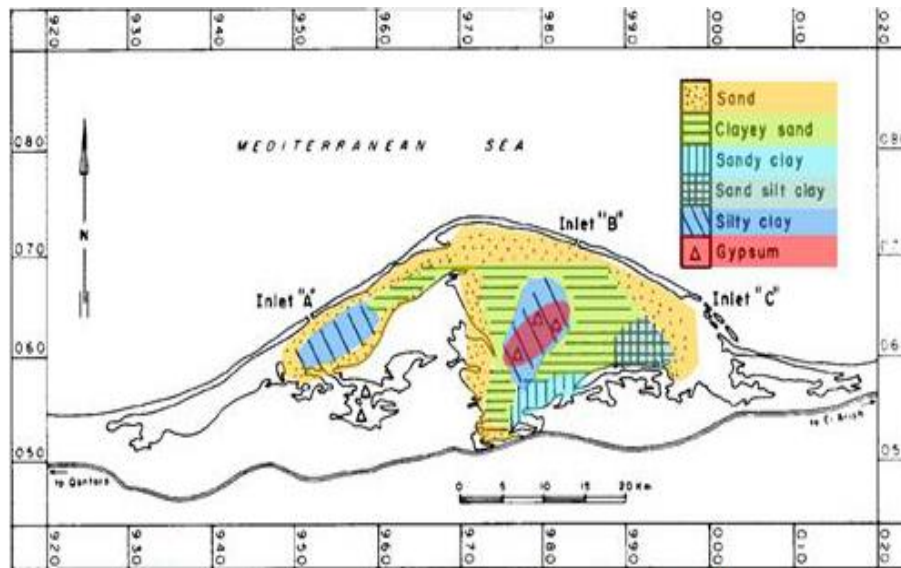


Figure 2-6: Types of sediment fractions within the lagoon (Piere, 2016).

- Longshore transport processes and inlet morphology:

Waves and the availability of movable sediment particles are important factors for the sediment transport processes. The longshore transport processes describe the movement of erodible sediment particles along the coast in longshore direction due to the action of oblique to shore waves (Bosboom & Stive, 2015; Mangor, 2018). The net longshore transport is determined as the sum of the opposite directed drift components presented along the shore whilst the bulk or total longshore transport is determined with the sum of their magnitudes (Bosboom & Stive, 2015; Linnarsund & Mårtensson, 2008).

Several studies have been performed to examine the longshore transport processes along the coast of Lake Bardawil. As described in section 2.1.1, the Port Said Subcell and Bardawil Subcell show the erosion and accretion patterns along the coast with the presence of the hard structures. The net longshore transport is eastbound directed and accurate sediment magnitude values have not yet been determined, since there is a high lack of data from the area (Linnarsund & Mårtensson, 2008).

According to studies which performed during 1970, thus before the construction of the breakwaters, the net east longshore transport rate at the Boughaz 1 inlet was found to be between 200,000 – 300,000 m³year⁻¹ and two time less than the net transport rate in the Boughaz 2 inlet. This is explained with the convex shape and direction of each inlet, but the opposite has been showed from studies done during 1983, 1991 and 2007 where 450,000 m³year⁻¹, 500,000 m³year⁻¹ and 40,000 m³year⁻¹ of net transport rate have been reported (Emanuelsson & Mirchi, 2007; Khalil & Shaltout, 2006; Linnarsund & Mårtensson, 2008). The gross longshore transport rates have been reported as well and can be seen in Table 2-1. The estimation of the longshore transport processes estimated with the C.E.R.C formula and aerial photography (Linnarsund & Mårtensson, 2008).

The strong effect of the existence of the hard structures in the Boughaz 1 inlet area is observed with the study done by Emanuelsson and Mirchi (2007), who measured the net eastward longshore sediment transport rate equal to 40 000 m³year⁻¹. The sediment transport values according to this research can be seen in Figure 2-7.

Furthermore, Klein (1986) introduced the entrapment volume in the inlets before the construction of the breakwaters according to two studies. Both gave reasonable estimations with an average value equal to 250 000 m³ year⁻¹ which indicates that large sediment volumes entrapped within the Boughaz

1 inlet. These values are important characteristics for the determination of the natural sediment bypass and the shoal formations and inlet morphology (Mangor, 2018).

Study	Direction	West inlet (m ³ /yr)	East inlet (m ³ /yr)
Inman, 1970	Net E	300 000	500 000
Vinja, 1970	Towards E	340 000	600 000
	Towards W	140 000	100 000
	Net E	200 000	500 000
	Gross	480 000	700 000
Suez Canal Authority, 1983	Towards E	576 000	360 500
	Towards W	149 500	54 500
	Net E	426 500	306 000
	Gross	725 500	415 000
Emanuelsson, et al., 2007	Net E	40 000	258 000

Table 2-1: Longshore transport processes along Lake Bardawil (Linersund & Mårtensson, 2008).

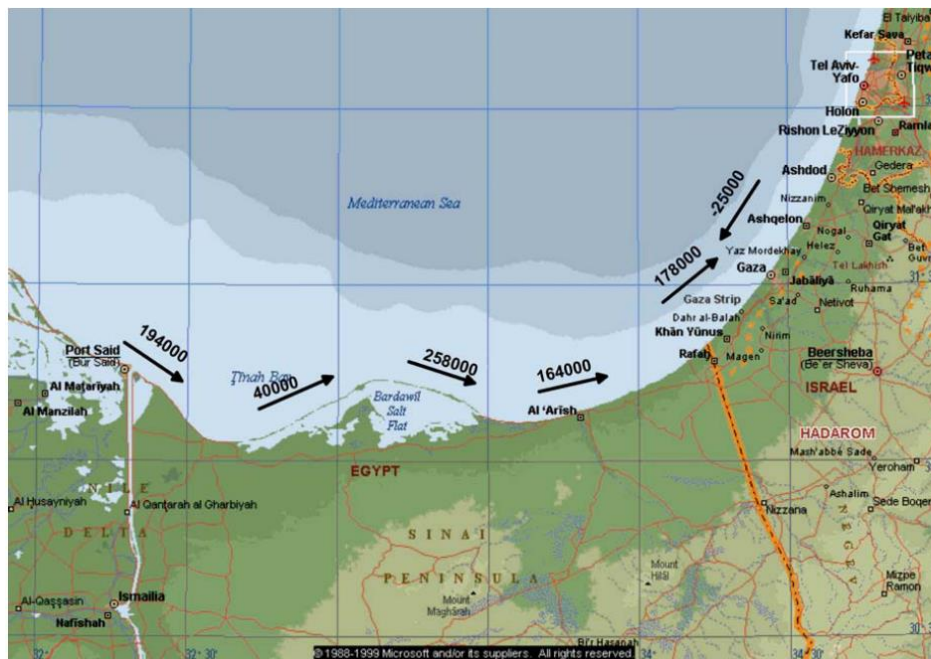


Figure 2-7: Volume and direction of net transport rates [m³/year] along the Sinai northern coast Emanuelsson and Mirchi (2007)

The morphological changes of the Boughaz 1 inlet are given in Figure 2-8. The shoreline retreat at the east side of the inlet is more evident after the construction of the breakwaters, while before the final constructions of the breakwaters the sedimentation within the inlet entrance is obvious. The removal of such structures, is crucial for the natural functionality of the system.

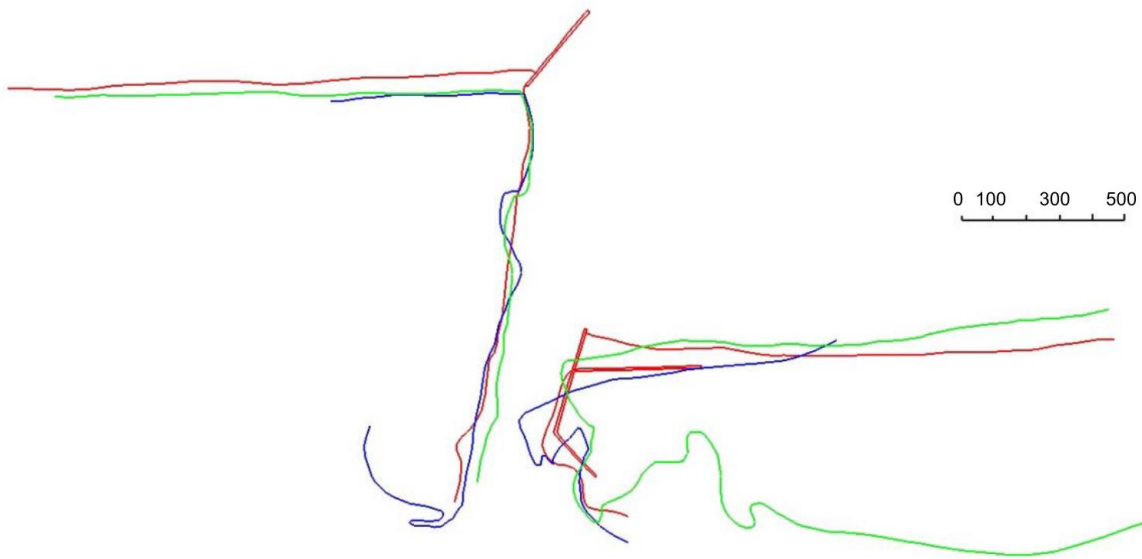


Figure 2-8: Morphological evolution of the Boughaz 1 inlet during 1991-1999. Green line:1991, blue line:1994 and red line: 1999 (Linersund & Mårtensson, 2008).

2.2 Stabilization of inlet systems and sediment bypassing

2.2.1 Stability models

The stability of coastal inlets can be determined according to two criteria. The first, which is proposed by Escoffier(1940), prescribes the dynamic equilibrium state of the cross-sectional area of the inlet with respect to hydrodynamics and sediment dynamics (Gao & Collins, 1994). The second criterion is based on the stability of the inlet according to Per Bruun and Gerritsen (1960) and Bruun (1978) (De Vriend et al., 2002). They introduce the stability with respect to sediment bypassing along the coast.

Stability in terms of Escoffier's model can be assessed according to the maximum velocity during the tidal cycle (u_e) in relation to the constant equilibrium maximum velocity (u_{eq}), see Figure 2-9, (Bosboom & Stive, 2015). The maximum flow velocity through the inlet throat was defined proportional to the tidal prism (P) and to the cross-sectional area (A_e) and tidal period (T) as follows.

$$\widehat{u}_e = \frac{\pi \cdot P}{A_e \cdot T}$$

As a first estimation, the equilibrium velocity according to Escoffier(1940) assumed to be constant and equal to 0.9 m/s and depends on the sediment properties only (Bosboom & Stive, 2015). Consequently, the dimensions of the inlet are of great importance for the stability of the system. The cross-sectional area should be such that the tidal prism can increase, and the flow velocity is larger than the critical to create erosive features through the inlet gorge until stable conditions can be reached (Point C in Figure 2-9).

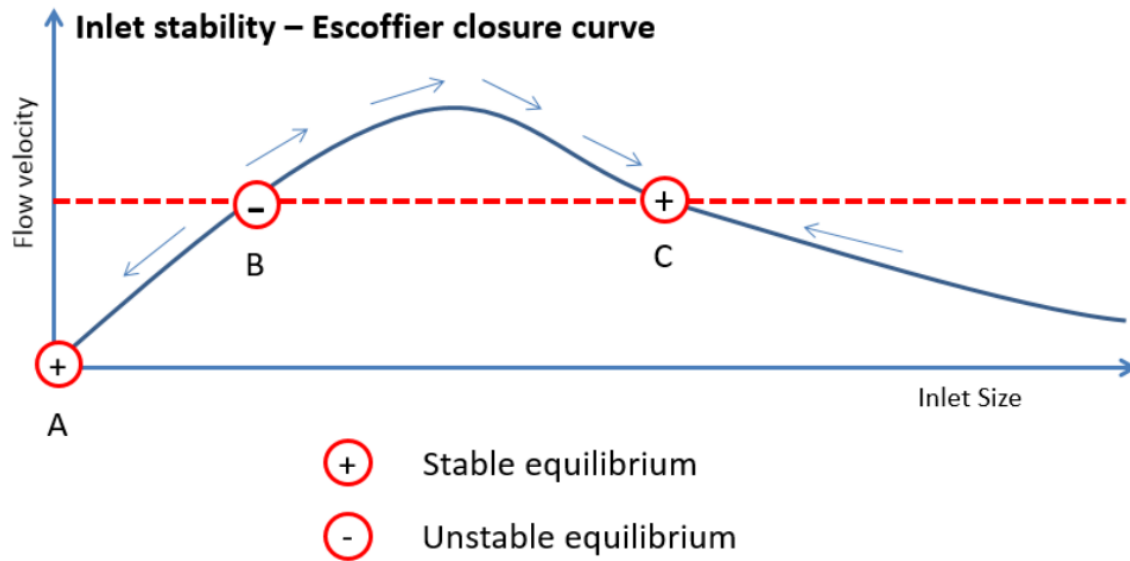


Figure 2-9: Escoffier's closure curve Lanfers (2016).

Furthermore, sediment transport plays crucial role to determine stability on the inlets and ebb delta. Study that has been done by Bruun and Gerritsen (1959), defined the stability of the inlet and ebb tidal delta with the stability factor, r factor, by calculating the mean value of longshore transport and the maximum discharge through the inlet. Lately Per Bruun and Gerritsen (1960) and Bruun (1978) defined stability and the type of natural bypassing in relation to the tidal prism and littoral drift (P. Bruun, J. Mehta, & G. Johnsson, 1978; De Vriend et al., 2002). They determine that with the stability factor as follows:

$$r = \frac{P}{Mt_{tot}}$$

In which:

- P [m³]: Tidal prism
- Mt_{tot} [m³/year]: Total littoral drift

The littoral drift passes through and along the inlet over time. The sediment on the outer delta is picked up by the wave-driven currents and/or the longshore currents and subsequently is transported to the downdrift/updrift islands depending on tidal action and wave direction. It is shown that during ebb conditions part or all of the sediment that is transported through flood conditions settles to the ebb channel and returns to the ebb tidal delta (Bosboom & Stive, 2015). This introduce the complexity of this feature. The r factor is applicable to inlets with limited freshwater discharge which this is the case for Lake Bardawil and is widely used and accepted (De Vriend et al., 2002; Gao & Collins, 1994).

There are four different stages which describe the stability of the tidal inlet system with respect to the r factor and accordingly four conditions related to the bypassing mode defined by P. Bruun et al. (1978) (van de Kreeke & Brouwer, 2017), see Table 2-2. For large r values the inlet channel is stable with litter bar and good flushing, for intermediate values between 50-150, well developed ebb shoal and clear main channel is presented whilst for the lowest r values the system becomes unstable (Bosboom & Stive, 2015; De Vriend et al., 2002). Referring to the latter, with low r values, there is a high variability of the location and area of the channel and a possibility of the existence of more channels which indicated that dredging and breakwaters required for maintaining the navigable depths. Furthermore,

deposition of sediment may lead to inlet closure during episodic events and no navigability is possible (P. Bruun et al., 1978; Tran, 2011). The last column of Table 2-2 illustrates the dominant processes defined based on several studies. Very large values of r , are mostly related to the tidal flow bypassing which is found in tide dominated coasts, whilst the wave dominated conditions are found with bar bypassers and small r values (Bosboom & Stive, 2015; van de Kreeke & Brouwer, 2017). P. Bruun et al. (1978) defined the bypassing mechanisms mainly to bar bypassing and tidal bypassing, however, during the passing years several other bypassing modes have been observed (van de Kreeke & Brouwer, 2017). These can be found throughout the study of Duncan M FitzGerald et al. (2000).

$r = P / M_{tot}$	Stability based on Bruun (1978)	$r = P / M_{tot}$	Bypassing mode related to channel stability	Dominant processes
$r > 150$	Good	$r \gg 150$	Episodic and tidal bypass	Tide
$100 < r < 150$	Fair	$50 < r < 150$	Bar bypass/Tidal bypass	Mixed energy (tide or wave dominance)
$50 < r < 100$	Fair to poor			
$r < 50$	Poor	$20 < r < 50$	Typical bar bypassing	Wave
		$r < 20$	Bar bypass	

Table 2-2: Stability and bypassing mode of a tidal inlet system related to the r factor (Bosboom & Stive, 2015; P. Bruun et al., 1978; De Vriend et al., 2002).

For mixed energy coasts Duncan M FitzGerald et al. (2000) proposed three models which describe the different types of sediment by-passing along natural inlets, see Figure 2-10 (De Vriend et al., 2002; Duncan M. FitzGerald, 2011; Duncan M FitzGerald et al., 2000). The first model describes inlet migration and spit breaching, the second describes the stable inlet processes and the third is about the ebb-tidal delta breaching. More detail information about these models can be seen in De Vriend et al. (2002), Duncan M FitzGerald et al. (2000) and Duncan M. FitzGerald (2011).

The type of sediment bypassing that was found according to study that has been carried out by FitzGerald et al (1978) in a mixed energy non-structured tidal inlet in South Carolina, is based on the migration of tidal channels and/or sand bars. This inlet is facing 1.5 m average tidal range and 0.6 m mean wave height. For non-migrating inlets, in mixed energy coast, the 2 and 3 models provided in Figure 2-10 were found to be representative for r ranging values between 50 – 150 (Duncan M. FitzGerald, 2011). Other study showed that in a tidal inlet named Wichter Ee which is located in the East Frisian Wadden Sea, the r factor is found approximately equal to 60 and its morphological response at a certain moment was found as the model 3 in figure below. The tidal prism in that inlet equal to about $42 \cdot 10^6 \text{ m}^3$ and the littoral drift is found to be lower than 1 million cubic meters per year (Bosboom & Stive, 2015). Examples provided from van de Kreeke and Brouwer (2017) show that spit formation is observed with poor stability and a very small r factor ($12 \leq r = P/M \leq 17$). However, all these processes and the shoal size to the adjacent coasts depends on inlet size, ebb tidal delta morphology, sediment transport rate in the inlet, and the type of by-passing system, and are difficult to precisely determined by comparing only the P/M values (stability) with the bypassing mode without any observations (Duncan M FitzGerald et al., 2000). This is also validated with the Price inlet. Even if the P/M ratio for this inlet is calculated equal to 80, its stability its defined as good with a tidal flow bypassing due to its sediment properties, see van de Kreeke and Brouwer (2017). Nevertheless, several years might be needed to obtain these processes and to well determine the by-passing mode of the system (Duncan M FitzGerald et al., 2000).

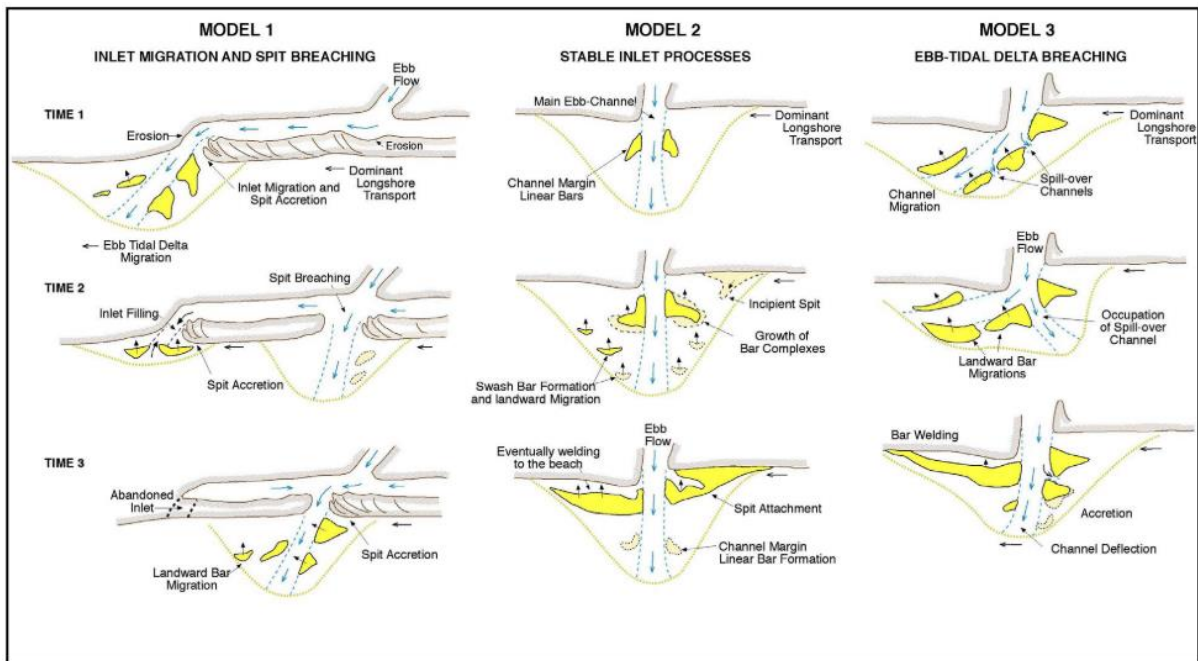


Figure 2-10: Models of inlet sediment by-passing Duncan M FitzGerald, Kraus, and Hands (2000).

Generally, all these sediment by-passing models can be presented in the inlet system either simultaneously either alternating (De Vriend et al., 2002). Even if, not (yet) universal background is derived to precisely provide the bypassing mode of the inlet system, as well as the relation to that with the P/M ratio, the field observations from these studies showed to be attractive for a general conclusion. Usually, similar morphological changes are expected to be observed when the coastal classification is the same (Duncan M. FitzGerald, 2011). Lake Bardawil is characterized with mixed energy climate which indicates that model 2 and 3 are most probable to be seen. Although, the morphological response of the ebb tidal delta of Boughaz 1 inlet is either not well observed with Google Earth images, see section 2.1.1, nor with available sources the model 2 and 3 might determine the bypassing mode of the system, while assuming that the inlet channel is not migrating and excluding the presence of breakwaters.

It can be concluded that the stability of the inlets depends directly to the interaction between waves, tide and sediment supply along the coast and the geometry of the tidal inlet system. Morphological variations exist over the time due to cycling variation of these processes and result in change of the position of the inlet channel as well as the possible growth and landward migration of shoals in the ebb-tidal delta system (Garel, Sousa, Ferreira, & Morales, 2014).

Several maintenance works have been made to keep the inlet systems open and stable mainly for navigation purposes (Garel et al., 2014). To provide a sufficient water depth in the inlets usually hard structures, such as breakwaters, are constructed to stabilize the inlet and maintenance dredging works are done to prevent sedimentation through the inlet gorge. However, tidal inlets need also to be stable for prevention of shoreline erosion and for aquaculture purposes as well (Bertin, Chaumillon, Sottolichio, & Pedreros, 2005). Although the reasons for the protection of the inlet systems are for high importance, the interruption of the prevailing conditions due to human interventions can lead to inverse conditions than expected. On the other hand, new coastal management methods such as the 'Sand Engine' pilot project, can provide efficient results for decades of years and allow the coast to grow naturally. Although, this design strategy has not yet been implemented near an inlet system and is still under investigation for the shoreline protection, the results until now show that the Sand Engine

can reinforce the coast to a large extent and for more years than the expected for the hydrodynamic conditions presented in the Dutch coast (de Schipper et al., 2014). According to that, the design strategies followed to understand the design requirements of this mega nourishment should be known such that the new innovative design investigation can be created for the functionality of Boughaz 1 inlet and the growth of the ecosystem. More detail information of this pilot project is given in Appendix A.

2.2.2 Stability studies of Boughaz 1 inlet

According to several studies, the construction of breakwaters in the tidal inlets, as this is the case for Boughaz 1, result in shoreline erosion where longshore sediment transport is disrupted. The stabilization of the inlet systems with the implementation of the breakwaters may lead to changes of the prevailing conditions near the coast. This disturbs the natural function of the system and worsen the conditions.

It is shown that the current situation in Boughaz 1 inlet (with the presence of breakwaters), is not able to prevent sedimentation inside the inlet gorge in the coming years without any maintenance works (Nassar et al., 2018). This implies, that the investigation of different and ecologically sustainable way for the limitation of sediment infilling is attractive.

The stability of the inlet cross sectional area without the presence of breakwaters was examined according to Escoffier's model. Bosman and Lanter (2018), modelled two different design conditions, considering the width and the depth of Boughaz 1 inlet, to estimate the maximum averaged flow velocity through the inlet channel and thus to predict the possibilities of achieving stable system. The width and depth of the channel in the first condition was 300 m and 7.5 m, respectively, whilst for the second a width of 200 m and a depth of 10 m were considered. The results showed that a deeper and narrower channel give more efficient results for achieving equilibrium conditions and the tidal prism in Boughaz 1 inlet can increase with about 48%. The maximum velocity in the channel for this case was found equal to 0.9 m/s. This can be considered as a reasonable value based on the suggestion that Escoffier assumes a good approximation for u_{eq} equal to 0.9 m/s (Bosboom & Stive, 2015). This implies that the point C in Figure 2-9 might be achieved. However, these values were determined with the presence of tidal currents only and the exclusion of wave impact and sediment properties. Furthermore, due to lack of data some inaccuracies are still presented with the model results. Thus, a better approach should be done, and more conditions should be considered to determine the maximum velocity and thus the possibility of attaining stable conditions.

Nassar et al. (2018) examined how the erosion process along the east side of the inlet can be avoided with six different scenarios. These scenarios were simulated for a 20-year period, from 2010 to 2030, with a combination of both hard and soft structures. The first scenario was related to the construction of eight long groins along the east coast which showed that high erosion levels between the intervals of the groins were expected. The second scenario was the construction of nine detached breakwaters which resulted in salient form behind the structure and with high erosion rates through the gaps between the breakwaters where high energetic conditions are presented. The third scenario was a combination of both constructions which did not show better results than the previous ones. Following that, Nassar et al. (2018) also examined the shoreline changes with the implementation of a sediment bypass system. This scenario resulted in reduction of accretion and erosion levels at the west and east side of the Boughaz 1 inlet respectively. Lastly, the inspection of the shoreline changes due to the presence of eight short groins with one-time nourishment (Scenario 5a -Figure 2-11) and with the inclusion of 100,000 m³ nourishment per year (Scenario 5b - Figure 2-11) were examined. The one-time nourishment was positioned evenly between the eight short groins as can be seen in

Figure 2-11 whilst the yearly nourishment of 100,000 m³ was implemented at the east side of the inlet to an extension of 1,400 m. These last two scenarios showed efficient results with respect to the reduction of shoreline erosion. The first scenario gave a reduction of erosion of 91.85 % whilst the second 71.47%. Even if the construction costs are higher for the Scenario 5a, it is conducted that, based on the methodology that was followed, this scenario is the most efficient one. For further indications to this research, reference is made to (Nassar et al., 2018).

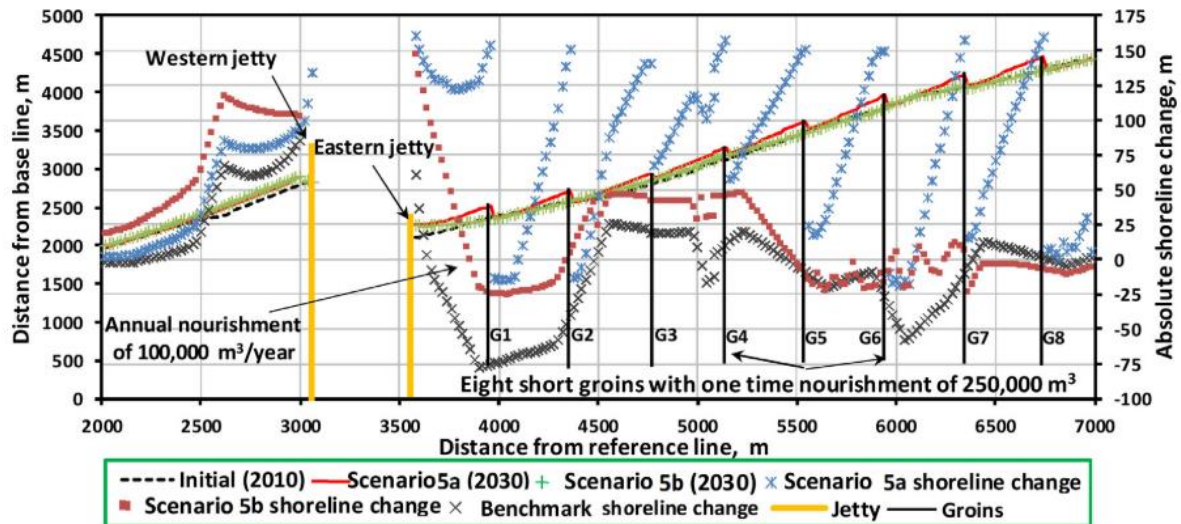


Figure 2-11: Shoreline evolution with two different maintenance works. Scenario 5a: Eight short groins with the inclusion of one-time nourishment. Scenario 5b: Implementation of yearly 100,000 m³ of nourishment at the east side of the inlet entrance (Nassar et al., 2018).

According to these design studies and considering the problems that Boughaz 1 inlet faces, a sustainable design should be found to endeavour inlet stabilization, thus better functionality. For that reason, in this research project the response of the different elements should be analysed such as to gain more inside how and if possible, to mimic nature.

2.2.3 Previous related study

Lanters (2016), related the hydrodynamics with the fish population in Lake Bardawil since the fish supplies in the lake have been reduced dramatically due to a combination of declining fish population with declining water quality and as a response, increasing fishing effort to juvenile fish. According to his research and the Institute for Marine Resources and Ecosystem Studies (IMARES), the fish population in lake Bardawil is expected to increase when the tidal prism is increased. Furthermore, the increase of the inlet depth equal to 10 m and the decrease of salinity levels are also correlated to the increase of fish supplies from the Mediterranean Sea. Another aspect to that was the examination of the wind influence. The wind affects the hydrodynamics and the circulation motion within the lake (Lanters, 2016). In this thesis project, the hydrodynamic response of the system was examined under different design conditions with the exclusion of wind to understand the influence of the tidal currents, wave effect and sediment properties. The model constructed from that study is used and modified for the adapted design methodology. For implications on this study, reference is made to the research done by Lanters (2016).

Lanters (2016), examined four different design phases and their influence on the hydrodynamic conditions. The first indicated the examination of the initial state of the system and the inclusion of a new inlet in the western part of Lake Bardawil. The second phase was related to the dredging of a gully which connects all the inlets while the third phase was contained yearly dredging of new gullies within the basin. In the last phase, a new innovative design was made. A Sand Engine was designed at the Boughaz 1 and the new western inlet. In all phases, the tidal prism, flow velocities in certain locations were examined. It has been showed that the tidal prism can increase to about 400% and the system can export sediment due to the difference in sediment size between the Mediterranean Sea and the lake.

The tidal range outside of Lake Bardawil was found to be different than the water level fluctuations within the lagoon. The spring tidal range at the offshore was found to be approximately equal to 0.4 m while within the basin in a certain location the tidal range was found to be below 0.10 m, see Figure 2-12. The flow velocities at this phase, which indicates the current state of the system, are different between the west inlet and east inlet. The flow velocities were found to be 0.7 m/s during ebb and flood at the west inlet and 0.9 and 1 m/s during ebb and flood at the east respectively. Furthermore, it was concluded that in the current state the system is importing sediment since the maximum flood velocities are larger than the maximum ebb velocities(Lanters, 2016).

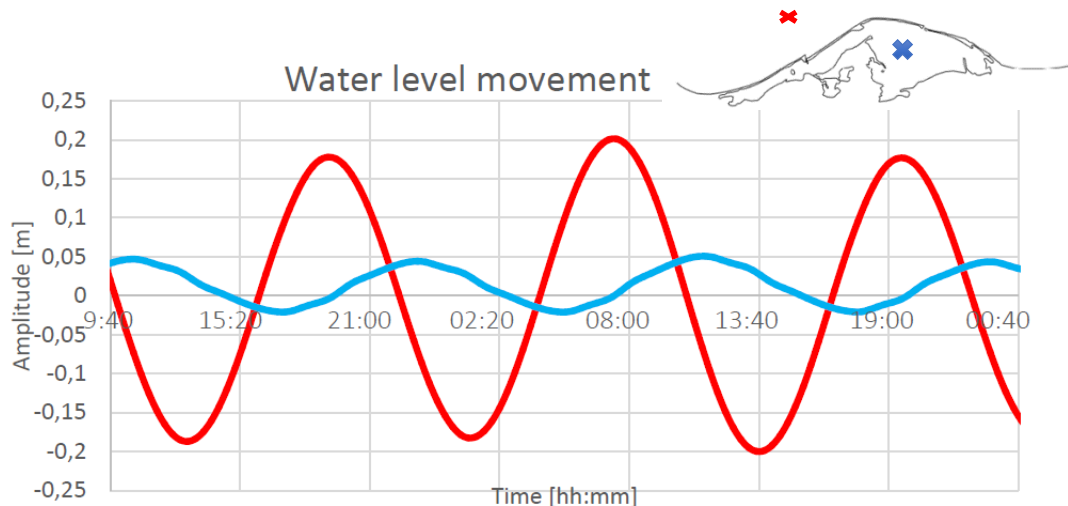


Figure 2-12: Water level variations outside and inside of the Lake Bardawil. Red line: Outside, blue line: Inside.(Lanters, 2016)

According to the design phases described above, it was conducted that the basin geometry plays crucial role for the changes of water level movement and flow conditions within the basin. The first phase which does not related to any change of the basin geometry did show an increase of the tidal prism, however the distortion of the flow conditions was still presented while in the last phases the reduction of the friction and resistance led to the increase of the water levels and the flow velocities in the area. This is clearly indicated in Figure 2-12.

The hydrodynamic response of the aforementioned phases was also examined under the influence of four different wind conditions. As indicated in section 2.1.2, the wind act surface forces in the water which affects the circulation motion within the lagoon. The influence of the wind in the initial state of the system affects the circulation within the lake which subsequently affects the ecosystem and the hydrodynamics (Lanters, 2016). With the presence of the wind forces, there is a net water export from the east inlet during the simulation period as depicted in the Figure 2-13. Furthermore, it was calculated that the tidal prism increases with the influence of the south-west (SW), west (W) and

north-northeast (NNE) winds to about 4.5% while a reduction of 3.3% was found with the west-northwest winds (WNW).



Figure 2-13: Water exchange between Mediterranean Sea and Lake Bardawil(Lanters, 2016).

3 | Methods

Herein, focus is made on the methodology that is followed throughout this thesis. A start is made with the explanation of the design methodology. A description is given for the main design elements which can mimic nature and are used to define the innovative tidal inlet design. The design parameters of each design element are depicted, and their values are provided considering specific criteria and requirements. This part concludes with the followed procedure. Followed that, the modelling methodology is described. The numerical models that are used are provided while the modelling approach is given with the associated data.

3.1 Design methodology

The objective of the design methodology is to find an initial design concept, the innovative tidal inlet design, that meets the functional requirements of the Boughaz 1 inlet system. This initial design concept, referred for clarity as a final combined design choice, determines the design of the initial phase of a general design process and it cannot be considered as the final detailed design.

In a design process, the functional and structural requirements are defined. The functional requirements of Boughaz 1 inlet that must be fulfilled are the increase of the water exchange, associated to the increase of the tidal prism and flow velocities and the need to limit sedimentation. These will lead to a healthier and functional tidal inlet system. The main structural requirement for this system is to guarantee its dynamic stability such as the aim to mimic nature and to minimize the maintenance dredging works to be valid. These requirements are important for determining and sizing the most important design elements of such as system.

The inlet is subject to a reduced tidal prism over the passing years, resulting in poor water quality in the lagoon, limited fish migration from the sea and sedimentation causes the need for dredging maintenance works. Although, the dredging maintenance works and constructed breakwaters can minimize the abrupt sedimentation through the inlet and provide more stable conditions in the short term, the natural behaviour of the system is gradually changing which might worsen these conditions in the longer term. For that reason, to determine the most suited design methodology we firstly need to define the elements that influence the functionality of the Boughaz 1 inlet and can mimic nature. Once we define those design elements, then we can assess their impact on the system and thus identify a final combined design, which aim to achieve the objective of the design methodology.

Each design element is influenced by several design parameters and thus range of values can be assigned to each parameter. However, in this thesis this range is narrowed by several criteria and design requirements. These are related to the stability criterion provided by Escoffier (1940), the Depth of Closure concept (DoC) given by Hallermier, the design limitations/requirements that are

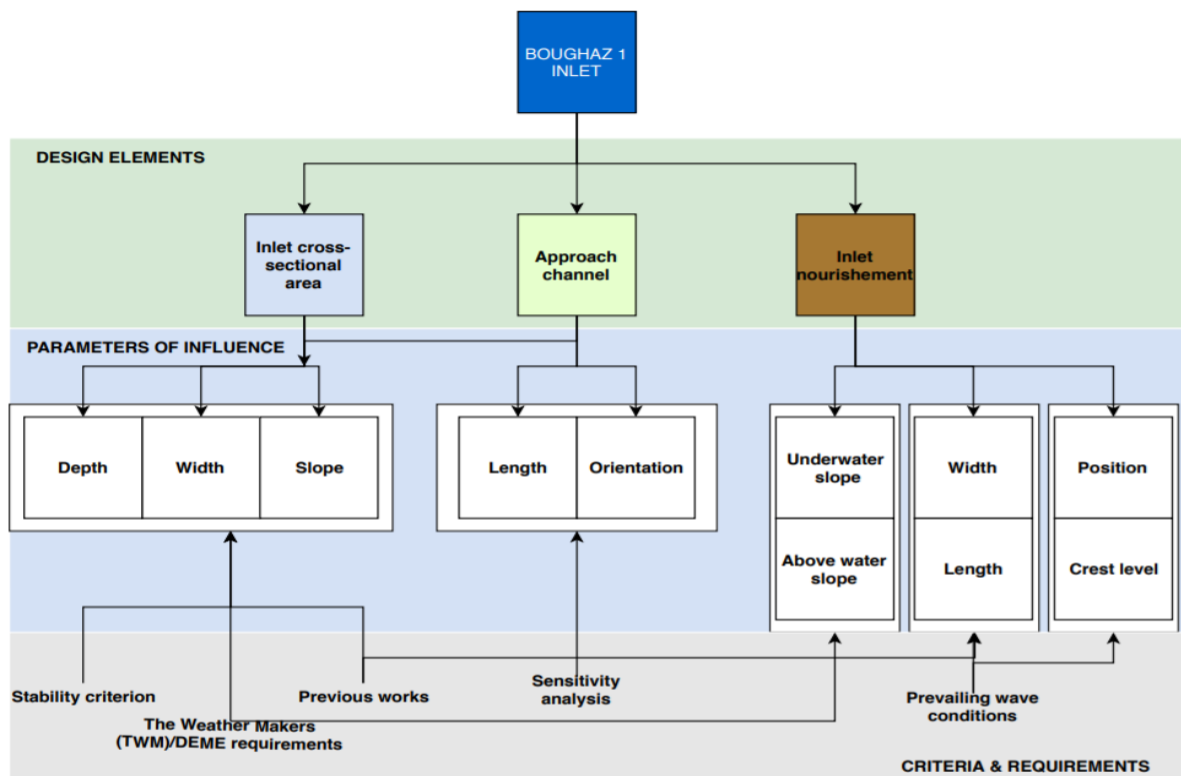


Figure 3-1: Concept of the design methodology.

given by The Weather Makers (TWM)/ DEME, from previous works and the prevailing conditions in the area while a sensitivity analysis is carried out to parameters that are not determined quantitatively before. The followed concept of the design methodology is discussed in detail in the following sections while an overview can be seen in the following chart.

3.1.1 Design elements

The aim of this study is to improve the functionality of the Boughaz 1 inlet while mimicking nature. By trying to mimic nature means that we allow the system functions naturally without the presence of any hard structures. This means that as a first step, the removal of the breakwaters should be considered for the design methodology. The presence of these hard structures leads to the blockage of the current flows through the inlet. The longshore sediment transport is disrupted in the updrift side of the structure, in the west side of the inlet entrance, and subsequently shoreline erosion downstream is observed which enhance the inlet instability.

The ability to mimic nature such as to improve the water quality, the enhancement of fish migration and the ecosystem, requires sufficient water exchange between the tidal system (van de Kreeke & Brouwer, 2017). This implies that a large tidal prism is required for the improvement of the functionality of the Boughaz 1 inlet. The tidal prism is the volume of water that enters and leaves the inlet during a tidal cycle (Bosboom & Stive, 2015). The tidal prism is directly related to the inlet cross-sectional area which indicates that the dimensioning of this element plays crucial role for the magnitude of the tidal prism, the flow velocities and subsequently the improvement of the functionality of the tidal inlet system. Based on that, the inlet cross-sectional area can be considered as the main design element for the tidal inlet system since can significantly alter its equilibrium conditions. On the other hand, though, can be considered as the bottleneck for the hydrodynamic response of the tidal inlet system if hardly any attention is given to its proper design.

Another important design element is found to be an approach channel. The so-called approach channel in that case differs from the standard access channel for ports. It should be noted that the design of such access channels are primarily based on navigational requirements whilst the approach channel in the Bardawil case is mainly designed for fish migration (Bosman & Lanter, 2018). This design element can concentrate the tidal and wave energy to enhance the tidal prism and the flow velocities through the system. This is an important indication for the water exchange between the lagoon and the Mediterranean Sea. The increase of the tidal flows to a larger extend can redirect the fish population within the lake. Since the need to mimic nature is of high importance, the so-called approach channel can also consider as one of the main design elements.

Last but not least, Bosman and Lanter (2018) examined the response of the implementation of a soft engineering measure, called inlet nourishment. This measure is intended to increase the water set up through the inlet, increase the tidal prism and reinforce the coast. The inlet nourishment is a submerged sand shoal near the inlet entrance in combination with a beach nourishment, see Figure 3-2. Such a design can lead to a potential increase of the residual flows at the west and east side of the inlet due to the reshaping of the barriers as well as concentrate the tidal flow. The residual tidal eddies are important for the sediment transport processes and the water exchange of the system (Bosboom & Stive, 2015; Yang & Wang, 2013). On the other hand, wave energetic conditions are important for the redistribution of the sediment along the coast (Luijendijk et al., 2017). According to that, the inclusion of such an innovative engineering measure can be multifunctional and thus should be clearly understood.

Since, the cross-sectional area, the so-called approach channel and the inlet nourishment can beneficially improve the functionality of the Boughaz 1 inlet and can mimic nature, their assessment

is important to be understood. Thus, before proceeding to the final combined design, certain design adaptations for each design element are followed to understand their effect to the system response. Each design element though is also determined by several parameters and requirements which need to be identified first.

3.1.2 Design parameters and requirements

Each design element comprised by several design parameters, see Table 3-1 and Figure 3-2. In general, each parameter can take a wide range of values. In this thesis, the values of each parameter are defined by several criteria and requirements such as narrower range of values need to be examined.

The parameters that define the design of the inlet cross sectional element are its total length, width, its main depth and slope. The approach channel element follows the same cross-sectional dimensions of the inlet cross sectional area while its total length and orientation are further examined. The design parameters of the inlet nourishment design element are its position, total length in longitudinal direction, its beach nourishment and its total width in the cross-shore direction, the submerged crest level and its above and underwater slope.

Table 3-1: Design parameters of the associated design elements.

Design parameter	Design element		
	Cross sectional area	Approach channel	Inlet nourishment
L_{cs}	Total length	-	-
W_{cs}	Total width	-	-
D_{cs}	Main depth		-
L_{ac}	-	Total length	-
a_{ac}	-	Orientation	-
D_s	-	-	Position from inlet entrance
L_s	-	-	Total length
W_n	-	-	Width of beach nourishment
W_t	-	-	Total width
C_s	-	-	Crest level from MSL
i_b	-	-	Above water slope
i	Underwater Slope		

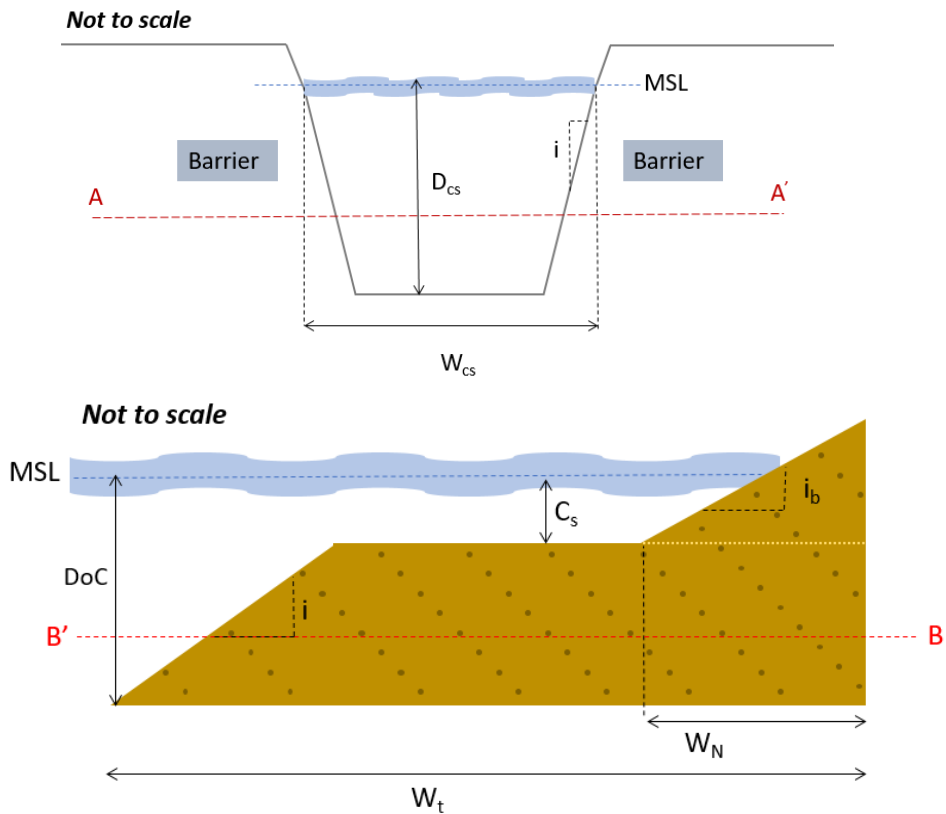
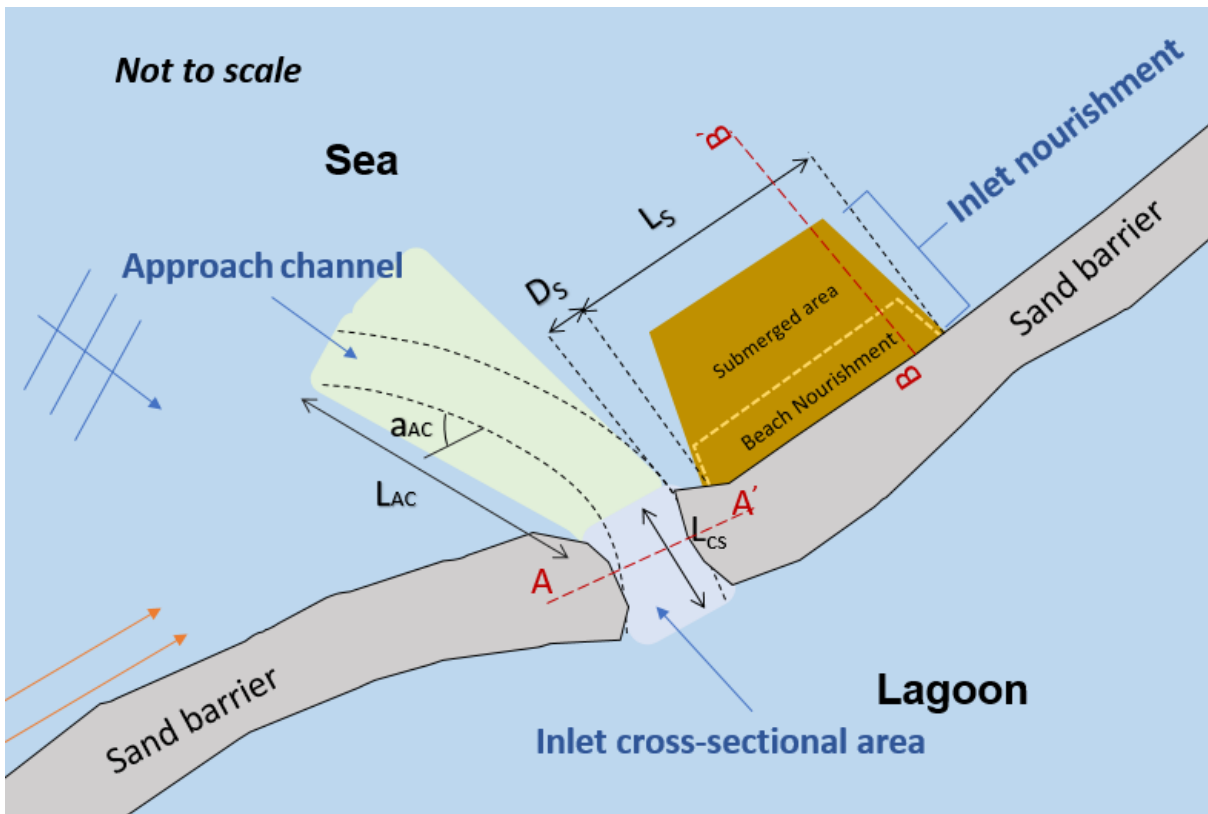


Figure 3-2: Overview of the design parameters of each design element. At the top, the top view graph is presented. The cross sections given in the top view graph are illustrated with further detail at the bottom of the figure.

The values of each parameter are determined based on the following concepts, criteria and requirements:

- **Stability criterion by Escoffier (1940):**

Escoffier (1940), related the equilibrium flow velocity in relation to the size of the inlet cross-sectional area as described in section 2.2.1. The increase of the inlet cross-sectional area can lead to a potential increase of the tidal prism and the flow velocities resulting in a stable inlet. Since this is an important criterion and its highly related to the functionality of the Boughaz 1 inlet its concept is considered. The size of the inlet cross-sectional area should be large enough such as the flow velocities within the inlet are able to choke off the material and can increase the tidal prism of the system. Thus, the initial size of the inlet cross sectional area of Boughaz 1 inlet is increased by taking into account this criterion.

- **Previous works/ Sensitivity analysis/ Prevailing wave conditions:**

Certain design adaptations of the inlet cross sectional area of Boughaz 1 inlet are examined by Bosman and Lanfers (2018). In total two different combinations are examined with an average size of the inlet cross sectional area equal to 2500 m² with a constant shape and varying width and depth. This size is considered as an initial value for assessing the response of the inlet with higher and lower values than that. This size is already larger than the initial state of Boughaz 1 inlet. The total length of this element is kept constant and equal to about 800 m for all the designs. Its total maximum width was varying to determine different design sizes while its minimum values is based on the design requirements provided by TWM as illustrated below. Furthermore, the shape, which is determined with its width and main depth, is further examined with a sensitivity analysis of three different design shapes. This is done since it is reported that also asymmetric shapes can lead to a potential increase of the ebb flows which is important for the exporting of sediment from the lagoon.

Lanfers (2016) in collaboration with the IMARES institute indicated that an inlet with a 10 m depth can increase of the fish supplies from the Mediterranean Sea towards the lagoon. Given that there is a substantial reduction of the fish migration to the lagoon and this extremely affects the living conditions of thousands of families in the area and thus the functionality of the inlet system, it is of vital importance to take this condition into account. Consequently, the 10 m depth is considered the maximum allowable main depth for the inlet cross-sectional area and approach channel design elements.

Moreover, Bosman and Lanfers (2018) indicated the length of the approach channel equal to 2400 m. This value is considered while a smaller length equal to 1200 m is also examined. The orientation of the approach channel is defined with sensitivity analysis based on four different design orientations. The first design adaptation with this parameter, is defined parallel to the inlet entrance, the second which is extended far offshore is considered perpendicular with the west barrier whilst the third adaptation is designed parallel with the west barrier. Lastly, a design orientation of the approach channel had an angle of 45 degrees with respect to the west barrier. The orientation of the design conditions is an important factor for the indication of the current flows approaching the inlet entrance.

The design of the Sand Engine pilot project in the Dutch coast was based on the climatic and hydrodynamic conditions presented in the Dutch coast, the sediment budget that was needed annually (de Schipper et al., 2014) and the requirements of multi stakeholders about several aspects such as nature development (Luijendijk et al., 2017). The directional spreading of the

waves in the area is important to assign the position of the nourishment such as higher sediment distribution can be observed. Since the inlet nourishment in this thesis is multifunctional, its general position is found based on that concept. In view of the fact that, the waves approaching the inlet from north west, the longshore currents are transported from west to east and the eastern side of the inlet is more vulnerable due to erosion, the inlet nourishment is placed at the east side of the Boughaz 1 inlet. This is in agreement with the study done by Nassar et al. (2018) who examined the shoreline response of the system. The specific position of the inlet nourishment is defined approximately equal to 300 m from inlet entrance based on sensitivity analysis.

The length of the inlet nourishment is considered equal to 2100 m to provide a large-scale nourishment design. The cross-shore distance, related to the total width of the inlet nourishment, is determined based on the concept of Depth of Closure defined by Hallermeier, see Appendix A. This concept in combination with the wave breaking criterion defined the width of the nourishment equal to 1300 m. The width of the beach nourishment was chosen initially arbitrary equal to 50 m while in later stage a new design approach of that element is defined with a larger beach width. These parameters determined a constant shape, rectangular form, of the inlet nourishment. For simplicity and to understand further the crest level of this design, the shape is kept constant for all the design configurations. The crest level of the inlet nourishment is defined from the prevailing wave conditions in the area. The mean significant wave height in the Lake Bardawil is found equal to 0.5 m. This value is taken into account while other values are considered as well. This is further explained in the next section.

- **Design requirements provided by TWM/DEME:**

The range of values is narrowed also by the limitations and design requirements provided by the company. These are determined based on previous works, the limitations determined by the construction equipment as well as the aim for limited dredging quantities and sediment properties in the area. The related values with the associated design parameters are given in Table 3-2.

The operation of the construction equipment is important to be known for the representative design adaptations. The Ambiorix CSD can disintegrate materials under a certain swing angle with successive steps. The dredged material is transferred through pipelines to a desired location. This type of dredger is productive at a minimum depth of 6 m while its maximum depth reaches 35 m (DEME, 2018). All the dredged material in the area are used for the construction of the innovative inlet nourishment. Another aspect which is considered important for the conceptual design of the Boughaz 1 tidal inlet system is the amount of the dredged quantities followed by the dredging operational works within the tidal inlet and approach channel. It is requested that the minimum value of these quantities can lead to a more desirable economical approach for the project. The exact amount of the dredging quantities is not considered within this thesis, but the general adaptation of this criterion is indicated.

The minimum depth of the inlet cross sectional area is defined equal to 7.5 m while its maximum equal to 10 m. These values are determined based on the construction equipment and the research done by Lanteris (2016) who found that these values are important for the fish migration towards the lake. The minimum width is defined based on the optimal swing angle of the construction equipment while its maximum value is determined with a sensitivity analysis and based on the previous works that defined the size of the inlet cross-sectional area.

The maximum slope is provided based on a sediment grain size found in the area. All these parameters are equally valid for the design of the approach channel. The above water slope of the inlet nourishment design is defined equal to 1/25 while an 1/6 underwater slope is used.

Table 3-2: Range values of each design parameter for the three design elements provided by TWM/DEME.

Design Elements	Design Parameters	Range values	Description/Dependencies	Reference
Inlet cross sectional area	Depth	-7.5m to -10m CD	Limitations Cutter Suction Dredger (CSD)	DEME equipment Ambiorix
	Width	Minimum 150m	Optimal swing angle CSD	
	Underwater slope	Max steepness 1:6	Based on grain size of 300 $m\mu$	-
Approach channel	Depth	-7.5m to -10m CD	Limitations Cutter Suction Dredger (CSD)	-
	Width	Minimum 150m	Optimal swing angle CSD	CUR152
	Length	No restrictions	Aim for reducing dredging quantities	DEME equipment Ambiorix
	Orientation	No restrictions		
	Underwater slope	Max steepness 1:6	Based on grain size of 300 $m\mu$	CUR152
Inlet nourishment	Length	No restrictions	-	-
	Width			
	Crest level	No restriction	-	-
	Shape/Size	No restriction	-	-
	Underwater slope	Max steepness 1:6	Based on grain size of 300 $m\mu$	CUR152
	Above water slope	Max steepness 1:25	Based on grain size of 300 $m\mu$	CUR152

3.1.3 Followed procedure

Before proceeding to the initial design phase, the hydrodynamic analysis of the current state of the system is examined to indicate in detail the current tidal prism, flow velocities and water level variations of the system before forming different design outlines within Boughaz 1 inlet. Subsequently, conclusions are made which are considered important for the execution of the design methodology.

The procedure that is followed to define the final combined design choice is based on a certain design sequence. The sequence of the most important nature-based design elements was analyzed based on the relation between the elements. Since both, the so-called approach channel and inlet nourishment depend on the presence of the inlet cross-sectional area, it was assumed that it is better to examine

first the response of this element. Sequentially, the approach channel and the inlet nourishment were studied separately. It should be noted though, that the sequence of such construction works starts with the approach channel, continue with the inlet cross-sectional area and ends with the design of the so- called inlet nourishment during construction phase. However, this sequence was not followed here since an inside of the response of each element is judged to be relevant. According to that, the inlet cross-sectional area was firstly examined with different design adaptations. The best in hydrodynamics conceptual design was considered as a primary design for the examination of the approach channel and the inlet nourishment measure. Followed that, the hydrodynamic analysis of the approach channel and inlet nourishment are indicated, and their optimal design choices are given. Afterwards, all the optimal to the hydrodynamics design choices are combined and determined the final combined design choice of the initial design phase. The dimensions of Boughaz 2 inlet are kept constant.

Subsequently, the final combined design choice is further examined with three different cases. This is done to confirm the scope of the design methodology. The first case, Case 1 is defined as the tide only scenario, Case 2 states the examination of the final combined design choice with the implementation of the tide and certain sediment properties while Case 3 outlines Case 2 with different wave conditions, see Figure 3-3 . All the design elements are examined under hydrodynamic response of the system, while an overview of the morphological impact is provided for the final combined design choice.

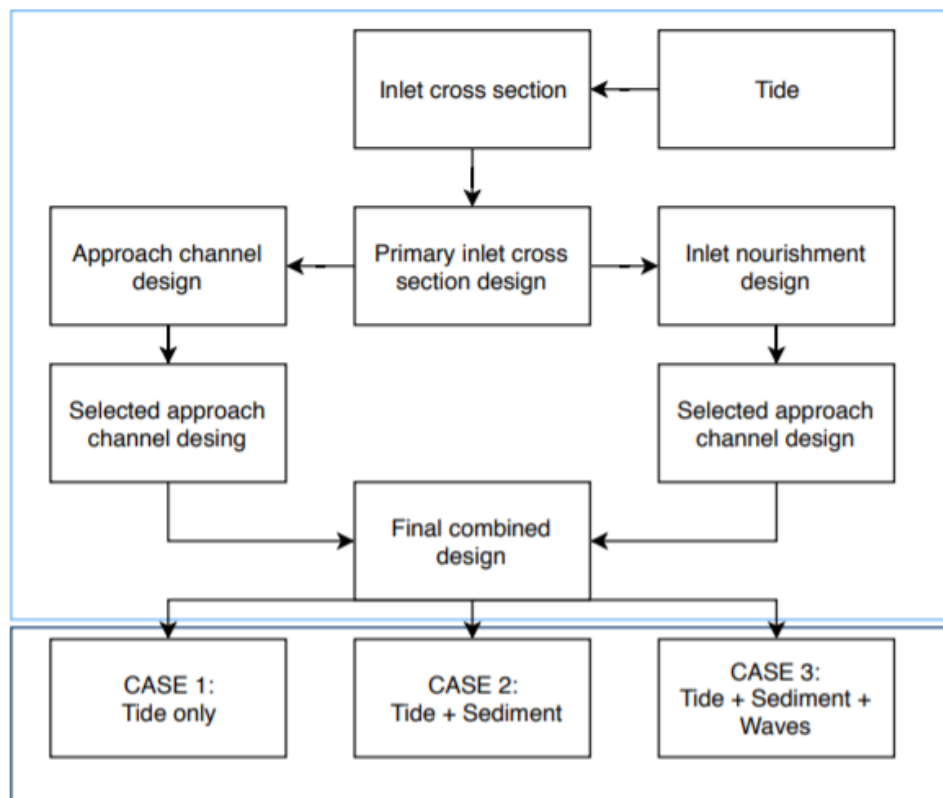


Figure 3-3: Flow chart of the followed design procedure of Boughaz 1 inlet. Within the light blue colour box, indication of the design sequence followed to examine the hydrodynamic response is given. The optimal design is selected. Within the darker blue colour box, the hydrodynamic and morphological response of the selected final combined design choice is examined under three different cases. Case 1: Tide only. Case 2: Tide + sediment. Case 3: Tide + sediment + waves.

3.1.3.1 Inlet cross sectional area

The initial average cross-sectional area of the Boughaz 1, west inlet, has rectangular shape with cross-section area about 1191 m². The cross-sectional area of the east inlet is 1236 m² (Lanters, 2016). The east inlet dimensions are kept constant while different design conditions are examined with respect to the west inlet.

In total, nine different designs of the inlet cross-sectional area were determined, see Table 3-3. The dimensions followed the design requirements provided before. The range of the size of the inlet cross sectional area is between 2245 and 3465 m². The maximum width is determined as 660 m while its minimum is taken equal to 300 m. The length is kept constant and equal to 800 m while its main depths are considered equal to 7.5 m and 10 m. Each design had a slope of less than 1/6 which was based on the soil properties in the area and the functionality of the construction equipment, see Table 3-3.

Three shapes were examined as shown in the Figure 3-4. As stated in Table 3-3, the trapezoidal shape with varying depth level, is based on the two different design depths. The choice to indicate such a design is the minimum soil removal and thus minimum dredging quantities as well as the possible growth of circulation motion which is beneficial for both ecology and sediment transport (Bosboom & Stive, 2015; Bosman & Lanters, 2018).

Table 3-3: Different design approaches of the cross-sectional design element.

Design element	Design parameters				
Cross sectional area	W_{cs} (m)	L_{cs} (m)	D_{cs} (m)	Shape number (Figure 3-4)	Size (m ²)
1	440	800	7.5	1	2790
2	440	800	10	1	3435
3	660	800	7.5	2	3242
4	500	800	10	2	3465
5	440	800	7.5	1	2650
6	300	800	10	1	2522
7	486	800	7.5	2	2527
8	400	800	10	2	2785
9	300	800	7.5/10	3	2245

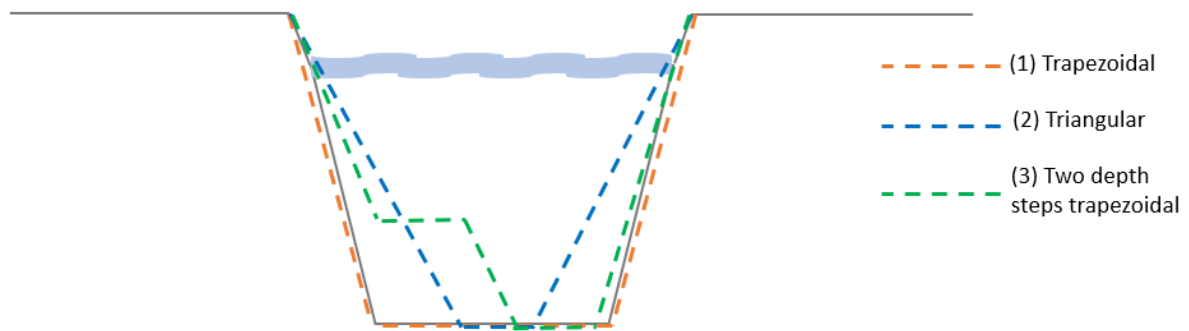


Figure 3-4: Shape configurations of inlet cross-sectional area. (1) Trapezoidal, (2) Triangular, (3) Trapezoidal with two depths.

3.1.3.2 Approach channel

The design of the approach channel was based on the selected most efficient design of the inlet cross-sectional area. Since both, the approach channel and the cross-sectional area are related to each other, the shape of the inlet cross-sectional area was used to define the cross section of the approach channel element. In that case the effect of the so-called approach channel was based on its orientation and length. The table below indicates the dimensions of each design.

Table 3-4: Different design approaches of the approach channel inlet.

Design element	Design parameters					
Approach channel	W_{cs} (m)	L_{ac} (m)	D_{cs} (m)	Shape number (Figure 3-4)	i	α_{ac} (°)
1	300	1200	7.5/10	3	$>1/6$	0 Parallel to inlet
2	300	2400	7.5/10	3	$>1/6$	90 Perpendicular to coast
3	300	2400	7.5/10	3	$>1/6$	0 Parallel with the west coast
4	300	2400	7.5/10	3	$>1/6$	45

A hydrodynamic analysis is carried out to define the primary design of the inlet cross sectional area. Its selected design parameters such as the width, depth and shape were determined and the design of the cross section of the approach channel is defined. The orientation and length of the approach channel were modified. The length of the approach channel varied from 1200 m to 2400 m. The different design adaptations can be seen in Figure 3-5.

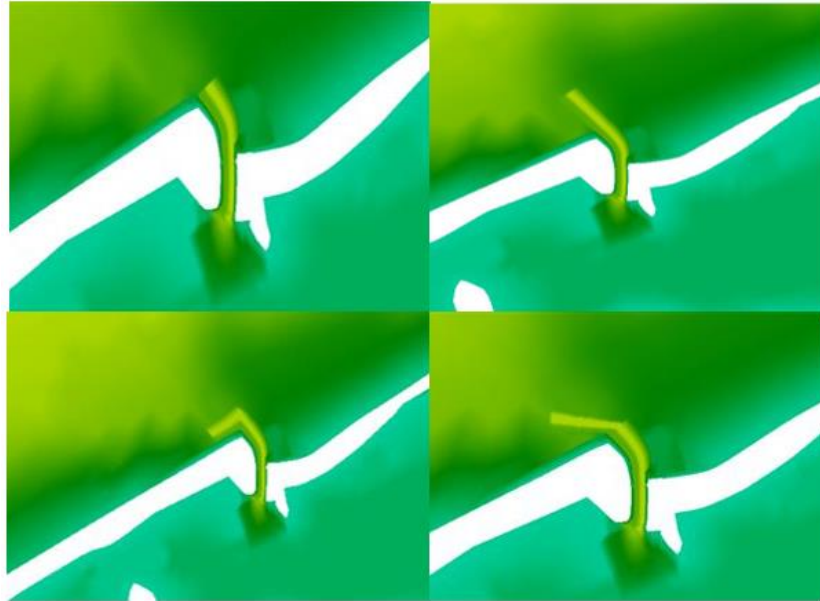


Figure 3-5: Top view of the designs of approach channel within the model Delft3D FM.

3.1.3.3 Inlet nourishment design

The design of such measure is directly depending on the wave impact and/or orientation. Incident waves under a certain angle with respect to the coast, tend to stir up sediment and create longshore currents which accordingly corresponds to sediment transport (Bosboom & Stive, 2015). This indication is important for the position and shape of such engineering measure to be able to fulfil its function. Herein, the choices of the initial position of the inlet nourishment are based on data provided by literature, concerning the wave orientation in the area. Since the waves in the area are reported to approach the lake from NW and the longshore currents are directed eastwards result in sediment transport. Considering that and according to previous works the inlet nourishment is placed at the east side of the inlet with a distance equal to 300 m from the inlet entrance.

Initially four designs have been determined with the same position distance, beach nourishment width, total width and length. The width of this measure is determined based on the criterion of DoC. DoC is widely used for the beach fill design of a coast and describes the most landward depth where limited morphological changes between nearshore and offshore are observed (Coastal wiki, 2015). Since it is requested to have the minimum quantities for this measure, this concept is considered important for the determination of the cross-shore distance, thus its width. This will allow the dumping of materials at the area of influence and not exposing them to more offshore locations while no needed. The determination of the DoC is based on the following equation:

$$D_c = 2.28 \cdot H_s - 68.5 \cdot \left(\frac{H_s^2}{g \cdot T^2} \right)$$

In which:

D_c (m): Depth of closure

H_s (m): Significant wave height at a nearshore location

T (s): Wave period of the specific wave height

$g \left(\frac{m}{s^2} \right)$: Gravitational acceleration

To define the DoC an assumption is made that along the shoreline this factor does not change. The calculation of this depth is based on 17-year wave record which indicates that for shorter or even larger wave record the DoC might be different. Based on that a more simplified condition is taken to understand the cross-shore extension of this measure such as no extra dredged material to be placed further offshore. The DoC was calculated equal to a depth of about 5.70 m. According to Emanuelsson and Mirchi (2007) the DoC was found to be 4.60 m with the assumptions used here. This deviation mainly depends on the source of wave data used in both cases. Since the DoC is strictly depending on that these deviations are accepted. The significant wave height nearshore was found with the ray model provided by BMT Argoss wave model. This is further illustrated in Appendix A.

To validate this condition and to provide more sustainable design, the need to capture the highest wave energy is important. For that reason, the wave breaking depth is defined to identify the location where the highest morphological changes can be seen. According to the Emanuelsson and Mirchi (2007), the maximum breaking wave height at three different locations of along Lake Bardawil were found to be between 2.18 m and 2.88 m. Taking that into account, a breaking depth is found to be between 2.80 to 3.69 m. This is defined with the following equation:

$$\frac{H_b}{h_b} = \gamma$$

In which:

$H_b(m)$: Breaking wave height

$h_b(m)$: Breaking wave depth

γ : Breaker index = 0.78

The varying design parameter in that case is the crest level of the submerge shoal of the inlet nourishment. To capture the most wave energy the crest level was found to be more effective at 0.5 – 1 times the significant wave height. The momentum contribution of waves can only be observed between trough and crest level. Thus, the crest submerge elevation of such measure should be such that these conditions are met. In Table 3-5 the initial design adaptations are given. The mean significant wave height near lake Bardawil was found to be 0.5 m with a mean period of 6.3 s (Embabi & Moawad, 2014). Since high lack of data presented in the area, this value was considered reasonable to be taken under consideration. Consequently, based on the criterion that the crest level should be at a range of 0.5-1 times the significant wave height values of 0.25 and 0.5 m were considered. Two more simulations were done to analyse if indeed these criterion is valid. Furthermore, erosion is expected when waves approach the shore under an angle. The angle of approach creates longshore currents which are directed either eastwards either westwards. To avoid any deposition of sediment within the inlet entrance, the submerge measure was placed at a distance 300 m away from inlet location. The position was approximately considered based on the research done by (Nassar et al., 2018). They indicate a position of the one-time nourishment as described in section 2.2.2. However, the exact position of this measure at the east side of the Boughaz 1 inlet is not well indicated and thus an approximately choice is made.

According to these concepts the initial designs that are examined are the following, see Table 3-5. Initially, the beach nourishment width in that case is extended at 50 m distance from land whilst the submerge area is extended smoothly until the DoC with a width of about 1300 m. For simplicity, the

shape of the initial designs is chosen to be a rectangular such as the effect of the other parameters can be understood better.

Table 3-5: Different design approaches of the inlet nourishment.

Design element	Design parameters				
Inlet nourishment	W_t (m)	L_s (m)	C_s (m)	W_n (m)	D_s (m)
1	1300	2100	0.75	50	300
2	1300	2100	1	50	300
3	1300	2100	0.5	50	300
4	1300	2100	0.25	50	300

3.2 Design modelling

In this section, all the data used within the numerical models are first indicated. These, include the wave data analysis, the tidal data and sedimentary properties, found to be representative for the study area. Then, a description of the model set up and modelling approach is provided. A start is made with the Delft3D FM model and following that the Delft3D model is described. The choice to use two software applications is based on the condition that the Delft3D FM is still under beta testing which indicates that the applicability of this software with the implementation of waves and morphological processes is not yet fully validated and calibrated and uncertainties might occur. For that reason, the hydrodynamic response of the different design approaches is followed with the Delft3D FM and the final design is examined with the Delft3D software.

3.2.1 Data collection

3.2.1.1 Wave data analysis

Near coastal areas many different complex processes arisen due to the presence of different physical conditions. One of them are the wave climatic conditions. When waves approach the shore they will alter due to several complex processes such as refraction, diffraction and shoaling, until their highest steepness is reached which will lead to wave breaking. When wave breaking occurs by waves which approach the shore under an angle, they will tend to generate longshore currents which are responsible for stirring and transporting of sediment (Mangor, 2018). This, in combination to other processes such as wind, tide etc, can lead to significant alternations in the hydrodynamics and morphology of the coastal area. For that reason, to understand the functionality of a certain design in a coastal area the wave conditions should be known.

To obtain a wave data in Lake Bardawil, the BMT Argoss model is used. BMT Argoss is a company specialised in meteocean, consultancy and weather forecasting (BMT Argoss). Reliable wind and wave statistics globally are provided from BMT Argoss wave climate service, for 26 years (1992-2017). The database is fully calibrated with satellite observations and long term global and regional model hindcasts. Information regarding the wind speed and direction, significant wave height, wave direction, mean and zero crossing wave period can be collected through the database and can be observed with timeseries, histograms, scatter tables (2D-3D) in yearly, seasonally or monthly conditions. This model provides valuable information for hydraulic engineering design facilities and is widely used.

According to several studies lack of wave data exists near the Lake Bardawil. Since in-situ measurements are not available for this thesis project, the Argoss wave climate model was considered to be a reliable tool for the prediction of the wave conditions in the area.

For the determination of the representative wave conditions in Lake Bardawil, an offshore model point was chosen. This offshore model point is located at 31° 45' N, 33° 00' E. The north distance from Lake Bardawil to this point is approximately 53 km and about 80 and 130 km from the Port Said (west distance) and at the borders of Israel (east distance) respectively as can be seen in the Figure 3-6. This wave model point was considered as a representative one since any land-sea breeze with the surrounding areas should be avoided and deep wave conditions should be met. Following that, a timeseries of 26 year's records (1992-2017) was extracted from BMT Argoss model for further analysis. In total 75976 observation points were extracted for the wave model point. Values regarding the significant wave height, peak period and direction were analysed to indicate a representative offshore wave climate in the area.



Figure 3-6: Location of the wave model point taken from Argoss model ("Lake Bardawil," 2015).

In literature, the wave climate conditions have not been analysed with Argoss model data, but different approaches were considered. One of them describes the implementation of a wave gauge in a water depth of 14 m near Boughaz 1 inlet (Nassar et al., 2018). According to that research, the predominant directions of the waves are NW (51%) and N (32%). A good correlation can be seen with BMT Argoss model which gives a predominant direction of the NW waves (35%), see Figure 3-7. However, difference is observed with the WNW waves and N waves. This difference depends on the different location that the wave measurements are considered, since the wave data taken from Argoss model is further offshore than the latter.

Based on the wave rose and scatter plot provided in Appendix B and extracted from BMT Argoss model the highest frequency waves occur between NW and WNW to about 35% and 34% respectively. Higher frequency of occurrence are the wave heights in a range between 0.2 to 1.2 with the 0.6 to 1 m to be the most significant ones. These directional wave heights create eastward longshore currents (Nassar et al., 2018). Less frequency waves are presented in the N and NNE which give west bound currents. Nassar et al. (2018), indicate that for 62-65% of the measurements show the predominant alongshore current direction is directed eastwards from NW waves. Since the longshore transport is an important factor for the feasibility study of the selected design, the NW waves are considered to be the most important ones and thus the wave data are analysed with this point of consideration. The shoreline orientated 60° from the true north which indicates that waves approaching the coastline to 330° do not create longshore currents. Waves normal to the coastline, perpendicular, are mainly responsible for the cross-shore sediment transport whilst longshore transport processes are observed when waves approaching the coast under an angle. The highest rate of sediment transport is under an angle of 45° (Bosboom & Stive, 2015).

All the wave conditions cannot be represented in a model performance due to the high computational demand. For that reason, wave climate reduction is needed to limit the computational effort. The reduction of the wave conditions can be based on different targets and with different techniques see Appendix B. Based on the wave climate reduction method, a choice of four different wave conditions was taken into consideration. The choice of four different wave conditions instead of 10-12 wave

conditions recommended from different studies, is based on the criterion that within this thesis focus is made with the hydrodynamic conditions and estimation of the morphological trends is considered.

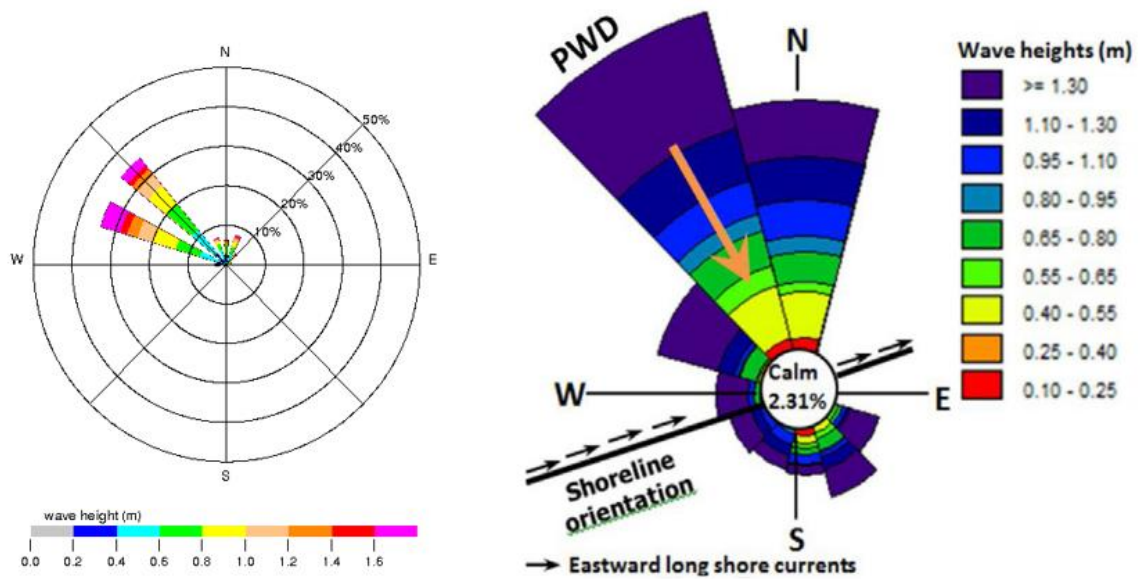


Figure 3-7: Wave roses near Lake Bardawil. Left: Wave rose for the offshore point(BMT Argoss). Right: Wave rose for a nearly nearshore point(Nassar et al., 2018).

Table 3-6: Wave conditions implemented within Delft3D model.

Wave conditions	Hs (m)	Tp (s)	Dir (°)
1	0.69	5.30	316
2	0.83	5.90	296
3	1.47	6.70	314
4	1.76	6.70	292

3.2.1.2 Tidal data

This thesis project is executed as an extension of a hydrodynamic thesis project done by Lanfers (2016) who examined the relation of the hydrodynamics to the ecosystem using a hydrodynamic model Delft3D Flexible Mesh (Delft3D FM). The prediction of the tidal components near Lake Bardawil is done by harmonic analysis (Lanfers, 2016). A Mediterranean Sea model was used to determine the water level boundary conditions. This model generate tidal components which are validated with 62 tidal gauges and are converted by interpolation to a boundary line (Gary D. & Erofeeva Y., 2002). The tidal constituents offshore from Lake Bardawil can be seen in Table 3-7.

Component	Amplitude[m]	Phase [°]	Period [Hrs]	Tidal character	Interaction
M2	0,109	236,5	12,42	Semi-diurnal	Lunar
S2	0,063	248,2	12,00	Semi-diurnal	Solar
N2	0,017	240,0	12,66	Semi-diurnal	Lunar
K2	0,018	243,7	11,97	Semi-diurnal	Solar
K1	0,027	268,0	23,93	Diurnal	Solar
O1	0,019	247,3	25,82	Diurnal	Lunar
P1	0,010	268,1	24,07	Diurnal	Solar
Q1	0,003	234,1	26,87	Diurnal	Lunar

Table 3-7: Tidal data implemented within the models (Gary D. & Erofeeva Y., 2002).

The main tidal components in the area are the lunar tide and the solar tide, M2 and S, respectively. The presence of the N2 and Q1 components owed to the variation of the moon's distance from the earth due to the elliptical moon's orbit whilst the K2 component modulated the frequency and amplitude of the main tidal lunar and solar components. The K1, O1 and P1 constituents in the express the moon's (sun's) declination and account for diurnal inequality (Bosboom & Stive, 2015). These components will be used as an illustration of the tidal boundary in the model area.

Lake Bardawil belongs to a micro tidal regime. The tidal range along the coast, outside of Lake Bardawil, was found to vary from 0.25 m to 0.55 m (Embabi & Moawad, 2014; Linnarsund & Mårtensson, 2008; Nassar et al., 2018). According to the tidal boundary conditions given above and the model performance done by Lanfers (2016) the tidal range at an offshore location was found at highest equal to 0.44 m during spring tide and 0.20 during neap tide.

3.2.1.3 Sediment data

Lake Bardawil consists mainly of sand. The average grain sediment sizes, 250 μm at the west side of the Boughaz 1 inlet and 200 μm at the east side. This is based on the only available source of sediment properties outside the lagoon (Piere, 2016). The higher sediment grain size of sand samples is found to be located within the inlets where high energetic conditions are presented, while lower energetic conditions, thus within the lagoon, smaller grain sizes are found (Khalil & Shaltout, 2006). Since the net longshore transport is eastward directed, it is expected that larger fractions of the grain sizes found at west side will be transported through the Boughaz 1 inlet. Thus, it is reliable to consider for further investigation the highest and lowest grain sizes present at the west side of the Boughaz 1 inlet, see Table 3-8. Subsequently, the minimum grain size of 180 μm and maximum grain size of 330 μm are considered.

Furthermore, since 1.9% of gravel properties are found within the eastern inlet, it might be also the case that gravel fraction is presented at the western inlet. However, since in total only 9% of gravel is presented within the lagoon and 1.9% of that is within the eastern inlet, the availability within the west inlet can be very low and subsequently no larger grain sizes than the aforementioned are considered.

Higher fractions of mud grains were found at the eastern area of the lagoon and it is reported that dredging operations led to the movement of this sediments (Khalil & Shaltout, 2006). Although the mud fractions presented in the lagoon are larger than the gravel sediment properties, there is hardly any mud sediment property within the inlet and thus the assumption not to considered this property is correct. For more reliable results, several fractions and layers of sediment properties should be investigated since the sediment properties within the lagoon differs than the Mediterranean Sea. However, for simplifications and minimum computational time it is chosen to examine the two sediment properties separately.

Table 3-8: Sediment grain sizes nearshore of Boughaz 1 inlet (Piere, 2016).

Sites Inlet "A"	Minimum D ₅₀ (µm)	Maximum D ₅₀ (µm)	Average D ₅₀ (µm)
West Boughaz 1	180	330	250
East Boughaz 1	160	280	200

3.2.2 Modelling approach and model set up

3.2.2.1 Modelling approach

As described in section 3, the hydrodynamic response of each element is firstly analyzed with the Delft3D FM. Sequentially, a final design choice is made by combining the optimal to the hydrodynamics designs of each nature-based element. This design is then optimized with the Delft3D software. This is done since the Delft3D FM is still under beta testing and thus for certainty the Delft3D software is chosen.

The simulation steps that have been followed both in Delft3D FM and Delft3D model are given with the following flow charts, Figure 3-8 and Figure 3-9.

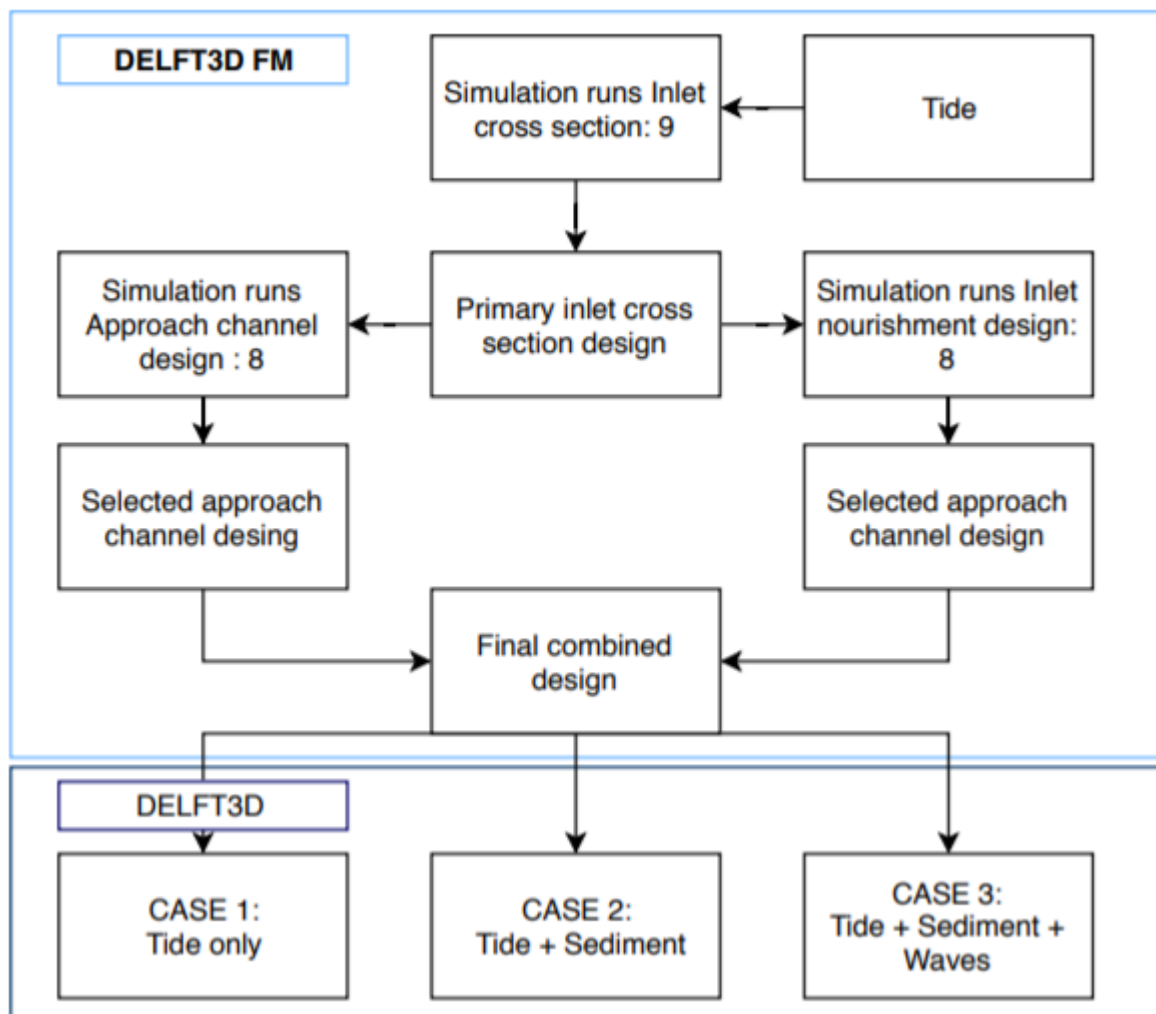


Figure 3-8: Flow chart of the production simulation runs based on the defined design methodology.

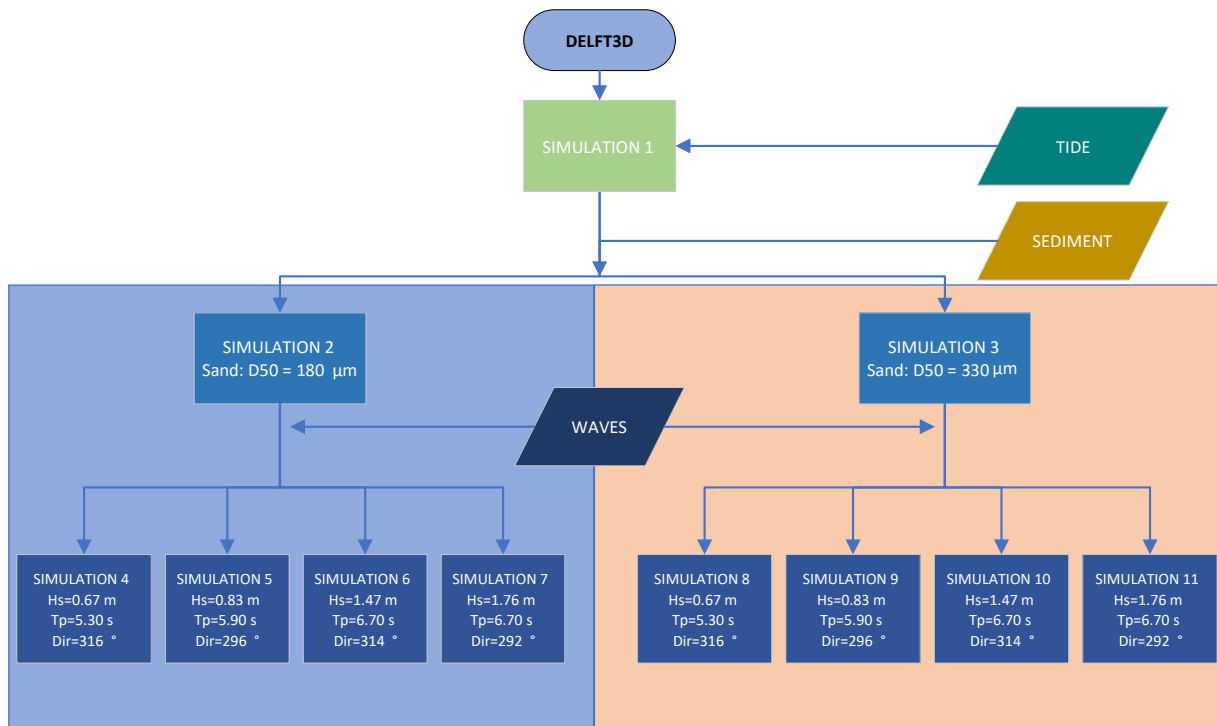


Figure 3-9: Flow chart of the simulation runs examined with the Delft3D. Simulation 1: Case 1, tide only condition. Simulations 2-3: Case 2, tide with two sediment properties. Simulations 4-11: Case 3, tide, sediment and waves. Simulation 2-7: Simulations with a grain size equal to 180 μm . Simulations 3-11: Simulations with 330 μm grain size.

The simulations started with the examination of nine different design approaches of the inlet cross-sectional area element. Then, it total eight and eleven simulations of the approach channel and inlet nourishment designs are simulated and analyzed before determining the final design. Following that, the final design is implemented within the Delft3D software where three different cases have been examined, see Figure 3-8. Case 1 indicates the tide only conditions. Case 2 indicates the examination of flow with sediment properties whilst Case 3, is the Case 2 with the inclusion of the four different wave conditions illustrated in section 3.2.1.1. Figure 3-9, provides in more detail the three cases examined within Delft3D. Case 1 is indicated as the simulation 1, Case 2 is the simulation 2-3 of Delft3D and Case 3 are the simulations 4 – 11. A division is made also between the two sediment properties examined with the Delft3D model. Simulations 2-7 provide the simulation runs that examined with the smaller grain size whilst simulation runs 3-11 are with the larger grain size.

3.2.2.2 Delft3D Flexible Mesh

The Delft3D FM is the newest version of the Delft3D software. Within this software different modules exist. In this hydrodynamic analysis the D-Flow FM module of the Delft3D FM was used. This calculates non-steady flow and transport phenomena under the influence of tide and meteorological conditions in unstructured grids (Deltares, 2016). The main advantage of such program is the flexible combination of different shapes of grids which make the design conditions easier in complex areas however the software is still under development.

Model set up

The hydrodynamic analysis is done to examine the influence of different design conditions in Boughaz 1 inlet with respect to the tidal prism and current flows. Different design conditions were examined based on the cross-sectional area, the approach channel and the inclusion of the inlet nourishment measure near the inlet. The model in Lake Bardawil were set up from Lanthers (2016) and was modified to satisfy the requirements for this project.

Grid structure

Since this model is based on the optimization of hydrodynamic conditions in Boughaz 1 inlet, the grid resolution near the inlet is increased in comparison to the other locations. This allows the model to configure more flow calculation steps for higher accuracy. The refinement though is done such as no loss of data is observed. Particularly, the grid within the inlet is approximately 10 m, at nearshore location is about 20 m whilst far offshore is in order of magnitude of 1000 and 5000 m, Figure 3-10.

Bathymetry

No up to date bathymetrical data exist within and nearshore the Lake Bardawil (Lanthers, 2016). The bathymetry within the lake was modelled with a relatively rough depth map whilst a sea map was used for the nearshore locations, see Appendix B. On the other hand, the offshore bathymetrical data were obtained from European Marine Observation and Data Network (EMODNET), which has sufficient accuracy.

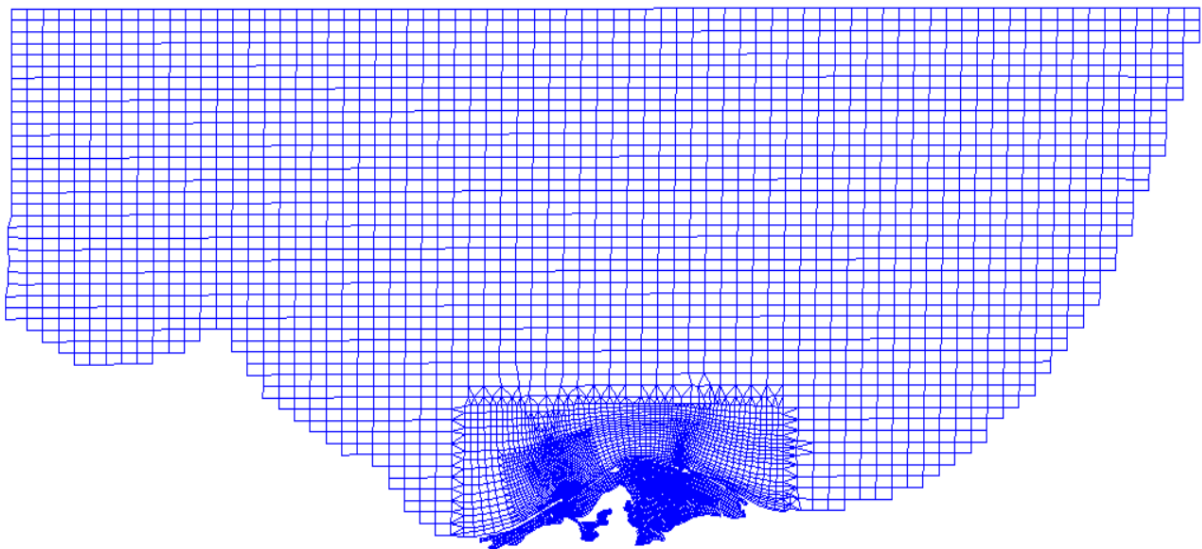


Figure 3-10: Flow grid within Delft3D FM.

Boundary conditions

The boundary conditions involved in the model are the tidal components. The inclusion of the wind and waves components are not yet considered. The meteorological conditions are already examined by Lanfers (2016), whilst the wave field is chosen to be examined with the Delft3D suite software. For Lake Bardawil, these boundary conditions were spread to a distance of 410 km of 140 points (Lanfers, 2016).

Physical parameters

The default values of the physical parameters, roughness, viscosity and constant values, are used. Referring to the first physical parameter, the manning friction formula is considered with a uniform friction factor equal to 0.023 and a free slip criterion. The horizontal eddy viscosity and diffusivity are set equal to $1 \text{ m}^2/\text{s}$ while the constant values referred to water density and gravity are set equal to 1000 kg/m^3 and 9.81 m/s^2 , respectively. These parameters have not be modified and are based on the previous research done by Lanfers (2016).

3.2.2.3 Delft3D

The Delft3D software has the same functionality with the Delft3D FM suite software. The main difference between these software's is the structure of the grid. The Delft3D software use rectilinear or a curvilinear, boundary fitted grid compared the unstructured grid of Delft3D FM. As mentioned earlier the choice to continue with the Delft3D software was decided such as the investigation of the hydrodynamic and morphological response of the system under the influence of the tidal flow with the presence of sediment properties and wave conditions can be observed. The Delft3D FM is still under beta testing and thus cannot (yet) implement surely these conditions.

According to that, two different modules are used. The Delft3D-FLOW and Delft3D-WAVES. The Delft3D-FLOW module calculates non-steady and transport flow phenomena of tidal and meteorological forcing calculations. The Delft3D-WAVES module (SWAN), calculates the propagation of random, short-crested wave conditions in coastal areas and describes the processes of wind-generated waves, dissipation due to white capping, bottom friction, wave breaking and non-linear wave-wave interactions. The coupling between these two modules give the opportunity to incorporate wave forces in the morphological behavior of the system (Deltares, 2011a, 2011c).

Model set up – Flow module

The final design selected from Delft3D FM was implemented within the Delft3D software. The choice of this design was based on the higher efficiency given by the three design elements to the hydrodynamics of the system.

Grid structure

The convex shape of Lake Bardawil introduces the complexity of designing a structured grid provided by Delft3D compare to the Delft3D FM. At curvy locations higher resolution is needed to follow the shape of the land boundary. However, higher resolution levels increase the computational time which should be avoided. For higher accuracy results, higher resolution is implemented at locations where the three design elements are located, Figure 3-11. The flow grid resolution at the Boughaz 1 inlet is 15 m alongshore and 22 m cross-shore and is extended to the location of the approach channel whilst within the Boughaz 2 inlet, the grid cell size is larger since the depth along this inlet is identical. Furthermore, within the inlet nourishment, the resolution at the cross-shore direction is 20 m and an average value of 50 m is presented alongshore. The grid cell size differences between the two software is only done for reduction of the computational effort. The accuracy of the results is mainly based on

the smoothness and orthogonality of the grid structure (Deltares, 2011b). To illustrate that, a 20% smoothness parameter is used to provide smooth structure of the grid and to provide smooth calculations between the grid cells according to the requirements. The criterion of the orthogonality is also met for more accurate results.

It should be noted the flow computational grid was extended to a smaller distance from Lake Bardawil than the constructed grid in Delft3D FM and thus the tidal boundary conditions are now shifted to different location. This was done since the wave computational grid should be larger than the flow grid to avoid any disturbances and the cover area of the Delft3D FM was already very large which indicates high computational time in coupling between flow and waves. The dimensions of the computational flow grid are 90 km alongshore and 40 km at the cross-shore direction.

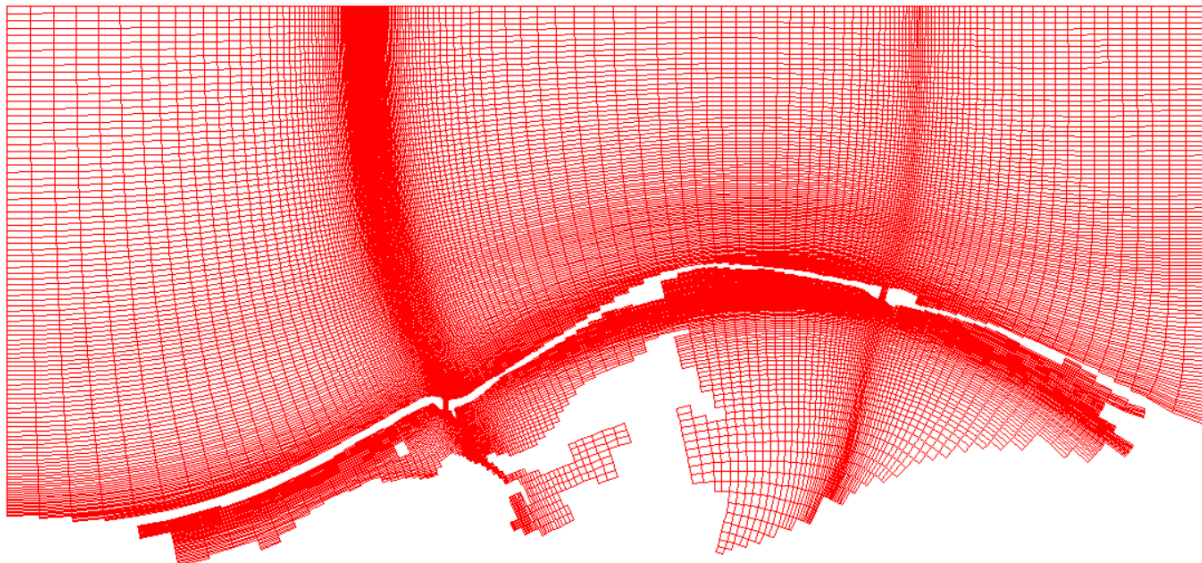


Figure 3-11: Computational flow grid. Higher local refinement along the land boundary and within Boughaz 1 inlet.

Bathymetry

The bathymetry of the final design selected from Delft3D FM was taken and implemented to the Delft3D software as samples file. Subsequently, triangular interpolation of the depth samples was done to provide the bathymetry on the new constructed grid of Delft3D.

Time frame

To indicate accurate results within the model a correct time step should be chosen. The accuracy of the results is based on the correct choice of the Courant (Friedrichs-Lewy) – number (CFL)(Deltares, 2011a). The CFL is mainly depended on the spatial scale of the numerical grid as follows:

$$CFL = \frac{\Delta t \sqrt{g \cdot H}}{\{\Delta x, \Delta y\}}$$

Where:

- Δt (s): Time step
- g (m/s^2): Gravitational acceleration
- H (m): (total) Water depth
- $\Delta x, \Delta y$: Horizontal grid cell sizes

With a time step equal to 6 s, the model gives a CFL number equal to 10.90. Most of the cases the CFL number should be at maximum equal to 10 whilst in some cases also larger values can be reached (Deltares, 2011a). To understand if the accuracy of the model results is affected with a CFL number equal to 10.90 a smaller time step, 4.5 s, is first examined with a sensitivity analyses described in Appendix C. Since the accuracy and the stability of the model results between a time step equal to 6 s and the 4.5 s is the same, for less computational time the 6 s is considered reasonable condition.

A total simulation period of 30.5 days is considered. The simulation period consists of a morphological spin up time equal to 12 hours, for the Cases 2 and 3. In Case 1, see Figure 3-8, where no morphological feedback is used, the simulation period is the same. The choice of one-month period is based on the condition that one full month tidal cycle should be examined as was the case with the Delft3D FM simulations.

Initial conditions

The initial conditions are set to the default value both for the water level and for sediment properties.

Boundary conditions

The grid consists of three open boundaries. A water level boundary is imposed at each boundary side with the tidal data provided in section 3.2.1.2. The choice not to implement Neumann boundary conditions at the lateral boundaries is based on the length scale of the grid. Since the grid size is very large and the water level gradients varying then uncertainties might be included with the model (Roelvink & Walstra, 2004). To limit though any reflection of the long waves propagating along the computational grid while imposing water level boundaries, a weakly reflection coefficient, Alpha, is used (Deltares, 2011a). The alpha coefficient is based on the length scale of the grid and thus an Alpha value between 5000 – 9000 is considered.

Physical parameters

The same constant, roughness, viscosity values are implemented within Delft3D FM, section 3.2.2.2, are considered also here.

Non-cohesive sediment properties are implemented within the model for Case 2 and 3. A choice of two different sediment conditions are examined based on the data collected from literature, see sections 2.1.2 and 3.2.1.3. Both, the $D_{50} = 180 \mu\text{m}$ and $D_{50} = 330 \mu\text{m}$ have a specific density equal to 2650 kg/m^3 , dry bed density and hindered density equal to 1600 kg/m^3 which are the default values provided from the model. The default transport formula of Van Rijn is considered for the morphological variations and all the related values left with their default values.

Model set up- Wave module

Grid structure

An orthogonal well-structured grid is constructed for the implementation of the wave conditions found in section 3.2.1.1. The wave grid is extended at the location where the wave model point is taken from Argoss model. Thus, the wave grid is extended 30 km far offshore from the most seaward (north side) grid point of the flow grid. At this cross-shore direction the depth is 40 m which indicates that the waves are not yet affected by bottom friction. Furthermore, to avoid any disturbances within the flow grid, a 50 km longshore extension of the wave grid is considered. This allows the waves that

are close to the boundary to refract first and smooth variations to be implemented within the flow grid.

As the case of the flow grid, higher resolution level exists within the area of interest. This is one of the requirements of the SWAN to illustrate accurately the effect of the waves due to bathymetrical and geographical changes (Deltares). The wave grid resolution closely in the area of interest is 123 x 123 and increases with a smoothness parameter of 20%, to about 1740 x 1740 m at the offshore boundaries, see Figure 3-12.

Bathymetry

The bathymetry of the final design selected from Delft3D FM was taken and implemented to the Delft3D software as samples file. Subsequently, triangular interpolation of the depth samples was done to provide the bathymetry on the new constructed grid of Delft3D-Wave.

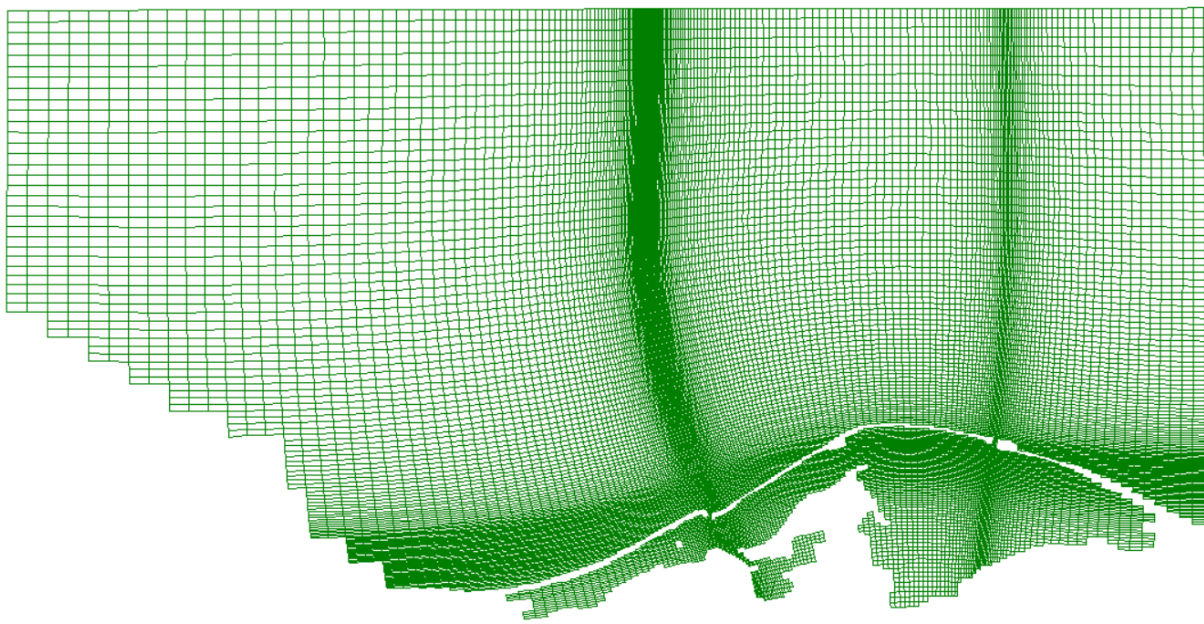


Figure 3-12: Computational wave grid. Higher local refinement area along Boughaz 1 inlet.

Time frame and coupling interval

The wave module is coupled with the flow module with a coupling interval equal to 60 minutes. The high coupling interval is recommended to correctly model the wave transformation in shallow depths which is affected by the water level variations.

Boundary conditions

The boundary conditions illustrated in section 3.2.1.1 are implemented in the northern boundary of the wave grid. An assumption is made that the wave conditions are not spatially and time varying and each wave condition is implemented uniformly in the offshore boundary. This is done after investigation of the wave roses in different locations along the offshore boundary which showed that all the wave roses were almost the same as the selected one. Though no extensive wave analysis is done for these points and further investigation is needed. A JONSWAP spectrum shape is considered

with a peak enhancement factor equal to 3.3, whilst a directional spreading is determined with the cosine power.

Physical parameters

The Battjes and Janssen model (B&J model) is used to indicate the effect of the depth-induced wave breaking with the Alpha and Gamma factors equal to 1 and 0.73 respectively. The bottom friction is described with the JONSWAP model with the default coefficient equal to $0.067 \text{ m}^2\text{s}^{-3}$. The non-linear triad interactions (LTA) are not taken into account. Although, this assumption might be important for the indication of the wave forces, their implementation might increase the computational time to an undesirable extent. Lastly, the diffraction effect is not considered since there is no shadow zone within the area of interest.

4 | Results

In this chapter the hydrodynamic results of both the Delft3D FM model and Delft3D are prescribed. Initially, the results given from the model simulation of the current state model are given. This indicates the description of the Boughaz 1 inlet, referring to west inlet and Boughaz 2 inlet referring to east inlet. Then, the hydrodynamic results of the west inlet that have been analysed from Delft3D FM with the different design scenarios are depicted. Following that a conclusion is made for the selection of the final design which is then implemented in the Delft3D software. Before describing the results of the final design in Delft3D software, a comparison is made between the results of both Delft3D FM and Delft3D. This is done to remark any possible differences might exist between the model results.

All the simulation runs are analysed with respect to the tidal prism, flow velocities and water levels at certain locations. Graphs that describe these values are essential to understand the hydrodynamic response of the system. The implementation of the final design within Delft3D software, is important for understanding the initial erosion and deposition patterns of the final design. This is beneficial for

the feasibility study of the design by imposing more processes and parameters such as wave effects and sediment properties respectively.

4.1 Design elements analysis

4.1.1 Initial state

The hydrodynamic analysis of the system is started with the Delft3D FM software. The initial state of the system as described in section 2.2.3 is important for the execution of different design scenarios. To understand the response of the current state of the system, the model provided by Lanfers (2016) is run and described. Predictions about the tidal prisms, flow velocities and water level conditions at different locations are given to illustrate the hydrodynamics of the tidal inlet system.

The average tidal prism per tidal cycle of the tidal system was found to be equal of 59 million m^3 . The influxes and outfluxes within each inlet were calculated to about 26 million m^3 and 33 million m^3 for the west (Boughaz 1) and east (Boughaz 2) inlets respectively.

The tidal flow in lake Bardawil is directed from west to east. The tidal elevation can be described as a harmonic component with the equation $n = a \cos(\omega t - ky)$ and with a flow velocity as $V = v \cos(\omega t - ky - \varphi)$ (Bosboom & Stive, 2015). This clearly indicates that there is a phase difference between the two inlets which increases towards the east inlet. Furthermore, phase difference is also obvious between the vertical and horizontal tide. The horizontal tide does not coincide with the vertical tide. This introduces the effect of friction which not only affects the phase difference but the amplitude and shape of the tidal elevation as well.

Different locations have been examined to indicate the water level variations and flow conditions of the system, see Figure 4-1. The tidal water range at most offshore location, as described in section 2.2.3 has a value of 0.40 m whilst within the inlets the tidal range decreases, see Figure 4-2. This indicates that there is a distortion of the tidal wave while it propagates within the two inlets. The tidal range at the west inlet is larger than the tidal range on the east inlet. The east inlet is in a sheltered side than the west inlet due to the convex shape of the barrier which indicates that the tidal effect is less in the eastern side than the western side due to geographical attenuation effects.

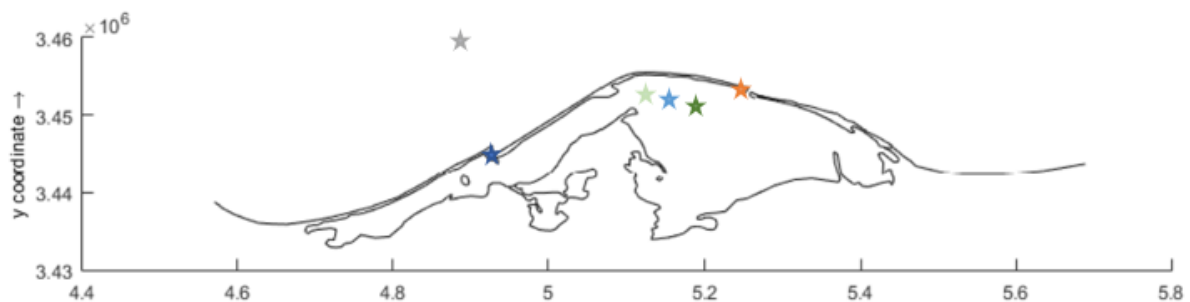


Figure 4-1: Locations of consideration. Grey: Offshore. Blue: West inlet. Orange: East inlet. Light blue: Slack point. Light green: Point 1. Green: Point 2.

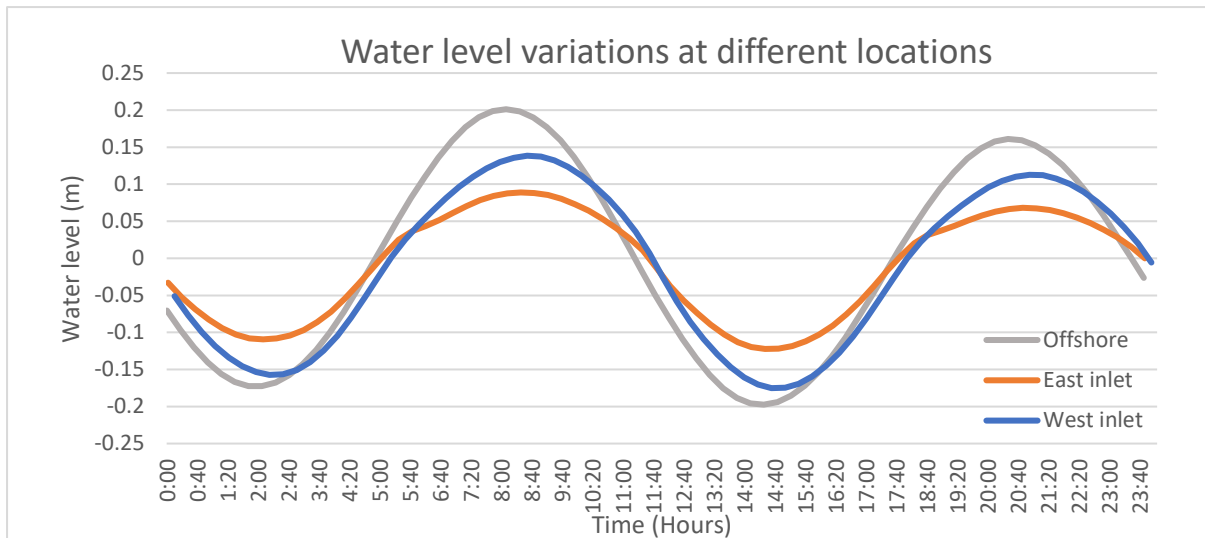


Figure 4-2: Water level variations at offshore and near the inlets. East inlet refers to Boughaz 2 inlet and West inlet refers to Boughaz 1 inlet.

The system can be characterized as a damped system due to the geometrical features of the basin. The ratio between the size of the lake and the size of the inlets is big which indicates that while the tide propagates the amplitude is reduced. This phenomenon can be explained with the concept of small basin approximation, see Appendix A. The ratio between the length of the basin and a particular tide is higher than 0.05 which indicates that the small basin approximation is not valid in Lake Bardawil. This implies that the water level variations within the lake differ than the sea water variations and no pumping mode is observed.

Within the lake, the tidal elevation and tidal flow decreases. Lanters (2016) examined the hydrodynamic response of several locations within the basin. The effect of friction and reflection is illustrated while analysing the flood end ebb flow velocities. For further illustrations reference is made to the thesis project done by Lanters (2016).

The flood and ebb duration differ over day with the longest to be during ebb. This means that the maximum flood velocities are larger than the maximum ebb (Bosboom & Stive, 2015) which is clearly visible in the east inlet where the maximum flood velocities equal to about 1 m/s while the ebb velocities are just below 0.9 m/s. According to that, the system can be characterized as flood dominant. However, the basin geometry plays crucial role for the function of the system. Since Lake Bardawil is very shallow lake, there is a large intertidal storage area which might counteract the effect of flood dominance conditions (Bosboom & Stive, 2015).

At a location between the two inlets, the tidal flow was found to be approximately zero whilst the water level variations between two points, one closer to the east inlet and one at the zero flow conditions, were found to have the same response (Lanters, 2016). This indicates a slack tidal wave which has a standing character. The tidal water level at the slack point is 0.05 m during flood and almost zero during ebb. This illustrates the intertidal flat formation which is flooded during flood and is exposed during ebb conditions (Bosboom & Stive, 2015). There, the tidal waves from the west and east inlet meet each other and lead to zero flow velocities. This, allow mostly the settling of the fine materials which are still in suspension and the creation of high turbidity levels (Bosboom & Stive, 2015; Lanters, 2016). These effects are clearly visible Figure 4-3 and Figure 4-4.

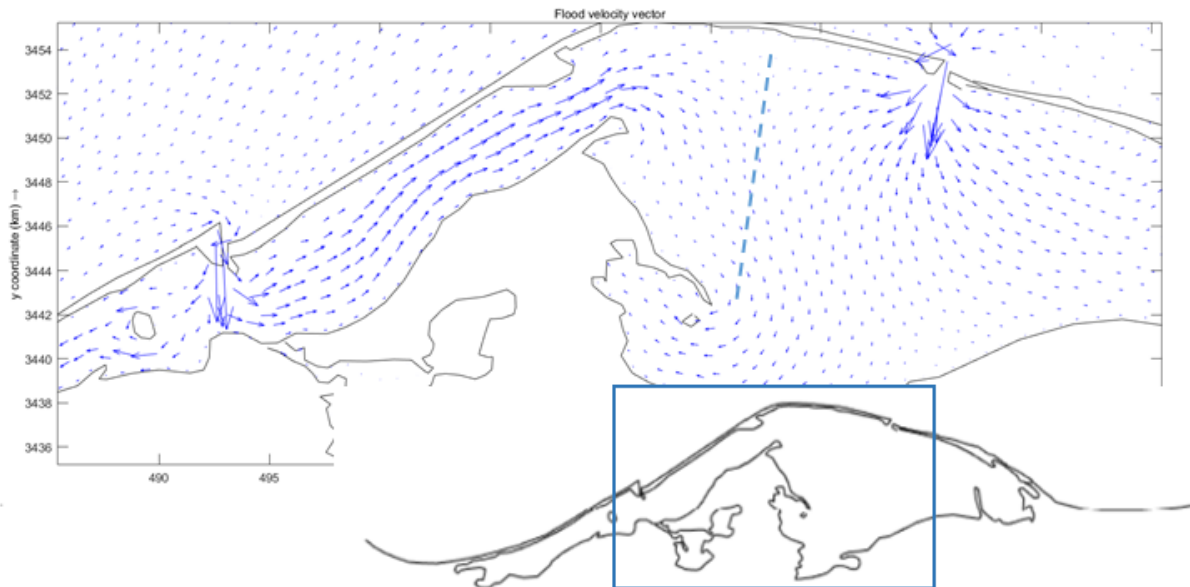


Figure 4-4: Flood velocity vector plot within the lake.

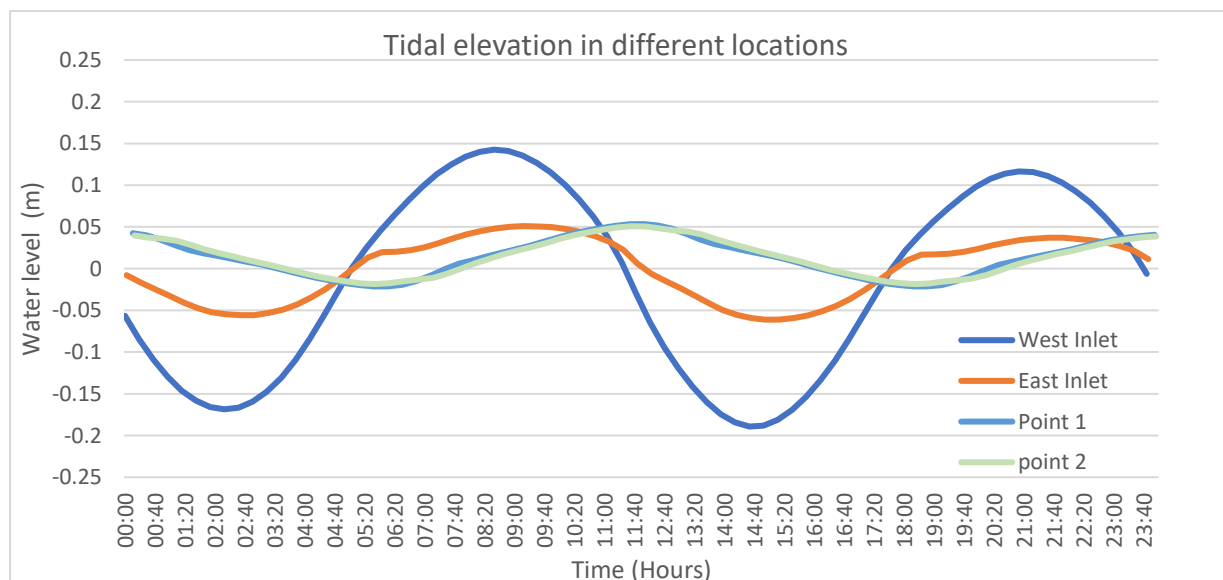


Figure 4-3: Water level variations at different locations within the inlets and lake.

Conclusions

Lake Bardawil is a very complex system and due to several uncertainties such as the lack of up to date bathymetry data (Lanters, 2016), its response it's difficult to be fully understood. Considering the hydrodynamic results described before the following conclusions have been arisen:

- The initial tidal prism in the lake is 59 million m³ in which 26 million m³ are discharged from the Boughaz 1 - west inlet.
- The flow velocities of the west inlet are 0.81 – 0.80 m/s whilst 1 m/s and 0.90 m/s are observed within the east inlet during flood and ebb respectively.
- The offshore tidal range during spring is 0.40 – 0.44 m, while within the west inlet reduces to 0.30 m and further inside to less than 0.15 m. During neap tide the tidal range is almost half than the spring tidal range. This head loss is observed due to the geographical attenuation effect provided in Lake Bardawil.
- The amplitude reduction from offshore to the nearshore and within the lake characterize the system as damped system. This is visible due to the large dimensions of the lake with respect to the tidal motion as well as due to the geographical features of the area. The shallower the inlet, the friction dominates inertia and more damping is observed.
- There is a phase difference between the inlets. The propagation distance of the tidal wave is large and this in combination to the barrier's shape, the tidal amplitude is reduced towards the east inlet.
- The system can be characterized as a flood dominant, but due to its complex shape and bathymetry and sediment properties between the lake and sea it might be the case that can function as an ebb dominant system (Bosboom & Stive, 2015; Lanters, 2016).
- Based on literature, the mixed energy coasts can be characterized with the bypassing models 2 and 3. Since Lake Bardawil belongs to a mixed energy conditions, the models 2 and 3 might be possible to presented in the area.

According to these remarks related to the functionality of the current state of the Lake Bardawil, the changes of the design within an inlet can deviate the hydrodynamics of the system. Thus, different design approaches can lead to beneficial results with respect to the tidal prism and flow conditions and subsequently to the functionality of the inlet. Focus is made on the design approaches of the Boughaz 1 - west inlet, by modifications in the inlet cross sectional area, inclusion of the approach channel and the implementation of an inlet nourishment. To understand how the tidal prism and flow conditions alter by modifying the design of the west inlet, the east inlet dimensions remained constant. Subsequently, the east inlet shape remained constant, in rectangular form with a depth of 3 m and a width of 420 m.

4.1.2 Inlet cross sectional area

Herein, the first design element which is examined is the inlet cross-sectional area of the Boughaz 1 inlet. The cross-sectional area highly affects the hydrodynamics of the system and thus is considered as the base element for the examination of the other design elements. The most beneficial to the hydrodynamic results provided by the different simulations are illustrated here while further results are provided in Appendix D. For each design of the inlet cross-sectional area the tidal prism, flow velocities and water level conditions within the west inlet are examined. Focus is put on the Boughaz 1 inlet, referring as the west inlet, which this thesis is based on, while reference to the Boughaz 2 inlet, referred as east inlet is indicated as well.

Tidal prism:

The tidal prism is determined as the inflowing and outflowing water volume during a tidal cycle (Bosboom & Stive, 2015; De Vriend et al., 2002). The Delft3D FM model can reproduce the discharge flowing in and out through the tidal inlets cross section. The calculation of the tidal prism is determined by the discharge calculation method (Umgiesser, Helsby, Amos, & Ferrarin, 2015) as follows:

$$P = \sum Q(t)\Delta t$$

Where:

P(m³): Tidal prism

Q(t) (m³/s): Discharge at certain time

Δt (s): The time interval between successive calculations

The tidal environment in Lake Bardawil is characterized as mixed energy mainly as semi-diurnal which indicates that two successive high and low waters can be seen during a tidal cycle. For that reason, the average tidal prism is calculated between two successive neaps of a period of fourteen days to indicate the average volume of inflowing and outflowing water. The spring and neap tidal prism are also determined for the whole system. For clarity, the tidal prism within the west inlet is presented in percentages and is compared with the percentage that covers the east inlet. This is done to see if the design methodology is also influencing the hydrodynamics of the east inlet, see Table 4-1.

Table 4-1: Tidal prism results related to the cross-sectional design element.

Design element	Mean tidal prism 10 ⁶ m ³	Spring tidal prism 10 ⁶ m ³ /tidal cycle	Neap tidal prism 10 ⁶ m ³ /tidal cycle	Tidal prism (%)	
				West Inlet	East Inlet
Initial state	59.3	72.1	44.1	44.1	55.9
2	71.9	89.0	51.8	54.1	45.9
6	70.9	87.4	51.4	53.3	46.6
9	70.5	87.0	51.1	53.1	46.9

In Table 4-1, only three out of the nine simulations with the different inlet cross-sectional design approaches are presented. These are the most efficient with respect to the tidal prism cross-sectional

design approaches. By modifying the design of the west inlet cross-sectional area, the tidal prism increases through the inlet and very small changes are observed at the east inlet.

The tidal prism increases more when the depth of the inlet cross-sectional area equals 10 m. This is observed for the inlet cross sections 2, 6 and 9 which have a size equal to 3435, 2522 and 2250 m² respectively. The largest mean tidal prism within the system is found for the largest inlet cross-sectional area. However, an inlet cross sectional area with about 2250 m² also gives a potential increase of the tidal prism. Cross section 2 which is about 169% larger than the initial cross-sectional area gives an increase of the mean total tidal prism to 21.3 % whilst an increase of 18.9 % is observed for a cross section 9 which is 73 % larger than the initial case. Both cross sections give reasonable increase of the mean total tidal prism but considering the design requirements in that case, cross section 9 is more efficient. Specifically, the tidal prism within the west inlet increases to about 49, 45 and 43 % for the cross sections 2, 6 and 9 respectively while only 1.35 % increase is seen within the east inlet. This might indicate that the effect of the design in Boughaz 1 inlet is not yet felt in the Boughaz 2 inlet for the considered simulation period.

Flow velocities:

For each design adaptation, the maximum cross-sectional velocities during a tidal cycle are defined. The flow velocities of the most effective cross-sectional area designs are given in the Table 4-2 and Figure 4-5.

The narrowest inlet cross-sectional area, which is the cross section 9, gives larger cross-sectional averaged flow velocities compare the other design approaches. The maximum flood velocities are 0.73 m/s while the ebb velocities are 0.70 m/s which indicates that the system can still be characterized as flood dominant. For the cross section 2, the depth averaged flow velocities are only 0.48 and 0.51 m/s during ebb and flood respectively, while ebb and flood velocities of the cross section 6 equal to 0.63 and 0.66 m/s.

The shape, and size of the cross-sectional design significantly affects the flow velocities through the inlet. The larger hydraulic radius, allow more water to pass through the channel. However, the larger wetted perimeter increases friction and reduces the hydraulic radius which this is the case for the cross sections compare the initial state. Besides that, the shape and form of the inlet gorge is influencing the distribution of the flow velocities within the inlet with the largest concentration to be within the deepest areas. Although, these conditions show that the initial state might have larger cross-sectional average flow velocities the effect of cross section 9 is more evident within the inlet cross-sectional area where more than 1 m/s velocities are seen at the deepest parts, see Figure 4-6. This is evident in the most inlets, where their asymmetric shape lead to higher flow velocities within the deepest areas and it is beneficial for the enhancement of the ebb flows(van de Kreeke & Brouwer, 2017).

Table 4-2: Maximum flood and ebb current velocities (m/s) based on cross-section design element.

Cross sections	West inlet		East inlet	
	Max ebb (m/s)	Max flood (m/s)	Max ebb (m/s)	Max flood (m/s)
Initial state	-0.81	0.80	-0.89	0.96
2	-0.48	0.51	-0.91	0.97
6	-0.63	0.66	-0.90	0.97
9	-0.70	0.73	-0.90	0.97

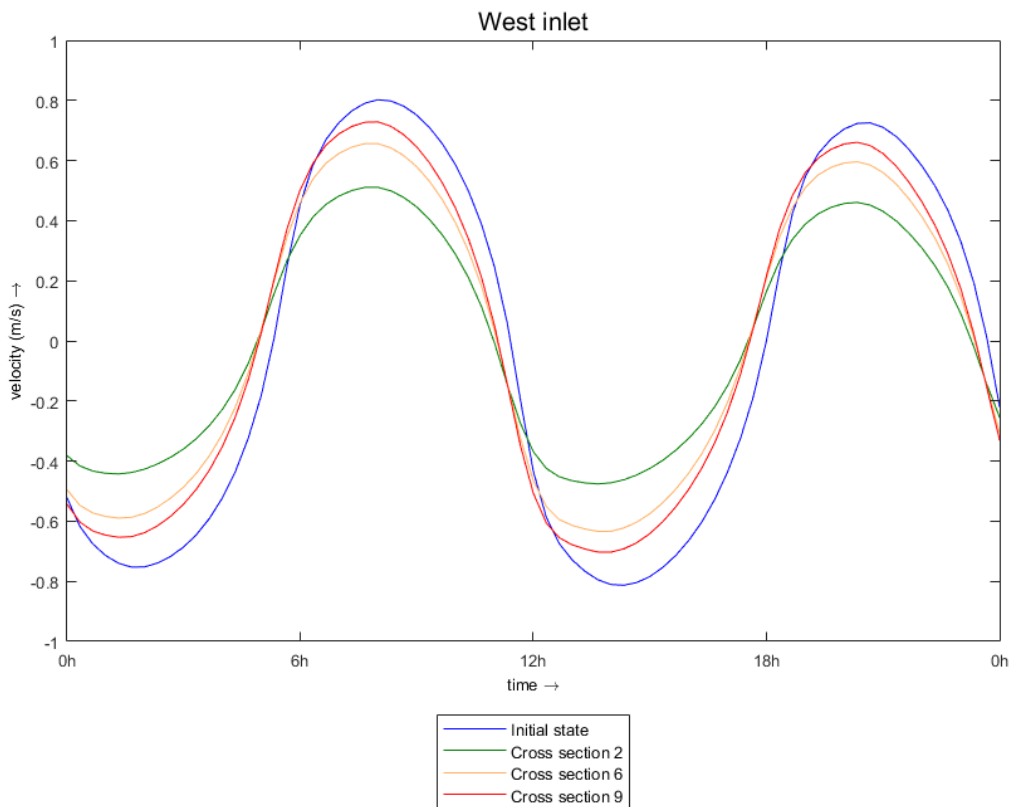


Figure 4-5: Cross sectional velocity of the most efficient design cross-sectional areas in the west inlet.

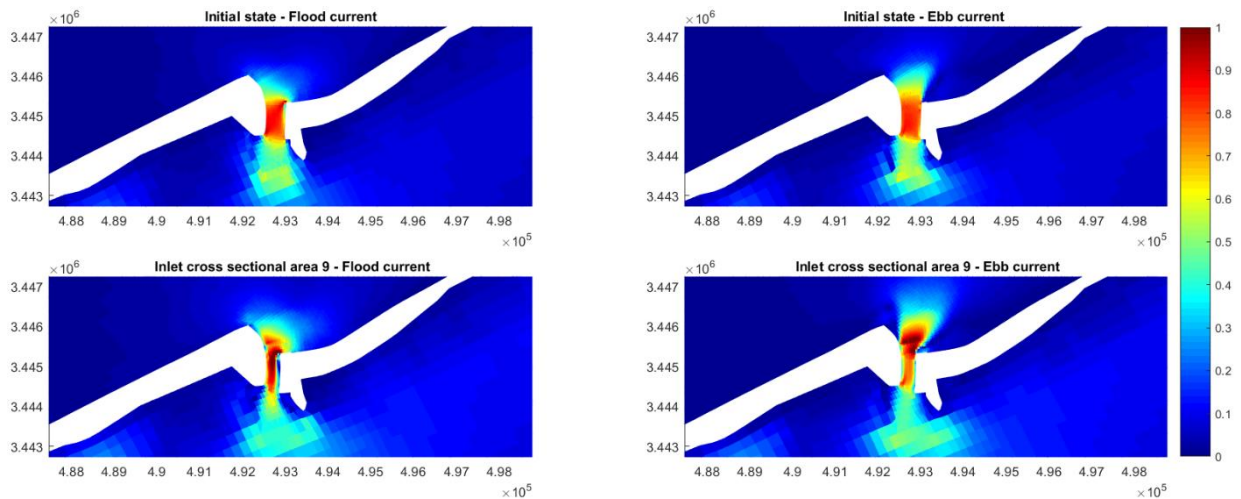


Figure 4-6: Current flows within the west inlet. The velocity magnitude (m/s) is presented during ebb and during flood for the initial state and inlet cross sectional area 9.

Water levels:

To understand the hydrodynamics of the system, the water levels at the deepest point of the inlet cross-section area are indicated. The water level range is varying between the 0.35 m for all the designs except from the inlet cross section 2. As indicated in Figure 4-7 the water level range for the largest cross- sectional area is about 0.38 m. Herein, the width of the inlet cross-sectional area in combination to the effect of friction increase the complexity of the energy concentration and or dissipation of the tidal wave and thus the determination of the water level variations (Bosboom & Stive, 2015). The larger width of this inlet cross-sectional area, indicates that the bank of the inlet cross section is further away from the point of consideration compare the other designs, which means that reduces the effect of the friction at that point and the tide has a progressive character compare the other cases. However, the inlet cross-section design 6 and cross-section 9 which have the same total area width, give almost the same variations of the water level and a reduction compare the initial state of the system.

Not in all cases the highest water level range coincide with the highest current flows, and this is obvious for the cross section 9. Although, the smaller water level range observed within inlet cross section 9 the flow velocities are larger than the cross section 2 where the tidal range is larger. For that reason, inlet cross section 9 is considered as the primary design for the examination of the rest design elements since the flow velocities are important for the functionality of the system.

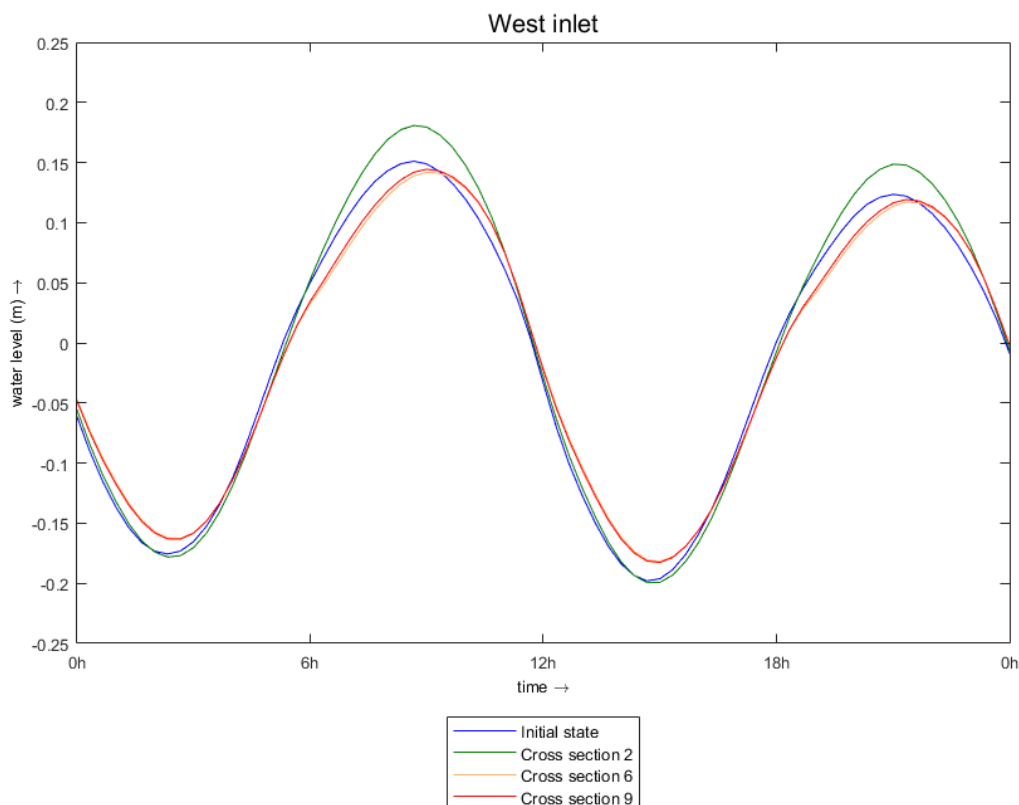


Figure 4-7: Water level variation during spring of the different cross-sectional areas designs within the west inlet.

4.1.3 Approach channel

Tidal prism:

The implementation of the so-called approach channel in combination to the optimal inlet cross-section 9 leads to an increase of the tidal prism, flow velocities and water level conditions within the inlet. Table 4-3 illustrates the tidal prism values for the Lake Bardawil and the percentage of tidal prism within the inlets separately.

An increase of the tidal prism of 4.7 % and 10.4 % from the primary design is observed for all the designs of the approach channel element within the lake and the west inlet respectively. The variables while examining this design element was the orientation and the length of the approach channel. The different design approaches did not influence the tidal prism value. To examine though if the tidal prism can increase much more than this value and different values can be obtained through the four design approaches, the lake is deepened to a large extend, similarly for all the designs. This is done since the depth of the lake is found to affect the tidal prism from the previous research. It is observed that the total average tidal prism in the system can increase to about 12.2 – 15.7 % and specifically to 26.90 - 32.60 % for the west inlet. The lowest percentage, thus 26.90 %, of increase is observed for all the designs based on the approach channels given in Table 4-3 except from design 2 which gave the highest percentage of increase. This design approach has a length equal to 2400 m and an angle 90 degrees from the inlet entrance.

Table 4-3: Tidal prism results related to the approach channel design element.

Design element	Total average tidal prism 10^6 m^3	Spring tidal prism $10^6 \text{ m}^3/\text{tidal cycle}$	Neap tidal prism $10^6 \text{ m}^3/\text{tidal cycle}$	Tidal prism (%)	
				West Inlet	East Inlet
Initial state	59.3	72.1	44.1	44.1	55.9
Base scenario Cross section 9	70.5	87.0	51.1	53.1	46.9
1	73.8	94.3	64.7	55.6	44.4
2	73.8	94.3	64.7	55.6	44.4
3	73.8	94.3	64.7	55.6	44.4
4	73.8	94.3	64.7	55.6	44.4

Flow velocities:

To examine further how the design and implementation of the approach channel is affecting the current flows within the inlets and specifically within the west inlet, the maximum flows are defined, see Table 4-4 and Figure 4-8. An increase of 14 % and 2.5 % from the primary inlet cross sectional area design and the initial state respectively, is observed with the implementation of the approach channel. All the design approaches show the same response to the tidal currents as well. The elongation of the

channel reduces the effect of friction and energy losses and allows the faster tidal flows within the inlet. Furthermore, during ebb flows, the currents are seen to extend far offshore than the case without the approach channel design. This is obvious Figure 4-10. By deepening the lake, the ebb and flood currents increases to maximum 55.7 % and 39.7 % from the base scenario respectively. Furthermore, it is observed that the ebb flows are larger than the flood flows and more than 1 m/s in the west inlet which indicates that the shallow lake is a limitation for the evolution of the system. Nonetheless, the flows remain almost the same within the east inlet.

Table 4-4: Maximum flood and ebb current velocities (m/s) based on approach channel design element.

Cross sections	West inlet		East inlet	
	Max ebb (m/s)	Max flood (m/s)	Max ebb (m/s)	Max flood (m/s)
Initial state	-0.81	0.80	-0.89	0.96
Base scenario	-0.70	0.73	-0.90	0.97
Approach channel	With shallow lake			
All designs	-0.80	0.82	-0.90	0.96
Approach channel	With deep lake			
1	-1.06	0.98	-0.89	0.95
2	-1.09	1.02	-0.89	0.96
3	-1.06	0.97	-0.89	0.95
4	-1.06	0.98	-0.89	0.95

A phase shift of 20 minutes from the base scenario is observed when the peak of the high flow velocities is reached. This shows that the approach channel design not only can increase the flow velocities within the inlet cross section but also reduce the effect of friction. Figure 4-9 shows the ebb and flood currents of the approach channel with and without the deep lake. By deepening the lake, both flood and ebb currents increases within the inlet cross section. It is found that up to 1.25 and 1.52 m/s can be reached during flood and ebb respectively. Furthermore, the ebb flows are extended more offshore while implementing the approach channel design, see Figure 4-10.

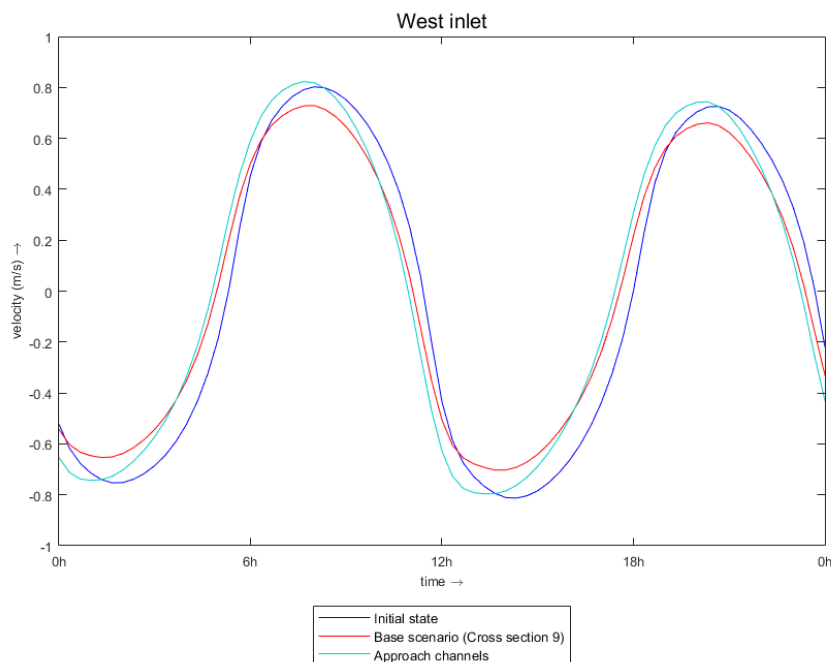


Figure 4-8: Comparison of the cross-sectional velocity between initial state, base scenario and approach channel designs.

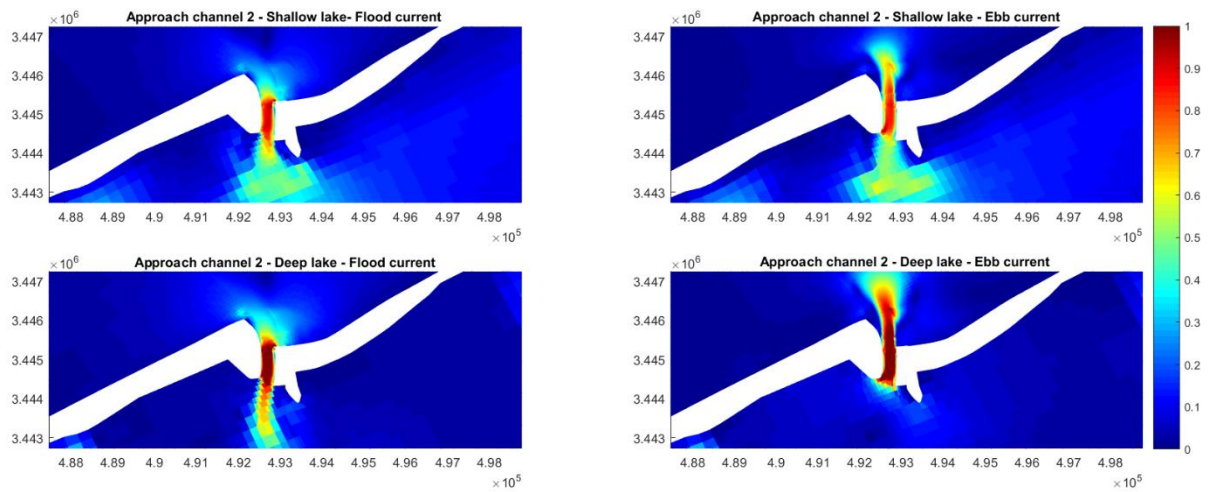


Figure 4-9: Current flows within the west inlet. The velocity magnitude (m/s) is presented during ebb and during flood for the approach channel design 2. The upper left and right figure indicates the approach channel with shallow lake and the bottom left and right the approach channel with the deep lake.

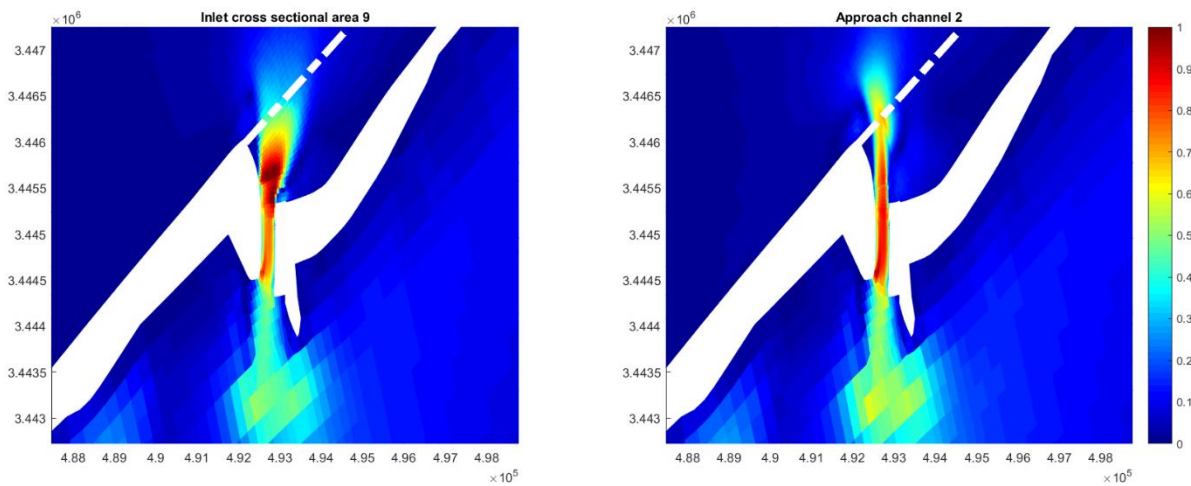


Figure 4-10: Comparison of current flows between inlet cross section design element and approach channel. The white dashed line is the reference line to indicate the extension of the current flows with and without the approach channel.

Water levels:

The water level range increases both during low and high tide respectively within the west inlet, see Figure 4-11. This shows that the implementation of the deep approach channel reduces the friction that act in the water column and thus allows the water level conditions to follow the same path as in more offshore locations. The maximum tidal range at a deepest point of the inlet is 0.40 m compare the 0.32 m obtained with the base scenario.

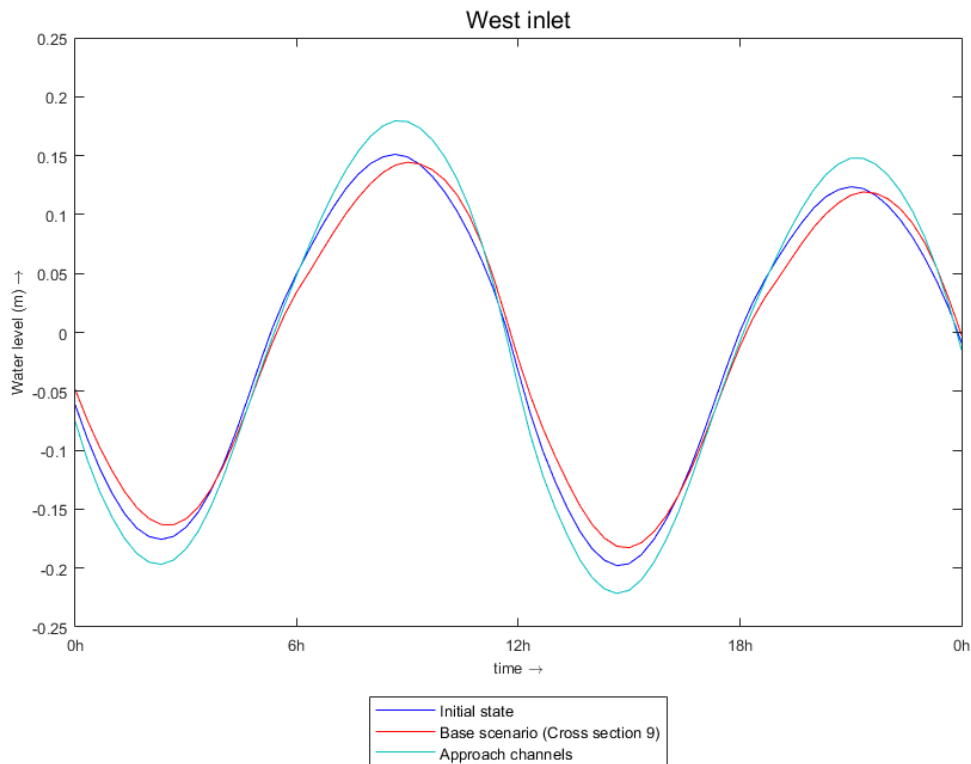


Figure 4-11: Water level variation during spring of the approach channel, initial state and base scenario.

4.1.4 Inlet nourishment

Tidal prism:

The inlet nourishment is examined separately from the approach channel. This is done to understand the response of this element to the hydrodynamics.

Table 4-5 shows the tidal prism results of all the design approaches of the inlet nourishment design element. As can be seen, the inlet nourishment does not positively affect the hydrodynamics within the inlet compare the results provided by Lanthers (2016). Although, a small reduction of about 1.5 % and 3 % from the base scenario of the mean total tidal prism and within the west inlet is observed, the effect of the inlet nourishment is not pronounced in the tidal inlet design. Since all the design approaches of the inlet nourishment have the same position and dimensions but different crest levels, it is considered more reliable to examine further the influence of these parameters.

Thus, the position, the beach nourishment width in combination to the reshaping of the west and east barriers, and the shallow lake are further examined. The followed new design approaches are based on a crest level equal to 0.5 m based on the prevailing wave conditions in the area. These waves while approaching the inlet nourishment measure will tend to become steeper until breaking will occur.

During breaking, waves from NW will tend to create longshore currents which can transport the excess sand of the inlet nourishment. Thus, the design 3 with a crest level equal to 0.5 m is redesigned.

By positioning the inlet nourishment design very close to the inlet entrance, the total tidal prism is reduced to about 7.2 %. Specifically, the mean tidal prism of the lake became equal to $64.25 \cdot 10^6 \text{ m}^3$ with about $31.2 \cdot 10^6 \text{ m}^3$ to enter the west inlet. This is considered as a not beneficial design approach and it is not further examined.

The berm width (beach nourishment) is extended and the west barrier is reshaped. This led to an increase of the tidal prism within the inlet equal to 2 %. Even though, small percentage of increase on the tidal prism might seem insignificant, it is important for the overall design approach. The beach nourishment width is defined approximately equal to 400 m. The western barrier is reshaped to allow a smoother entrance of the tidal flow within the inlet and not to block any tidal current. The final results of the new design of the inlet nourishment, give a tidal prism equal to $69.9 \cdot 10^6 \text{ m}^3$, and $37.19 \cdot 10^6 \text{ m}^3$ passes within Boughaz 1.

Table 4-5: Tidal prism results related to the inlet nourishment design element

Design element	Total average tidal prism 10^6 m^3	Spring tidal prism $10^6 \text{ m}^3/\text{tidal cycle}$	Neap tidal prism $10^6 \text{ m}^3/\text{tidal cycle}$	Tidal prism (%)	
				West Inlet	East Inlet
Inlet nourishment					
Initial state	59.3	72.1	44.1	44.1	55.9
Base scenario Cross section 9	70.5	87.0	51.1	53.1	46.9
1	69.2	85.1	50.3	52.0	48.0
2	69.4	85.4	50.4	50.0	50.0
3	69.2	85.1	50.3	52.0	48.0
4	68.8	84.5	50.1	51.7	48.3

Flow velocities:

Herein, the flow velocities all the design approaches of the inlet nourishment are indicated, see Figure 4-13. The flow velocities are reduced within the inlet entrance with the same rate as the tidal prism values. The new inlet nourishment design, give the same maximum flow velocities as the base scenario, 0.70 and 0.73m/s, which indicates that the inlet nourishment design still does not affect the flow conditions in the area. However, the implementation of the inlet nourishment shows that concentrates the flow energy within the inlet channel such as the design results provided by the approach channel design see Figure 4-12 . The construction of the inlet nourishment might lead to residual eddies which their length scale and magnitude are affected by the width and orientation of the inlet channel (Yang & Wang, 2013). This is obvious when the west barrier is reshaped. The reshaping of the west barrier leads to larger length of the tidal residual eddies and smooth flow during flood, see Appendix D. These eddies can lead to potential changes in water exchange and sediment transport (Yang & Wang, 2013). According to that, the inlet nourishment can lead to potential influence of the water and sediment exchange, however its response to that need further

investigation. Taking into consideration that the inlet nourishment extends the ebb flows further offshore, concentrate the tidal flows within the inlet and lead to increase of residual flows its new design approach is taken into consideration.

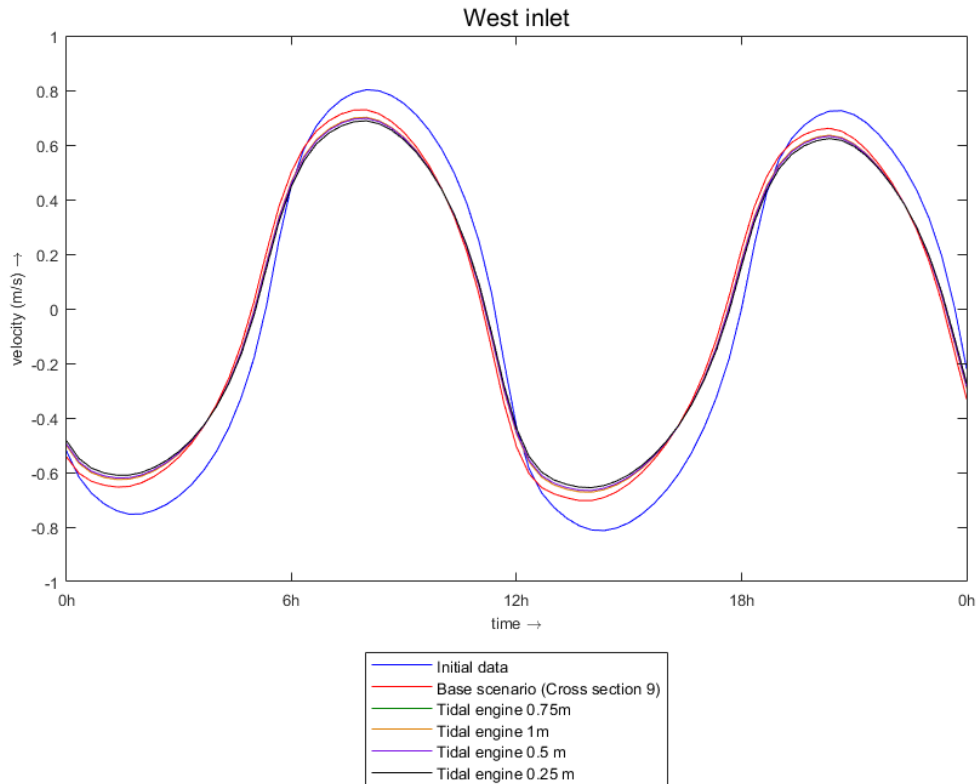


Figure 4-13: Comparison of the cross-sectional velocity between initial state, base scenario and inlet nourishment designs.

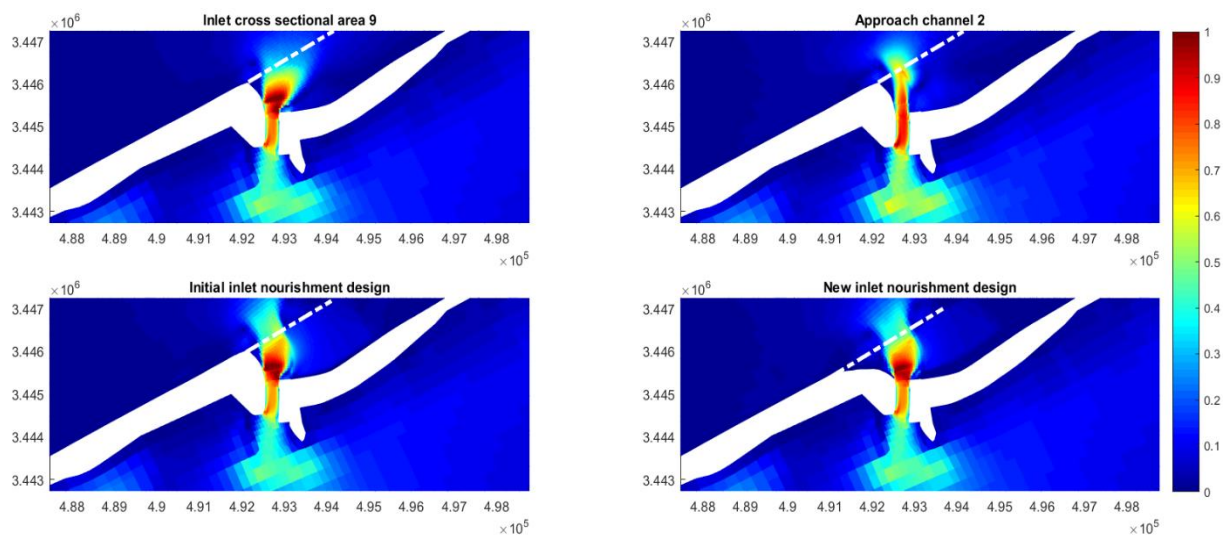


Figure 4-12: Comparison of the current flows between inlet cross section design element, approach channel and inlet nourishment. The white dashed line is the reference line to indicate the extension of the current flows during ebb.

Water levels:

As it is the case for both tidal prism and flow velocities, the water level range decreases while considering the inlet nourishment design. A reduction of the low water level is observed which indicates that the inlet nourishment might block the current flows at the east side of the inlet. However, while changing the inlet nourishment design, the water level range is the same as the primary design of the inlet cross sectional area.

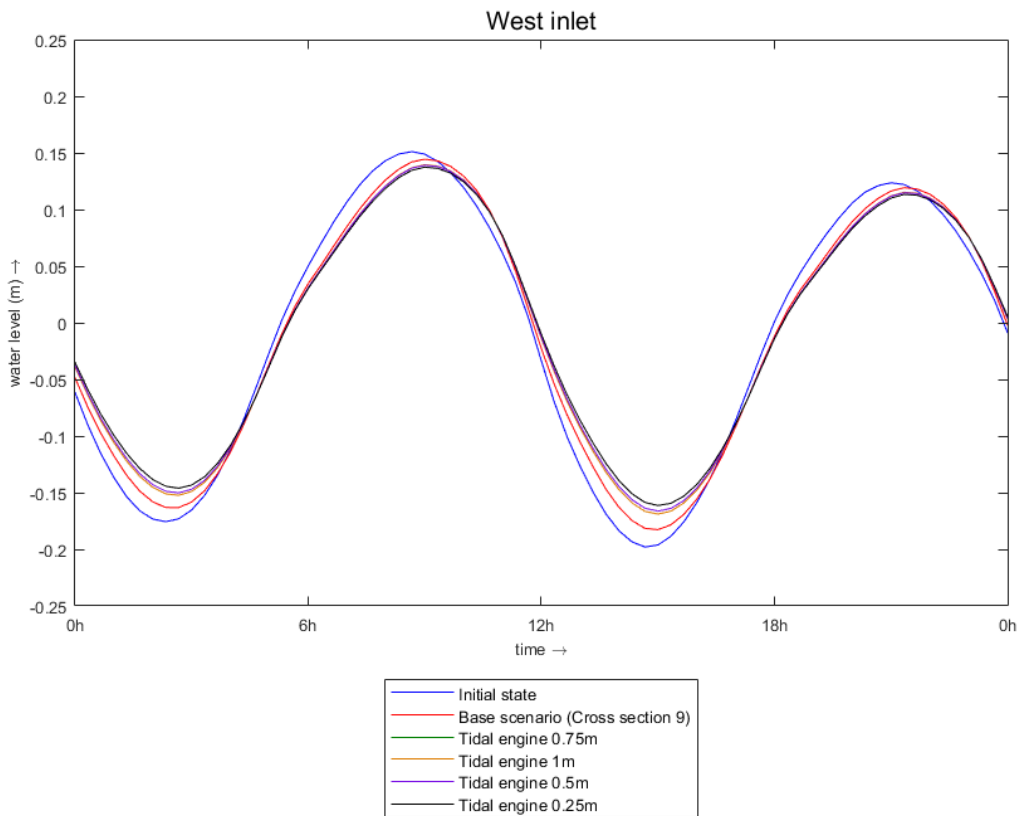


Figure 4-14: Water level variation during spring of the inlet nourishment designs, compared with the initial state and base scenario.

4.1.5 Conclusions and final combined design choice

The final design is selected based on the hydrodynamic response of the west inlet to the associated design elements, see Figure 4-18. To indicate the reason of this design, some concluding remarks for each selected design element are provided.

The cross section which is considered as the primary design for the examination of the approach channel and the inlet nourishment, is the cross section 9 which has a size equal to 2250 m². The asymmetric shape of this inlet cross section provides higher flow concentration at the deepest part of the inlet and its 10 m depth provides an increase of the tidal prism. The tidal prism equal to 70.5 10⁶ m³, in which 53.1 % is within the Boughaz 1 inlet. The flow velocities within the inlet cross section of the Boughaz 1 inlet are equal to 0.7 and 0.73 m/s both during ebb and flood currents respectively. The maximum water level range within the inlet is equal to 0.32 m.

The inclusion of the approach channel with the optimal inlet cross-sectional area design increased the tidal prism to more than 10 %. The orientation and length of the approach channel did not present any difference in hydrodynamics results between the designs, but the deep lake showed that the approach channel 2, with an orientation perpendicular to the west barrier, influence more the hydrodynamics. The shallow lake is defined as a strong obstacle for the representation of the tidal flows within the inlet gorge. The maximum cross-sectional flow velocities are increased to 0.82 m/s during flood and 0.80 m/s during ebb and the maximum water level follows the offshore water level range of 0.40 m.

The inlet nourishment does not lead to extensive increase of the hydrodynamics within the inlet. However, it is observed that the new inlet nourishment design with a crest level equal to 0.5 m and a berm width equal to 400 m in combination to the reshaped western barrier, allows the smooth flow of the tidal wave within the inlet, concentrates the energy within the main ebb channel and extend the ebb current more offshore than the initial case and primary design of the inlet cross sectional area design. For that reason, the new inlet nourishment design is chosen to be combined with the other two elements.

Combining all these design elements together, the mean tidal prism is found equal to **74.0 10⁶ m³** in which about **55.4 %** belongs to the design determined in Boughaz 1 inlet. The cross-sectional flow velocities during ebb and during flood equal to 0.80 – 0.81 m/s respectively in Figure 4-16. The water level within the inlet can reach up to 0.40 m as the offshore water level range. The response of this design methodology efficiently shows the improvement of the functionality of the Boughaz 1 inlet, the west inlet. This is clearly indicated in Figure 4-15.

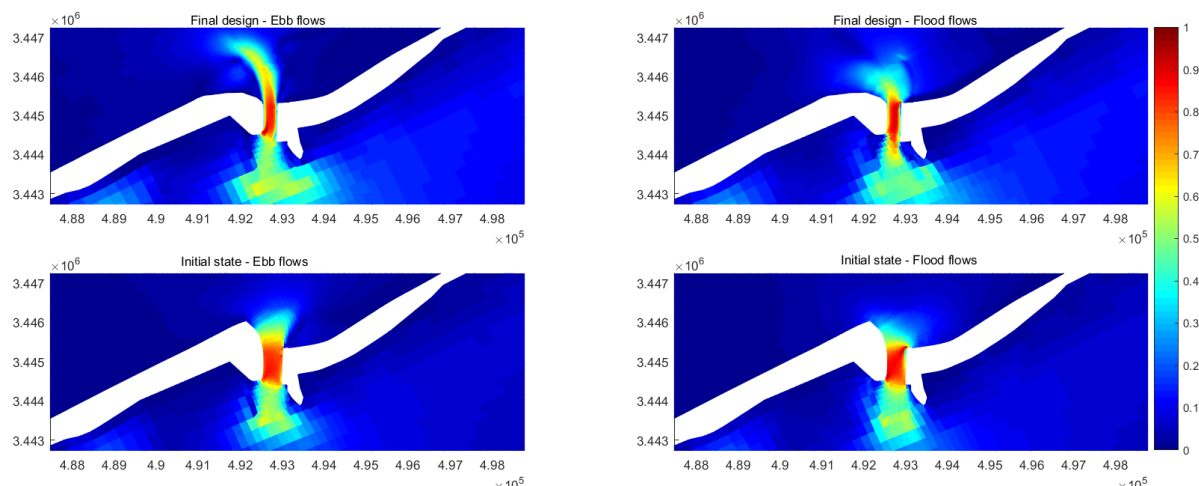


Figure 4-15: Comparison of the current flows between the final state and the initial state of Boughaz 1 inlet.

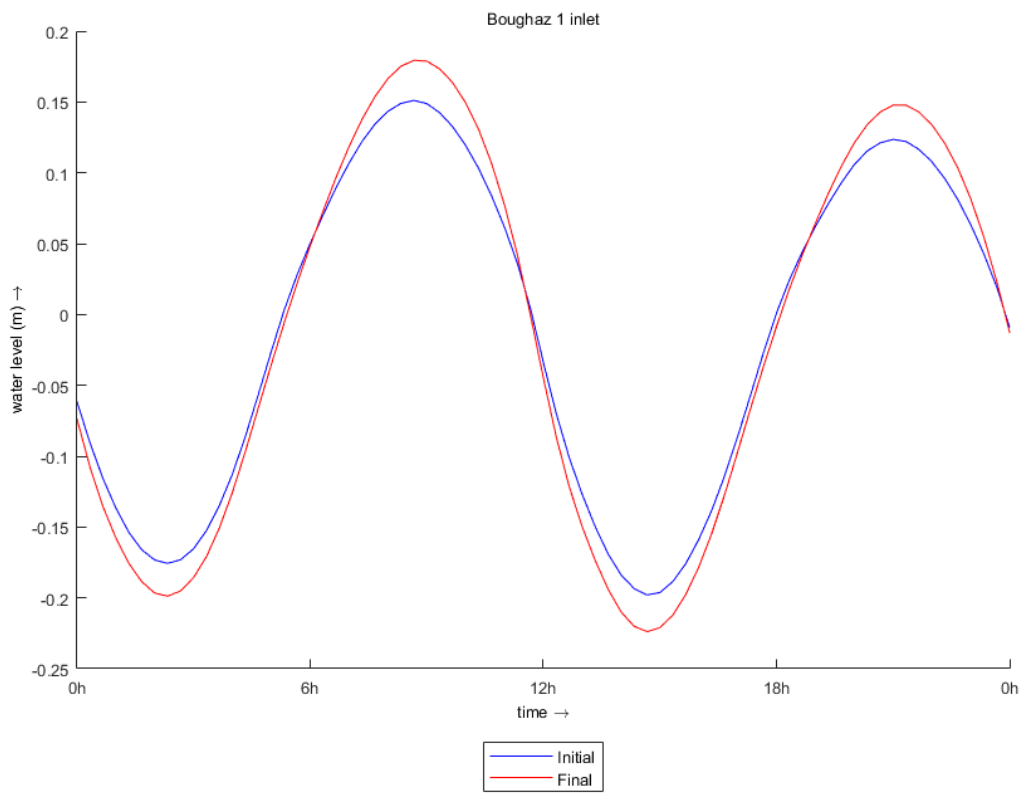


Figure 4-17: Water level variation. Comparison between initial state and final design.

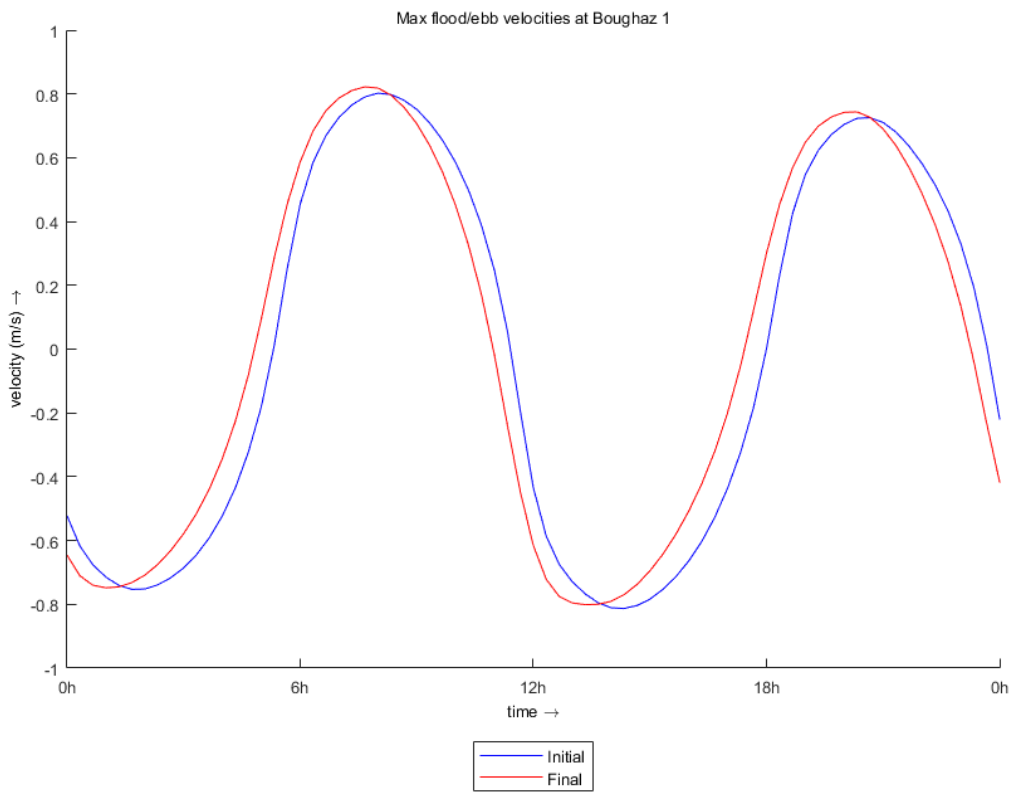


Figure 4-16: Velocity variation. Comparison between initial state and final design.

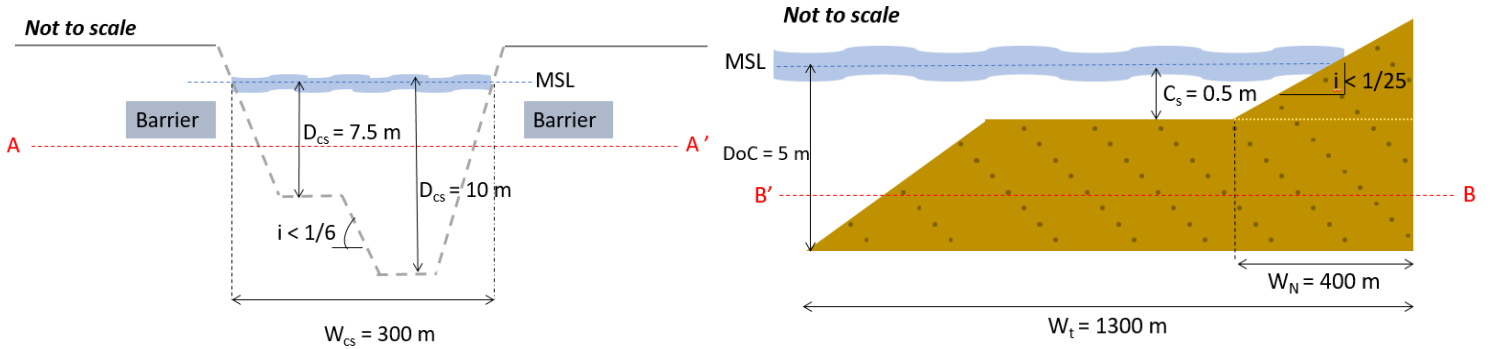
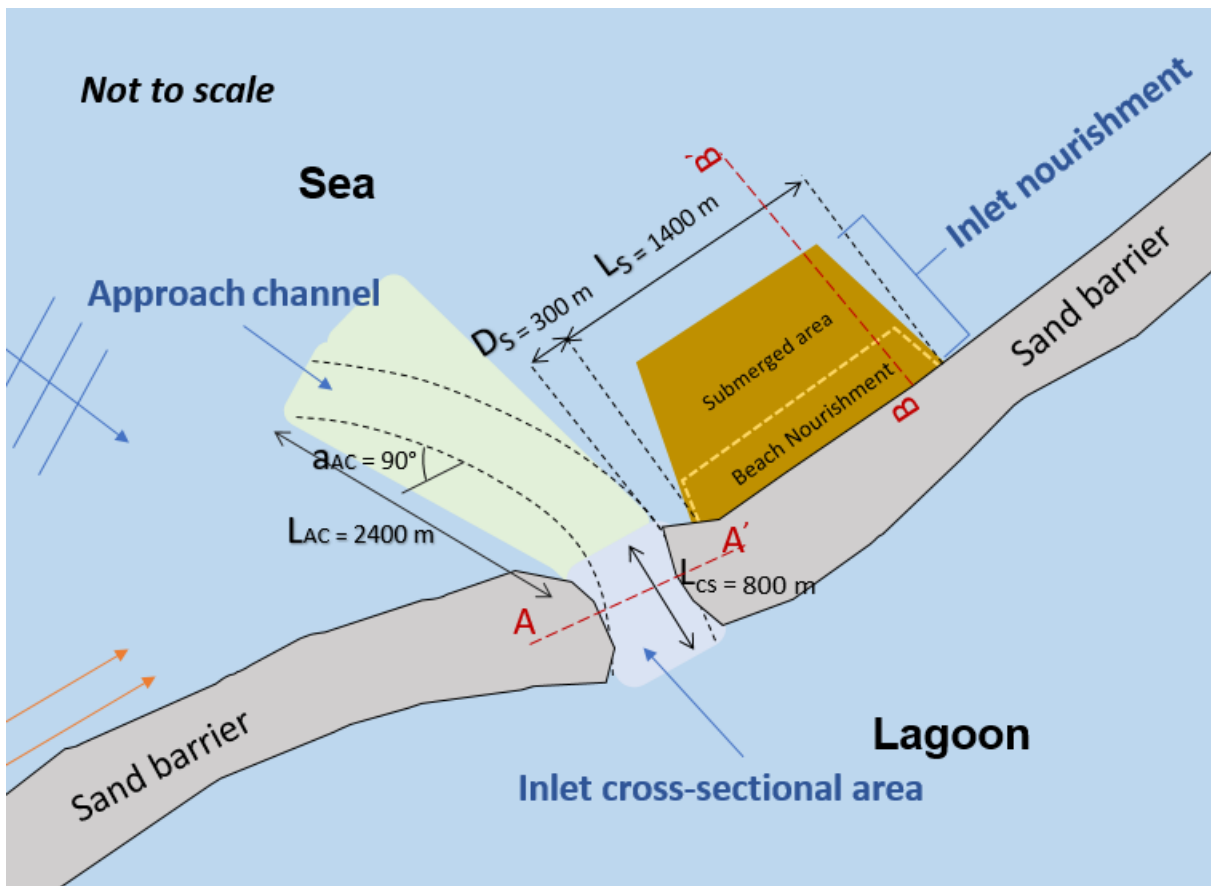


Figure 4-18: Final combined design approach. Determination of the optimal to the hydrodynamics design. Each design element is depicted with the associated defined parameter values.

4.2 Final combined design analysis

The final design determined with the Delft3D FM software is examined further with the inclusion of the waves and sediment properties. The flow chart provided below, illustrates the procedure followed with the Delft3D software. For clarity, the results are depicted with the associated number of the simulation given in the flow chart.

In this section, the hydrodynamics are depicted with the tidal prism values obtained from the model while the morphological effects are illustrated with the control volumes in certain areas. A sensitivity analysis is found crucial since the morphological model predictions cannot be validated. Lastly, a representation of the stability and thus the functionality of the design methodology is given.

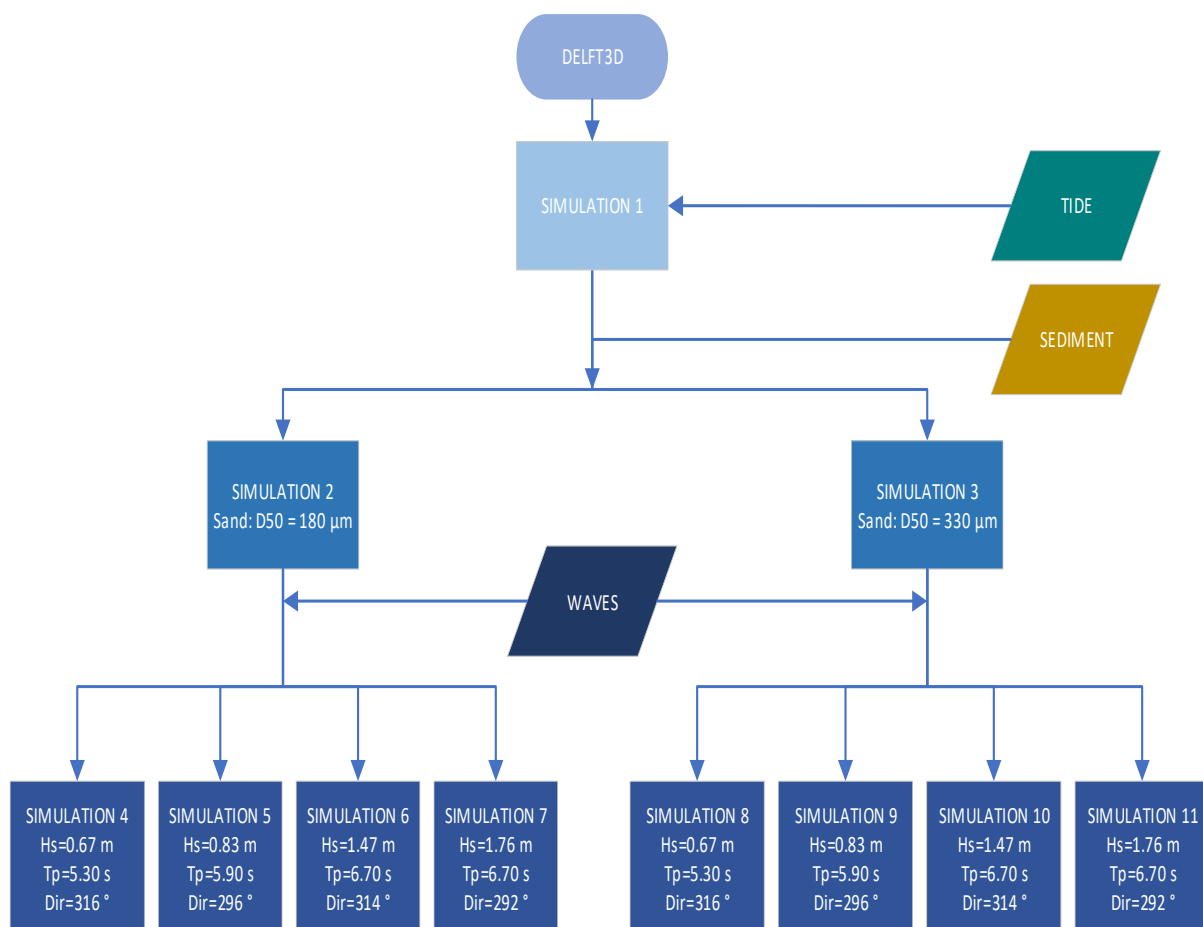


Figure 4-19: Flow chart of the simulation runs within Delft3D.

4.2.1 Hydrodynamics

The tidal prism is an important parameter for determining the water exchange between sea and lagoon. Many studies do not consider the effect of waves while examining the hydrodynamics, however their implementation can deviate the hydrodynamic response of the system. For that reason, it is important to indicate the tidal prism of the total system as well as separately the tidal prism value within the west and east inlets. According to that, the tidal prism of all the simulations is provided to understand how waves as well as the morphological changes with the certain sediment properties impacting the hydrodynamics in Lake Bardawil.

The average, the spring and neap tidal prism within both inlets are calculated. Herein, the average tidal prism values are indicated, see Table 4-6, the neap and spring values can be found in the appendix.

Table 4-6: Average tidal prism for all the simulations carried out with the Delft3D software. With grey colour the tide only case is indicated, while with light blue and orange are the simulations of $d_{50}=180 \mu\text{m}$ and $330 \mu\text{m}$ respectively.

Models	Simulations	Average tidal prism (10^6 m^3)			Percentage (%)	
		Lake Bardawil	West	East	West	East
Delft 3D FM	Final design	74	41.8	33.7	55.4	44.7
Delft3D	1	74.1	43.4	31.4	58.0	42.0
	2	76.9	43.7	33.9	56.3	43.7
	3	74.9	43.5	32.1	57.5	42.5
	4	77.2	43.5	34.4	55.8	44.2
	5	77	43.6	34.2	56.0	44.0
	6	71.5	42.8	29.3	59.4	40.6
	7	75	43.1	32.6	56.9	40.1
	8	74.4	43.2	31.8	57.6	42.4
	9	74.5	43.3	31.8	57.6	42.4
	10	66.5	42.4	24.8	63.1	36.9
	11	71.5	42.9	29.3	59.4	40.6

The first simulation of the Delft3D provides the hydrodynamics of the tide only condition to indicate and validate the hydrodynamics between the two software. Both give identical tidal prism within the lake but a difference of 3.7 % is observed within the west inlet. This difference is obtained due to the grid cell formation within the Delft3D software. The grid resolution is different than the Delft3D FM which indicates that the bathymetry interpolated differently. However, this difference is very limited and since the relative difference between the model results need to be understood, it is conducted as an acceptable condition.

The morphological updating within the model increases the total tidal prism in the area. The total average tidal prism increased by 3.8 and 1.1% when consider a median grain size equal to 180 and 330 μm respectively. Precisely, the tidal prism within the west inlet remains almost the same and most of the increase is observed within the east inlet. This indicates that the east inlet is mostly affected due to that.

Analogously, the wave conditions change the total tidal prism and particularly the tidal prism values within the west and east inlet. To illustrate that, a separation is made between the tidal prism changes found while examining separately the morphological changes of the finer and coarser material.

Based on the morphological changes obtained with the finer material, the total tidal prism, thus the tidal prism within Lake Bardawil, shows no more than 0.30 % increase of the tidal prism with the wave conditions 1 and 2 given in Table 4-6. Although a very small change is observed, the tidal prism value within the west inlet is not affected with these wave conditions (max > 0.45%) while 1.5 % of change from the tide and sediment only condition is seen within the east inlet. Nonetheless, these changes are very limited to indicate that these wave conditions affecting the tidal prism in the inlets. On the other hand, the wave conditions 3 and 4 of Table 3-6, modify the tidal prism values. The total tidal prism changes by 7 % while taking into consideration these wave conditions. Specifically, the tidal prism within the west inlet reduces at maximum by 2 % while the tidal prism within the east inlet reduces at maximum by 13.5 %.

Now focusing on the coarser sediment material, the tidal prism of the Lake Bardawil is reduced to about 0.7 % while considering the wave conditions 1 and 2 compare the small increase obtained with the finer material. This can be explained by the settling time of the finer material. In front of the inlet, more suspension of fines might be seen compare the bed load material and thus these differences are observed between the coarser and finer material. However, these changes are very limited as the case with the finer grain size. The same response is seen with the wave conditions 3 and 4. These wave conditions in combination to the morphological changes decrease the tidal prism by 11.2, 2.5 and 22.7 % in Lake Bardawil, west and east inlet respectively. Again, the east inlet shows to be affected more by the presence of these phenomena while the west inlet does not show any influence with the associated effects.

4.2.2 Morphology

The aim of this study is based on the evaluation of the design methodology while examining the hydrodynamic response of the Boughaz 1 inlet under different design adaptations. The scope of the thesis is to create an innovative tidal inlet design which can improve the functionality of the inlet and can mimic nature. The need to mimic nature is important for the healthier functionality of the system. For that reason, it is of great importance to examine the morphological response of the west inlet. To capture this, the morphological features as described in section 1.1, are indicated by calculating the volume change within different control areas as provided in Figure 4-20. By determining the volume changes within the specified areas, ones can analyse the natural behaviour of the system. Following that, the response of the inlet channel cross section and the inlet nourishment was found crucial to be further described.

The water volume change within the three main areas that can mimic nature is examined. The approach channel in control area 2 in the figure below is further divided into three subareas. These were describing the marginal flood channels and the main ebb channel. The main ebb channel is defined as the deepest part of this control area. This in combination to the control area of the inlet nourishment determine the ebb tidal delta of the tidal inlet system. The control areas 3 and 4 cover the inlet gorge area and flood area respectively.

All the simulations are examined taking as a reference point the initial bathymetry of the model and comparing with the final bathymetrical changes. The net processes are defined as an accretion or erosion within the polygons to provide an inside of the morphological response of the system with the associated wave and sediment data. The choice to provide this method, is based on the lack of validation of the morphological model Delft3D.

Table 4-7 provides the results related to each simulation and accordingly the design element. Erosive features are observed within the inlet, the marginal flood at the left side of the main ebb channel and

the inlet nourishment while accretion is seen within the ebb channel, marginal flood at the right side of the channel and the flood delta.

The inlet channel shows to be affected mostly by the presence of the tide only and specifically with the finer materials. The waves reduce the erosion within the inlet channel entrance as it is in the case of the hydrodynamics. The marginal flood at the left of the ebb channel shows higher erosion when the highest waves approaching the shore both in fine and coarse materials while considering the tide only currents no changes are seen. The same holds for the inlet nourishment. The inlet nourishment is not affected by the presence of the tide currents only scenario, but its shape formed when waves dissipating at this design element. There, the waves approaching the west inlet almost perpendicular and mainly onshore transport is observed within the model. This indicates that the inlet nourishment design might not yield to longshore sediment transport since it is unclear whether the inlet nourishment spread sediment alongshore. Although the flood delta and the ebb channel are accreted, the rate of change is very limited. Lastly, the marginal flood at the right of the main ebb channel is accreted. There, the waves and ebb - flood channels meet each other as a result in settling of suspended material. This is more obvious while indicating finer grain sizes.

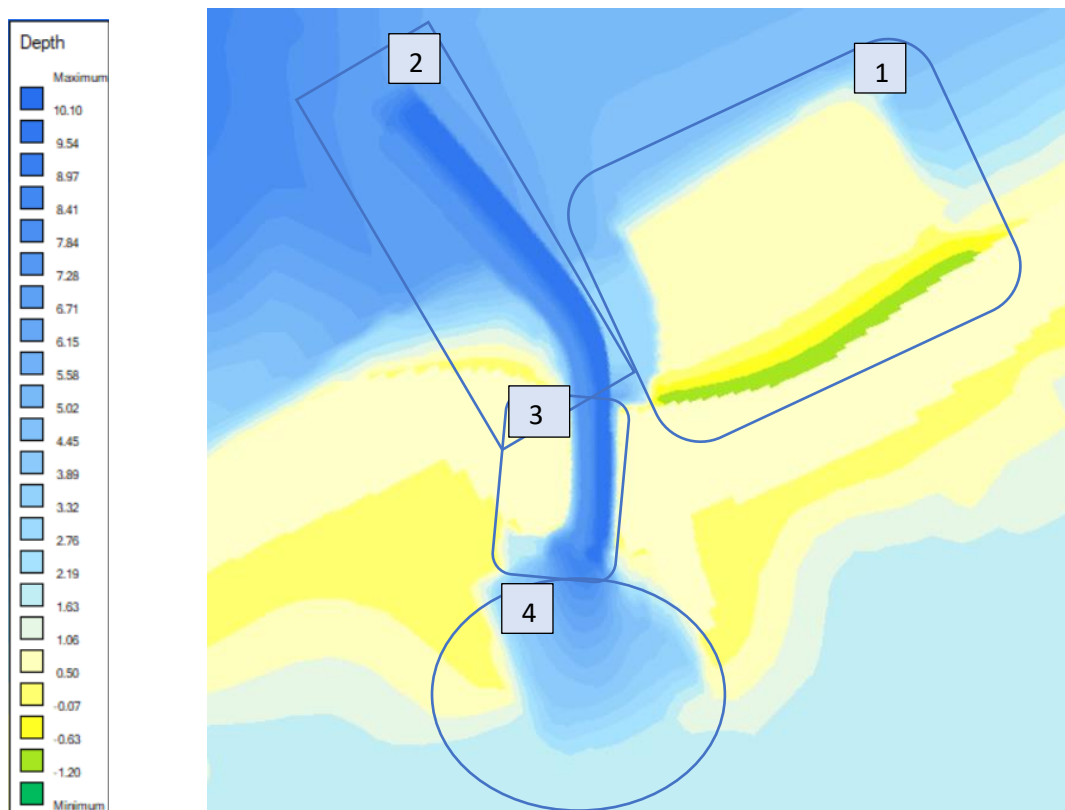


Figure 4-20: Control areas of the most important features in the tidal inlet system. 1 - 2 : Inlet nourishment and approach channel which cover the ebb-delta area, 3: Inlet gorge, 4: Flood delta.

The response of the inlet channel as well as of the inlet nourishment are provided in Figure 4-21 and Figure 4-22 for simulation 7, the related simulation results are provided in the appendix D. The inlet channel is eroded for all the simulations. The inlet is deepened more in the deepest part of the cross section where the flow velocities are larger. The shape of the inlet cross-section enhanced the flows at the deeper part as described in section 4.1.2. Erosion is also obvious at the left side of the inlet cross section while a small accretion is observed at the steeper area as well as in the bank of the inlet cross-section where the flow velocities are smaller. The inlet nourishment design is eroded by the presence

of the waves. At the front slope enormous erosion is observed while accretion is seen landwards which entails an onshore transport process. The onshore transport is related to the angle of approach of the waves. Since the inlet nourishment acts as a headland, and all the wave dissipation is observed at the tip of the design, the highest transport is generated towards the land. However, this behaviour is limited to be evaluated within Delft3D model, see section 4.2.3. Besides that, the DoC concept is validated when examining the morphological behaviour of the inlet nourishment design. No significant morphological changes are observed at this location point. This is more obvious while considering low energy wave conditions.

All these features are representing the morphological evolution of the tidal inlet system and specifically the changes seen within the inlet nourishment and the inlet cross section area. However, the morphological changes at each area of consideration are very limited which do not involving reality. These changes are mainly affected by several morphological factors within the model, such as the current related transport factors, wave related transport factors and the erosion of adjacent dry cells. These are the morphological calibration factors within the Delft3D model. For that reason, a sensitivity analysis is carried out to indicate their effect both in the hydrodynamics and the morphological features of the system.

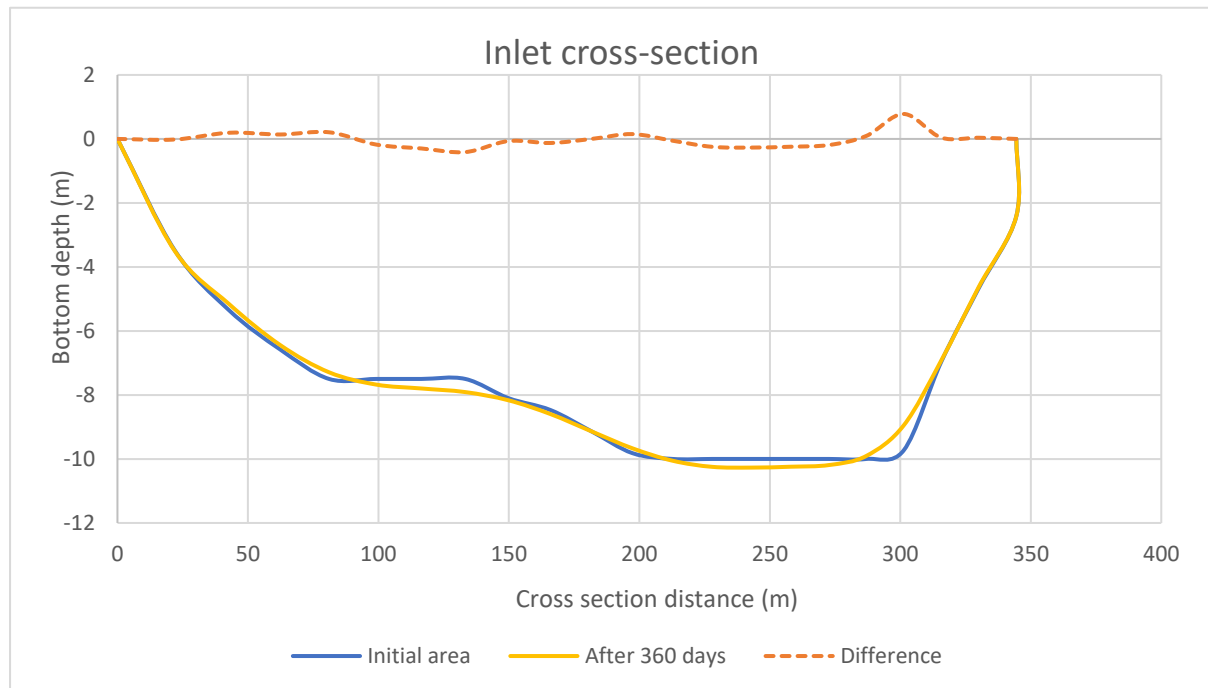


Figure 4-21: Morphological changes of the inlet cross-section of simulation 7.

4.2.3 Sensitivity analysis

The morphological changes are highly determined by different factors within the Delft3D model. Since the model is not morphologically validated due to lack of data, a sensitivity analysis is carried out to determine the effect of these related factors to the adjacent calculate control volume values. The rate of change of the tidal prism is also defined to observe the effect of these factors to the hydrodynamics as well.

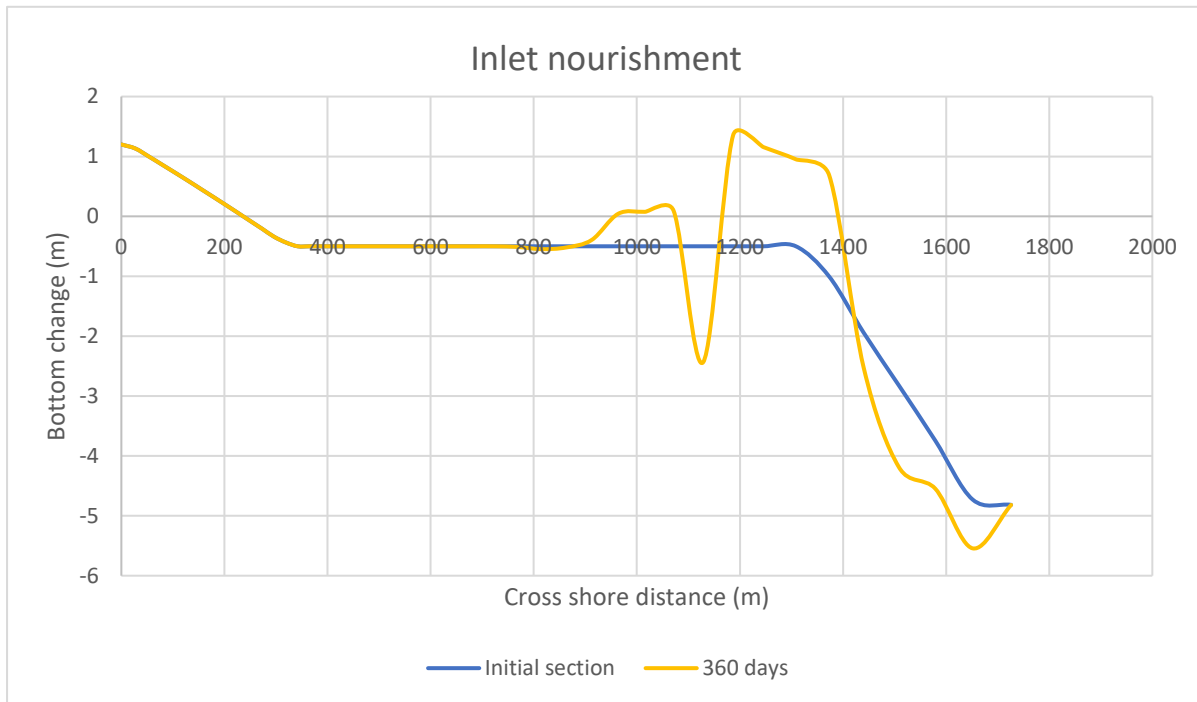


Figure 4-22: Morphological changes of the inlet nourishment of simulation 7.

The default values of the Delft3D and specifically, the wave related suspended and bed load transport are found to be not representative for the morphological changes of the model (Trouw, Zimmermann, Mathys, Delgado, & Roelvink, 2012). The default values increase the onshore transport due to waves in unrealistic manner since the Delft3D model is not capable to consider the effect of undertow. Furthermore, the current related factor which is related to the transport due to currents, increases the sediment transport when this factor is large enough. Lastly, the factor of erosion of adjacent dry cells is related to the redistribution of the erosion to the dry cells. Based on that, a sensitivity analysis of these factors is carried out while examining the effect of the simulations 2, 3, 7 and 11 in Figure 4-19. According to the literature, the parameter values are indicated. The wave related transport factor is found reasonable to be between 0.1 – 0.25, the current related transport factor is used from some studies equal to 10 and 20 while the last factor is chosen to be 0.5 and 1. The tidal prism changes as well as the morphological changes can be seen in Table 4-8 and Table 4-9.

The erosion of adjacent dry cells does not change either the hydrodynamics either the morphology of the tidal inlet system. The erosion of adjacent dry cells, smoothens at some areas the deep scour holes that are created (Deltares, 2011a). The current related transport factor increases the tidal prism of the system to about 6.5%. At maximum of 2.2% increase is observed within the west inlet while 12.5% is seen within the east inlet. Related to the morphological changes, the inlet is eroded by 5.5 % while increasing the current related transport factor. High percentages are also seen in relation to the inlet nourishment and the marginal flood channel. The wave related transport factor, increases the total tidal prism through the lake but almost no increase is obtained within the west inlet. This shows that the waves in combination to the morphological changes do not influencing the west inlet compare the east inlet where an increase of 7.2% is observed when the wave related factor is reduced.

Table 4-7: Control volume changes at the morphodynamic features of the tidal inlet system.

Control volume - Volume of water		Inlet		Approach channel						Inlet nourishment		Basin	
Simulations		Inlet gorge	Change (%)	Marginal flood channel_ left	Change (%)	Ebb channel	Change (%)	Marginal flood channel right	Change (%)	Engine	Change (%)	Flood delta	Change (%)
Initial	Reference volume	1.71E+06		7.43E+06		8.25E+06		4.06E+06		8.66E+06		9810220	
360 days	2	1.74E+06	1.62	7.43E+06	0.00	8.24E+06	-0.13	4.05E+06	-0.33	8.66E+06	0.00	9.79E+06	-0.21
	3	1.72E+06	0.41	7.43E+06	0.00	8.25E+06	-0.03	4.06E+06	-0.15	8.66E+06	0.00	9.80E+06	-0.09
	4	1.74E+06	1.47	7.48E+06	0.63	8.24E+06	-0.12	4.04E+06	-0.56	8.72E+06	0.78	9.79E+06	-0.19
	5	1.74E+06	1.46	7.47E+06	0.52	8.24E+06	-0.11	4.04E+06	-0.43	8.72E+06	0.69	9.79E+06	-0.19
	6	1.74E+06	1.36	7.63E+06	2.73	8.24E+06	-0.16	4.03E+06	-0.72	9.01E+06	4.04	9.79E+06	-0.17
	7	1.74E+06	1.38	7.60E+06	2.27	8.24E+06	-0.15	4.03E+06	-0.70	8.88E+06	2.63	9.79E+06	-0.18
	8	1.72E+06	0.32	7.47E+06	0.59	8.25E+06	-0.02	4.06E+06	-0.15	8.74E+06	0.93	9.80E+06	-0.08
	9	1.72E+06	0.32	7.46E+06	0.43	8.25E+06	-0.02	4.06E+06	-0.14	8.73E+06	0.88	9.80E+06	-0.08
	10	1.72E+06	0.33	7.63E+06	2.68	8.25E+06	-0.04	4.06E+06	-0.08	8.98E+06	3.68	9.80E+06	-0.07
	11	1.72E+06	0.31	7.57E+06	1.90	8.25E+06	-0.03	4.06E+06	-0.17	8.90E+06	2.83	9.80E+06	-0.07
Net Processes			Erosion		Erosion		Accretion		Accretion		Erosion		Accretion

Table 4-8: Sensitivity analysis of the tidal prism.

Calibration factors	Range of increase of tidal prism (%)					
	Lake Bardawil		Boughaz 1		Boughaz 2	
	Min	Max	Min	Max	Min	Max
Erosion of adjacent of dry cells	0	0	0	0	0	0
Current related transport factor	1.9	6.5	0.5	2.2	3.7	12.5
Wave related transport factor	1.5	3.1	0	0.2	3.4	7.2

Table 4-9: Sensitivity analysis of the morphological features within the west inlet.

Calibration factors	Range of change of the control volume area (%)											
	Inlet		Approach channel						Inlet nourishment		Basin	
	Inlet gorge		Marginal flood channel left		Ebb channel		Marginal flood channel right		Engine		Flood delta	
	Min	Max	Min	Max	Min	Max	Min	Max	Min	Max	Min	Max
Erosion of adjacent dry cells	0.0	0.0	0.0	0.0	0.0	0.0	0.0	0.0	0.0	0.0	0.0	0.0
Current related transport factor	2.1	5.5	0.0	3.2	-0.2	-0.5	-0.8	-1.6	0.0	2.6	-0.4	-0.9
Wave related transport factor	0.3	1.3	0.5	0.8	0.0	-0.1	-0.2	-0.8	0.1	0.6	-0.1	-0.2

4.2.4 Stability

To examine the stability, thus the functionality of the depicted design methodology, the stability factor r (P/M) is used, see section 2.2.1. The r factor is determined with the ratio of the tidal prism and the littoral drift in the area. Since the model is validated based on the hydrodynamics, the morphological implications are not considered valid to be applied for determining the longshore sediment transport within the system. For that reason, the littoral drift in Boughaz 1 inlet is taken from different sources found from literature, see section 2.1.2. Dissimilarity is obtained within the determination of the longshore transport patterns in Boughaz 1 inlet from the different studies. This is highly related to the uncertainty of the data used to evaluate the response of the system. However, to understand the feasibility of the design methodology, the P/M ratio is determined with the tidal prism values defined during neap, mean and spring tide and the littoral drift from the two different studies, see Table 4-10. The littoral drift values are found before 1985 thus before the construction of the breakwaters in the Boughaz 1 inlet.

Table 4-10: Stability factor r . P/M ratio defined for the Boughaz 1 inlet.

Initial state					
	P (10^6 m ³)	M ₁ (m ³ /year)	M ₂ (m ³ /year)	P/M ₁	P/M ₂
Neap	19	480000	725500	41	27
Mean	26	480000	725500	54	36
Spring	32	480000	725500	66	44
Final design					
	P (10^6 m ³)	M ₁ (m ³ /year)	M ₂ (m ³ /year)	P/M ₁	P/M ₂
Neap	33	480000	725500	69	46
Mean	43	480000	725500	90	60
Spring	54	480000	725500	112	74

The r factor at the initial state of the west inlet has a value ranging from 27 to 66. This indicates, that the west inlet is characterized mainly with poor stability, to a fair to poor stability during spring. The poor stability of the initial state is governed mainly when the littoral drift is large such as the M_2 in the table above, while with the M_1 and during spring conditions the system can be considered with fair to poor stability. On the other hand, considering the final combined design, the tidal system can be characterized mainly with fair to poor stability. However, the inlet stability can be even be fair during spring with the minimum littoral drift, while poor when the littoral drift is large and neap tide conditions are presented in the area. Comparing though the initial state and the final design of the west inlet, it is obvious that the stability thus the functionality of the west inlet is much better with the latter. The uncertainty of the data though is high which might considerably change the depicted results. Nonetheless, the relative difference between the initial state and the final design to the tidal prism already shows that the increase of the tidal prism lead to higher water exchange and better stability of the west inlet which this highly determines the functionality of Boughaz 1 inlet.

Not only stability, but the bypassing mode can be described with the P/M ratio. The initial state of the system is governed mainly by typical bar bypassing when the r factor is below 50 while above 50 bar bypass and/or tidal bypass. The final design is mainly described with a combination of bar bypass and tidal bypass which indicates that the entrance bars are still pronounced (De Vriend et al., 2002). Since the r factor is between 50 – 150 and the inlet seems to not migrate, the 2 and 3 natural sediment transport mechanism models' type can be observed in the system based on the examples provided in section 2.2.1. It is uncertain whether both models might exist or if one of the two is the most

dominant. This is related to the long term morphological processes and not accurately definition can be provided.

However, considering the morphological processes calculated in section 4.2.2, and the assumption that the inlet throat is not allowed to migrate within the modelling, an explanation of the possible dominant by-passing mechanism presented in the inlet can be given as follows. Firstly, neither the inlet nor the main ebb channel are migrating. An erosion is observed within the inlet while small accretion is observed in the main ebb channel for a year of simulation period. This accretion might be presented due the behaviour of the inlet channel. Furthermore, onshore sediment transport is observed with the considered wave conditions. These characteristics are highly correlated to the morphological behaviour of stable inlet processes model, model 2 in Figure 2-10, which indicates that this might be the dominant natural bypassing mechanism in the Boughaz 1 inlet with the associated design methodology. Nonetheless, this need further research to be validated.

5 | Discussion

Reflecting upon the available data, the assumptions that are considered, the design procedure and the modelling approaches that are followed some remarks should be provided. These are important indications for assessing the limitations, possible errors and uncertainties might exist within this thesis. In this chapter, the limitations, assumptions as well as important points of consideration are provided.

5.1 Available data

There is a great lack of data in Lake Bardawil. These include the bathymetrical data and sediment properties in the area. The offshore bathymetrical data are obtained from the European Marine Observation and Data Network (EMODNET) while for the more nearshore and inside to the lake data a depth map is used, see Appendix B. However, there are a lot of uncertainties whether this map is the most recent one, since it is reported that these bathymetrical features are found between 1856 and 2001 (Lanters, 2016). Although the hydrodynamic response of the system showed high correlation with the available data in literature, there are concerns regarding the morphological response of the system due to bathymetry. Furthermore, the sediment properties found from literature are based on sediment samples taken during 2009, (Piere, 2016). Since the dynamic changes of the system are seen throughout the years, the composition of different sediment properties might have been changed. Lastly, the deviation between the longshore sediment transport values found from literature is extremely large which enhance the uncertainty of the available data in the area.

5.2 Methodology

Herein, a discussion related to the methodology followed through the thesis is made. Precisely, a discussion to the entire project itself is given and then emphasis is provided to the topic of this thesis, thus in Boughaz 1 inlet.

Project description – Lake Bardawil:

As described in chapter 2, Lake Bardawil comprised by three inlets. The two are man-made inlets while the last is natural and is closed due to sedimentation. The project itself contains three different inlets which are important for the functionality of the whole system and the interaction between them. The natural inlet is not taken into consideration due to its small dimensions and the indication that seldomly is considered open. In this thesis though, focus is put on the one of the other inlets, the Boughaz 1 inlet, but it was found crucial to indicate the hydrodynamic response, related to the tidal prism, of the Boughaz 2 inlet due to the interactive relation between these systems. However, due to the limited time no further research is done to the hydrodynamic behaviour of the Boughaz 2 inlet and its response is found significant for the precise representation of the functionality of the Boughaz 1 and the Lake Bardawil.

Topic description – Boughaz 1 inlet:

The topic of this thesis is based on the design methodology of three design elements considering mainly the hydrodynamics through Boughaz 1 inlet and observing at the last phase its morphological and stability features. In general, the hydrodynamics and morphodynamic are broad fields which can extend to different subsets. However, due to limited data within this thesis focus and extensive research is done in the hydrodynamic field and the morphological part is based on estimations of control volume changes to obtain the tidal inlet features. Subsequently, the longshore sediment transport patterns, littoral drift, are not calculated and representation of the stability of the system is based on the available data from literature which involves uncertain results.

Stability relationships:

Focusing on the design methodology of the Boughaz 1 inlet, each design was based either of previous researches either on stability criteria such as the Escoffier criterion and the r factor defined by Bruun and Gerritsen (1960), Bruun (1978). Although, there are several stability approaches such as the A-P relationship provided by O'Brien, see Appendix A, which is well known and accepted, the uncertainty to indicate the exact values of the C , q coefficients is considered an important part for not take into

account this formula. Even if for different conditions and places all over the world these parameters have been determined, within the Mediterranean Sea no (yet) values are indicated which shows that one of the most important stability relationships cannot be considered accurately. On the other hand, Escoffier represents the stability of the system with the equilibrium flow velocity (~ 0.9 m/s). According to R. Brouwer, Van De Kreeke, and Schuttelaars (2012) the equilibrium flow velocity provided by Escoffier is related to the littoral drift and the cross sectional area. This indicates that according to the area of consideration different equilibrium flow velocities can be adapted which can be either larger or lower than the value illustrated generally by Escoffier. This introduces the uncertainty of the empirical relations to quantitatively indicate the design adaptations of nature and time varying elements, such as the inlet cross sectional area.

Another important limitation with respect to stability conditions is that Boughaz 1 is one of the two presented inlets in Lake Bardawil. This means that the Lake Bardawil is a double inlet system and cannot be evaluated separately with respect to the stability conditions. The examination of the stability within multiple inlet systems is examined analytically and numerically with O'Brien relationship and Escoffier's stability concept but with several adaptations to that. To determine quantitatively the exact inlet cross-sectional area the O'Brien relationship can be used when all inlets are phenomenological similar with respect to the wave driven littoral drift, tidal characteristics, sediment properties and similar geometrical features (Bosboom & Stive, 2015). Furthermore, Escoffier (1940) assumed uniform water level fluctuations within the basin to determine the stability of a double inlet system (R. L. Brouwer, Schuttelaars, & Roos, 2013). However, these conditions are not presented in Lake Bardawil and high deviations might exist for the precise determination of the inlet cross-section size. The concepts though are applicable and an insight into the response of the cross-sectional design can be found.

Design simulations and sequence:

The total design simulations are based on different parameters such as the width, depth, of the three design elements respectively. Although, the number of combinations that have been done can be considered high enough for the representation of the design elements, there is a relatively wide range of values that can be assessed. The choice to apply the specific design conditions is based on the design requirements, previous works and criteria, which are considered important for the best assessment of the requirements of the system.

Another aspect which is important for a design methodology is the assessment of the defined design under different conditions. In this thesis, focus is put on the evaluation of the design under the functional requirements of the inlet system. However, the objective of a design process is to define a concept which not only complies the functional and structural requirements but also is feasible under cost-benefit ratio, social and legal acceptance.

5.3 Modelling

Delft3d FM → Delft3D

As described in Chapter 3, two different structure software are used. The model in Delft3D FM software was provided by the company and it was validated based on the hydrodynamic conditions in the area. This model is constructed with unstructured grid for flexible and better resolution along the boundary of the system. All the design combinations are examined with this software. However, the Delft3D FM is under beta testing and the implementation of morphological features as well as the wave forcing was not possible to be done. For that reason, the structured based software, Delft3D, is constructed which is fully validated and calibrated through the years. Even if the results of the final

design were found to be similar, except of a minor difference between the inlets results, the structured form of the grid within the Delft3D limited the resolution at the curvy locations of the land boundary.

The larger flow grid of the Delft3D FM was changed to a smaller flow grid in the Delft3D software due to high computational time. The grid construction requirements in combination with the computational efficiency of the model did not allow the same grid resolution in the area of interest within Delft3D. The bathymetrical samples from Delft3D FM are interpolated to a different resolution grid in the Delft3D model. This might lead to inaccuracy of the model results specifically to the morphological updating. However, the errors are not observed in the hydrodynamic results which are considered of crucial importance.

Delft3D model set up

The input parameter values within the Delft3D model are kept the same as the Delft3D FM to avoid any differences in the model results. This showed that indeed the models are able to provide the same hydrodynamic results.

The grid is formed with the same manner as within the Delft3D FM, thus the grid cells did not cover the land boundary surface area. Though, this did not allow the morphological migration, if any, of the inlet.

The model results based on the morphological parameters, such as the wave and current related transport factors, the sediment formulas, the sediment thickness etc, are case sensitive in the model. Since the model results related to morphological changes were not able to be validated due to high lack of data, sensitivity analysis is carried out. The sensitivity analysis based on the calibration factors provided in the model showed that the model results vary. The wave related transport factors are mainly influence the cross-shore transport while the current related transport factors the longshore movement. High values lead to high transport processes and the default values are found to be not representable mainly for the cross-shore transport processes which the model is not capable to reproduce well enough.

Input reduction technique:

The input reduction technique that is used to involve four different wave conditions in the model is based on the energy flux input method. Since no available sediment properties were exactly known this method was considered the most applicable one. The direction and the significant wave height were the most important parameters for the binning method. However, the assumption to apply four wave conditions in the model do not represent reality. In most cases 10-12 wave conditions are applied to model the morphodynamic development of an area with an input reduction method based on sediment transport processes. However, since this thesis mainly focus on the tidal prism values and the tidal flow currents, the target for the input reduction method is to examine the brute forcing of these four wave conditions and not the exact representation of the morphological effects to the system, thus, these are considered reasonable assumptions.

6 | Conclusions – Recommendations

In the final chapter of the thesis, concluding remarks and recommendations are provided. Initially the main question is answered and is further analysed by providing the answers of the sub questions given in chapter 1. The second part of this chapter, illustrates several recommendations related to the improvement of this thesis, as well as further research that might be needed.

6.1 Conclusions

Different design adaptations have been applied in tidal inlet systems worldwide to improve their functionality. Some of them are related to the implementation of hard structures while others are related to the yearly dredging operation maintenance works. This is applicable to the design approaches followed in Boughaz 1 inlet in Lake Bardawil. The inlet is subject to a reduced tidal prism over the passing years, resulting in poor water quality in the lagoon, limited fish migration from the sea and sedimentation causes the need for dredging maintenance works. Although, the dredging maintenance works and constructed breakwaters can minimize the abrupt sedimentation through the inlet and provide more stable conditions in the short term, the natural behaviour of the system is gradually changing which might worsen these conditions in the longer term. For that reason, the aim of this thesis is the determination of an innovative design and associated methodology which is based on natural design elements and can improve the functionality of the Boughaz 1 inlet.

The conclusions arisen from this thesis are provided following the main research question and the associated sub questions:

Can the functionality of Boughaz 1 inlet be optimized by mimicking nature?

The functionality of the system is highly related to the increase of the tidal prism, flow velocities, water level condition within the inlet, and the need to mimic nature such as the associated problems to be prevented and/or to be minimized. The design methodology is essential for determining and sizing the important natural design elements which highly influence the functionality of the system. Each natural design element, namely inlet cross-sectional area, approach channel and inlet nourishment in combination with their different design parameters and adaptations is designed to positively influence the response of the Boughaz 1 inlet. Numerical models (Delft3D and Delft3d FM) are used to assess the influence of the different designs on the functionality of the system.

The depth of the lagoon and the orientation of the barriers are found to be crucial factors that determine the tidal prism and flow velocities in the system. The procedure to select a combined design is found valuable for the improvement of the hydrodynamic response of the Boughaz 1 inlet since the tidal prism exceeded 60 % compared the initial state. Furthermore, the flow velocities and the water level within the inlet are increased with the specific design approach. The former is calculated equal to 0.81- 0.80 during flood and ebb respectively, while the latter is found equal to 0.40 m. The hydrodynamics of the selected design are not affected by sediment properties and wave conditions. This entails that the design methodology that is adapted to a tide dominant system is appropriate. The aim to mimic nature is validated with the examination of the erosion and deposition patterns of the selected design. However, further research is needed to understand extensively the detailed morphological behaviour of each element on longer timescales. This will assess the period of the maintenance dredging works as well as the bypassing mode of the system.

To provide detail to the answer given above the conclusions are elaborated using the associated sub-questions below:

- Which are the most important elements that can mimic nature?

The inlet cross-sectional area and the approach channel, extensively determined the hydrodynamics within the tidal inlet systems, referring to the water exchange, stability and ecology of the system (Escoffier, 1977; van de Kreeke & Brouwer, 2017). Additionally, an inlet nourishment is found essential for the increase of hydrodynamics and reinforcing of the coast while mimicking nature.

This indicates, that the inlet cross-sectional area, approach channel and an inlet nourishment are important design elements for the functionality of Boughaz 1 inlet. The first two are directly related to the tidal prism, flow velocities and water level conditions of the system and thus found to be important (Bosman & Lanter, 2018). The inlet nourishment is a combination of a beach nourishment with a submerged shoal is not regularly implemented near inlet entrances. However, previous studies showed that this design can lead to potential increase of the hydrodynamics and thus is considered as an important element as well. The implementation of these elements in Boughaz 1 inlet can be seen in the following figures.

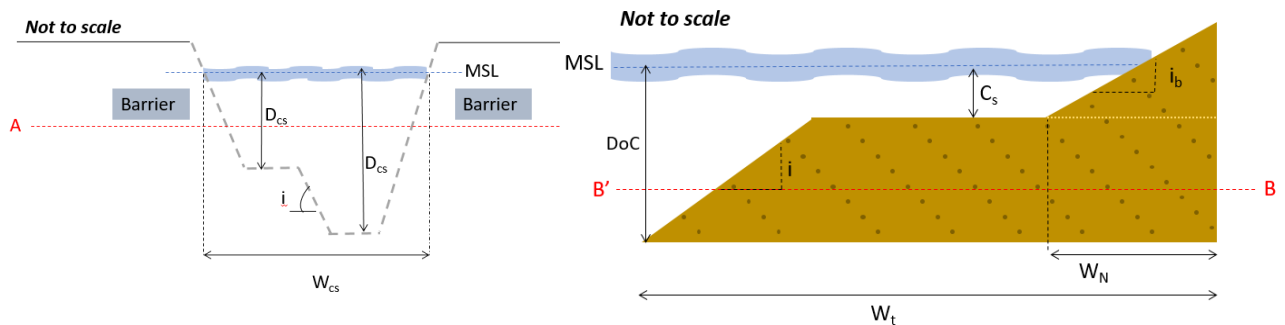
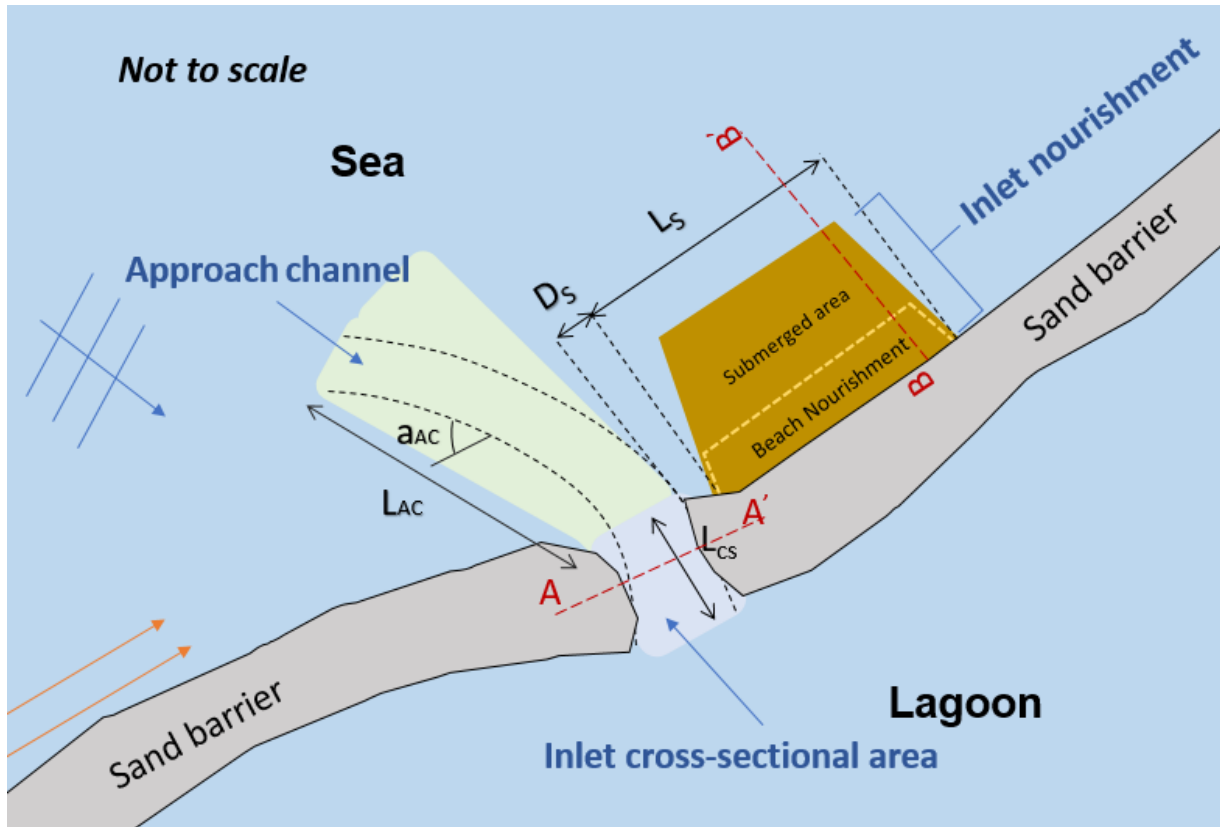


Figure 6-1: The most important design elements which can mimic nature with their associated parameters.

- **Which parameters affect the hydrodynamic response of each design element?**

Each design element is determined by several design parameters. These are defined based on the stability criterion provided by Escoffier, the depth of closure criterion, the design limitations given from The Weather Makers company and from previous works resulting in a certain range of values of each design parameter.

It is found that the size and shape of the inlet cross sectional area are important parameters for the increase of the tidal prism and tidal flows respectively. The largest inlet cross sectional area led to the larger tidal prism while an asymmetric, narrower and 10 m depth cross-sectional area led to the higher flow velocities, more than 1 m/s at the deepest parts.

The response of the approach channel is well understood when the depth of the lake is increased. This showed that, a perpendicular to the west coast channel orientation provides larger tidal prism, higher flow velocities and water level range in the inlet.

The width of the inlet nourishment was found to be an important parameter for the functionality of the system. The increase of the beach nourishment width in combination with the reshaping of the western barrier were essential for positively influence the tidal prism and flow velocities within the inlet cross section. The total width of this design, in the cross-shore direction, is validated with the associated criterion of depth of closure.

- **What combination of design element can optimize the functionality of Boughaz 1 inlet and what us the final combined design choice?**

Different design adaptations are found important for understanding how to improve the functionality of Boughaz 1 inlet with the three defined natural elements and with a final combined design choice. Each design element is influenced by different parameters. The design adaptations to these parameters are related to several criteria and requirements. To that, a specific range of values are determined to identify the different design configurations for each natural design element. In a tidal inlet system though, the natural elements are highly influenced by each other. Thus, the followed design methodology for each design element and their associated design configurations is stated with a certain sequence to identify a selected design:

1. Inlet cross sectional area

In total nine different design adaptations of the inlet cross sectional area have been examined. An inlet cross-sectional area with a size of about 2250 m² is considered as the primary design for the assessment of the approach channel and inlet nourishment. The chosen design is considered the one which improved the functionality of the Boughaz 1 inlet, related to tidal prism, flow velocities, water level conditions and satisfies the design requirements. With this specific inlet cross sectional the tidal prism is increased by 43 % from the initial state and provided flow velocities equal to 0.73 and 0.70 m/s during flood and ebb respectively while the water level range is calculated equal to 0.32 m. In this scenario, flood dominated processes are observed.

2. Approach channel

The cross-section design of the approach channel followed the design of the inlet cross sectional area of 2250 m², while with sensitivity analysis its orientation and length have been determined. It is found that the lagoon depth is an important factor for choosing the most efficient design adaptation for this element. Deepening the lagoon, the tidal prism and flow velocities have been increased substantially for all the design adaptations and ebb dominant conditions are observed. Three out of four designs

show the same response while one responded differently. This is related to the approach channel which is perpendicular to the western barrier, has a length of 2400 m and same cross-sectional dimensions as the inlet cross section. With this design approach, the tidal prism is increased by 36 % more than the inlet cross section design only. Without taking into account the deep lagoon case, this design increased the tidal prism more than 10 % from the inlet cross section area design only. The flow velocities became equal to 0.81-0.80 m/s during flood and ebb respectively which shows that the system reaches slowly equilibrium conditions. The water level range at the deepest point of the inlet cross section reached the value of 0.40 m.

3. Inlet nourishment

A large-scale nourishment at the east side of the inlet entrance, with a submerge shoal, did not affect the hydrodynamics of the system in this thesis, but seemed to be important for the concentration of the current flows within the inlet cross-sectional area. A new design approach is considered essential for further assessment of this element by examining its position and its width. The new width of the beach nourishment and the reshaping of the western barrier are determined as important parameters for the increase of the tidal prism to about 2 % and seem to smoothen the tidal flows within the inlet entrance. This new design approach is based on the increase of the beach nourishment width equal to 400 m while the western barrier is reshaped to align both sides of the inlet.

4. Final combined design

All these design adaptations are combined to provide the final design choice. The exact values of each parameter can be seen in the table below. The final combined design choice gave a tidal prism 61 % larger than the initial state of Boughaz 1 inlet, flow velocities equal to 0.81-0.80 m/s and a water level range 25 % larger than the initial state. This demonstrates the improvement of the functionality of the Boughaz 1 inlet.

Table 6-1: The determined parameter values for the final combined design of the initial phase of the design methodology.

Design parameter		Design element		
		Inlet cross sectional area	Approach channel	Inlet nourishment
Length	Lcs (m)	800	-	-
Width	Wcs (m)	300	300	-
Main depth	Dcs (m)	7.5/10	7.5/10	-
Length channel	Lac (m)	-	2400	-
Orientation channel	Aac (°)	-	90° from western barrier	-
Position from inlet entrance	Ds (m)	-	-	300
Length nourishment	Ls (m)	-	-	1400
Width beach nourishment	Wn (m)	-	-	400
Total width beach nourishment	Wt (m)	-	-	1300
Crest level	Cs (m)	-	-	0.5
Underwater Slope	i	<1/6	<1/6	<1/6
Above water Slope	ib	-	-	<1/25

- **How sensitive are the hydrodynamics associated with the selected design of the Boughaz 1 inlet to certain sediment properties and wave conditions?**

Focusing on the design followed in Boughaz 1 inlet, the implementation of the sediment properties in the model do not significantly change the hydrodynamics of this inlet. Limited changes are observed for both grain sizes, 180 and 330 μm , which did not exceed the 0.70 % from the tide only condition. The design methodology followed in Boughaz 1 inlet, showed not to be affected by the implementation of the waves. A maximum decrease of 2.5 % of the tidal prism is observed for both sediment properties and all the wave conditions respectively. This case is indicated with waves that approaching the design almost perpendicular and two sediment properties presented at the west side of the inlet entrance.

- **How sensitive is morphology associated with the selected design of the Boughaz 1 inlet to certain sediment properties and wave conditions?**

The ebb-flood delta system created in the model shows that the design in Boughaz 1 inlet can mimic nature. Specifically, within the inlet cross sectional area erosion is observed, the approach channel shows limited accretion while erosion is seen in the inlet nourishment. At the east side of the main ebb channel, a swash bar is formed, which shows the high interaction between wave and tidal currents. The morphological changes within the inlet are mainly influenced by the tidal currents and thus the design system can be characterized as a tide dominated while the inlet nourishment design is highly affected by the presence of the prevailing wave conditions.

- **Is the stability related to the functionality of the Boughaz 1 inlet system, improved in the new design?**

In this assessment, the stability is defined with the stability factor provided by Bruun and Gerritsen (1960). The stability factor provides the ratio between the tidal prism (P) and littoral drift (M). The M is taken from literature in two periods of year where the gross longshore transport processes are determined. Although, there is a high uncertainty whether this M is reliable to be considered, the P/M ratio in Boughaz 1 inlet has increased with the specific design methodology. This P/M ratio shows that the stability with the new design approach can reach the fair conditions, which is two levels more than the initial state of the inlet. During neap and high littoral drift the design methodology has a poor stability while during spring and same littoral drift the stability becomes fair to poor. However, if the littoral drift is less the stability increases substantially, up to fair conditions, which indicates that relative to the initial state there is greater system functionality. The bypassing models 2 and 3 might exist in the area, with the first to be judged as the dominant one. However, more observations are needed to accurately provide this conclusion.

6.2 Recommendations

In this chapter some recommendations are provided. These are related to the improvement of this study as well as future work might be needed.

- **Field observations and data survey**

The high lack of data in the area is highly affecting the accuracy of the results. Field observations are essential to provide detail information regarding the waves, wind, tides, tidal currents, littoral drift, salinity and temperature in the area. Furthermore, bathymetrical and sedimentary survey are needed to provide correctly the up to date depth and sedimentary maps. These will effectively can be gathered as an input in the model for adjusting the reality.

- **Design methodology:**

The design stage is an iterative process which in the engineering field no absolute solution can be found simultaneously but relative best solution can be the base for proceeding to the detail design. The first step to determine a design are the objectives of the project. Since this thesis is an extension of the work done by Lanthers, the design methodology is based on several design requirements and criteria, the stability related relations to enhance the water exchange and mimicking nature conditions. These requirements led to an optimal conceptual design which efficiently can improve the water exchange and flows within the inlet, that meets the functional requirements of the design process. However, the final combined design is defined based on specific sequence and with narrow range of values while different sequence and wider range of values can be examined as well. One of this can be based on the construction phase that is followed in field, thus the examination of the design approach channel first, then the development of the inlet cross-sectional area and finally the implementation of the inlet nourishment.

Furthermore, the design methodology is based on the initial phase of a design process and the assessment of the design under its functional requirements. However, it is important to examine the design also in terms of cost-benefit conditions, social and legal acceptance. This is essential for the accurate determination of a final detailed design which can be applied in a latest stage.

- **Delft3D model improvement / Model input:**

The parameter values related to the roughness, eddy viscosity and diffusivity within the Delft3D model are set the same as the validated to the hydrodynamics model Delft3D FM. However, several improvements can be done for better representation of the morphological response of the model. One of them is the sediment input properties within the model. A uniform fraction of sediment grain size is assumed. Two different grain sizes are examined, separately covering the whole model area. However, the sediment fractions differ from place to place and this should be taken into account. Although, at maximum 99 fractions can be implemented in the model, a very precise and detail grain size/sediment properties map is required for that. Equivalent to that is the detailed bathymetrical map. Besides that, the grid area should be constructed such as the inlet cross section to be allowed to migrate for better and accurately representation of the bypassing models.

Furthermore, an extensive sensitivity analysis is needed for several factors and formulas included in the Delft3D model. One sensitivity analysis that can be done is with the different transport formulas provided in the model related to coastal areas. The model is run with the default formula of Van Rijn, however, most robust formulas such as the one suggested by

Bijker can give different although more adjustable results. Another important factor is the morphological factor. The morphological updating is case sensitive and always need a proper attention. Different morphological factors should be examined to see the sensitivity of the model results.

The wave conditions in the model as well as the coupling interval between the flow and wave module are important points of consideration. The representation of a full, to model, wave climate is the implementation of 10 – 12 wave conditions with a certain morphological factor based on the percentage of occurrence. This will indicate a more reliable morphological behaviour of the system.

- **Further research in Lake Bardawil**

Through this thesis, it is found that the design methodology followed can improve the stability and current flows within Boughaz 1 inlet while mimicking nature. Lake Bardawil consist two inlets and further research is needed to examine the response of the whole system. The water exchange between sea and lagoon is important for the stability and functionality not only of the tidal inlet system but for the lake as well. Although, Abohadima et al. already performed an approach which can increase the flushing rate between lagoon and sea, their application had not be performed with the design methodology provided here and did not take into account the morphological processes involved outside the inlet entrances. Thus, it is suggested to further investigate the effect of the specific design methodology to the Lake Bardawil by:

1. Apply the design methodology followed in this project to Boughaz 2 inlet.
2. Identify the P/M ratio. Does the stability increases?
3. Implementation of a new inlet in the western side of the Lake.
4. Identify P/M ratio. How much is still needed?
5. New wetlands within lake, creating gullies which can connect the three inlets.
6. How large is the tidal prism increase?

According to van de Kreeke and Brouwer (2017), the increase of the tidal range in combination to increase of surface area and less littoral drift can lead to more stable inlets within multiple inlet systems. Thus, the suggested steps are essential for the functionality of the Lake Bardawil.

Although these steps can provide an increase of the tidal prism change, the morphological model need first to develop to provide an inside of the morphological response of the system.

Lake Bardawil is characterized as hypersaline lake. Several studies showed that the effect of salinity, high temperature, evaporation rate, as well as the way of living conditions in the area are the causes of the ecological collapse of the system (Abohadima et al.; El-Bana et al., 2002; Ellah & Hussein, 2009; Khalil & Shaltout, 2006; Lanter, 2016). In this study, these effects did not take into account since Lanter (2016), already adjusted the response of the hydrodynamics to the ecosystem collapse and showed with 2DH model that the salinity, depth and tidal prism are important parameters for the enhancement of the fish population and the improvement of the living conditions in Lake Bardawil. The salt intrusion and density differences due to that significantly can alter the sediment transport processes and thus the flushing rates along the inlets. Subsequently, further research is needed to adapt the design methodology with the salinity levels and thus the flushing rates within the Boughaz 1 inlet.

The tidal range in Lake Bardawil is very limited which entails that the stability of the tidal inlets with certain design adaptations might need several years to be understood. This implies that long term adaptations should be modelled to realize the changes of the tidal inlet stability and if dredging operations are needed. In many areas around the world, dredging maintenance works are carried out within a period of year due to very large tidal range conditions. In this study, a year of simulation period was considered since focus is put on the hydrodynamic response of the system.

Last but not least, the forcing conditions in combination to the shape of the lake, inlet entrances and dimensions etc, are important for the development of residual currents. The direction of the tidal currents with the wave-induced currents, as well as the phase and magnitude difference between ebb and flood currents and water level conditions can lead to the growth of spiral flows within the inlet entrance which accordingly creating a natural sand by pass and possible spit formation (Tran, 2011). This was not efficiently observed within this study since the waves approached the tidal system in Boughaz 1 inlet perpendicular to the coast and the tidal currents outside the inlet are very limited to create sand by pass, thus further research is needed for that.

7 | References

- Abohadima, S., El-Bagoury, D., & Rakha, K. Numerical simulation for flushing rate in Bardawil Lagoon, Egypt.
- Bertin, X., Chaumillon, E., Sottolichio, A., & Pedreros, R. (2005). Tidal inlet response to sediment infilling of the associated bay and possible implications of human activities: the Marennes-Oléron Bay and the Maumusson Inlet, France. *Continental Shelf Research*, 25(9), 1115-1131.
- BMT Argoss (Producer). Google Retrieved from <http://www.bmtargoss.com/about-us/about-bmt-argoss/>
- Bosboom, J., & Stive, M. J. (2015). *Coastal Dynamics I: Lecture Notes CIE4305*. Delft: Delft Academic Press (VSSD).
- Bosman, G., & Lanfers, M. (2018). *Restoration of Lake Bardawil*.
- Brouwer, R., Van De Kreeke, J., & Schuttelaars, H. (2012). Entrance/exit losses and cross-sectional stability of double inlet systems. *Estuarine, Coastal and Shelf Science*, 107, 69-80.
- Brouwer, R. L., Schuttelaars, H. M., & Roos, P. C. (2013). Modelling the influence of spatially varying hydrodynamics on the cross-sectional stability of double inlet systems. *Ocean Dynamics*, 63(11), 1263-1278. doi:10.1007/s10236-013-0657-6
- Bruun, P., & Gerritsen, F. (1960). Stability of coastal inlets. *Coastal Engineering Proceedings*, 1(7), 23.
- Bruun, P., J. Mehta, A., & G. Johnsson, I. (1978). *Stability of Tidal Inlets: Theory and Engineering* (Vol. 23).
- Coastal wiki. (2015). http://www.coastalwiki.org/wiki/Closure_depth.
- de Queiroz, B. (2017). Input Reduction Analysis for Long-term Morphodynamic Simulations.
- de Schipper, M. A., De Vries, S., Stive, M., de Zeeuw, R., Rutten, J., Ruessink, G., . . . van Gelder-Maas, C. (2014). Morphological development of a mega-nourishment; first observations at the Sand Engine. *Coastal Engineering Proceedings*, 1(34), 73.
- De Vriend, H., Dronkers, J., Stive, M., Van Dongeren, A., & Wang, J. (2002). Coastal inlets and tidal basins.
- Deltares. Delft3D Modelling Guide. Retrieved from <https://publicwiki.deltares.nl/display/D3DGUIDE/Delft3D+Modelling+Guide>
- Deltares. (2011a). DELFT3D-FLOW. In *Simulation of multi-dimensional hydrodynamic flows and transport phenomena, including sediments*. Delft: Deltares.
- Deltares. (2011b). Delft3D-RGFGRID. In *Generation and manipulation of curvilinear grids for Delft3D-FLOW and Delft3D-WAVE*. Delft.
- Deltares. (2011c). DELFT3D-WAVE. In *Simulation of short-crested waves with SWAN*. Delft: Deltares.
- Deltares. (2016). 1D/2D/3D Modelling Suite for integral water solutions: Delft3D Flexible Mesh Suite 1-408.
- DEME. (2018). Ambiorix, Cutter Suction Dredgers. Retrieved from <https://www.deme-group.com/technology/ambiorix>

- El-Bana, M., Khedr, A.-H., Van Hecke, P., & Bogaert, J. (2002). Vegetation composition of a threatened hypersaline lake (Lake Bardawil), North Sinai. *Plant Ecology*, *163*(1), 63-75. doi:10.1023/a:1020351704409
- Ellah, R. G. A., & Hussein, M. M. (2009). Physical limnology of Bardawil lagoon, Egypt. *American-Eurasian Journal of Agricultural and Environmental Science*, *5*(3), 331-336.
- Emanuelsson, D., & Mirchi, A. (2007). Impact of coastal erosion and sedimentation along the northern coast of Sinai Peninsula.
- Embabi, N. S. (2017). *Landscapes and Landforms of Egypt: Landforms and Evolution*: Springer.
- Embabi, N. S., & Moawad, M. B. (2014). A semi-automated approach for mapping geomorphology of El Bardawil Lake, Northern Sinai, Egypt, using integrated remote sensing and GIS techniques. *The Egyptian Journal of Remote Sensing and Space Science*, *17*(1), 41-60.
- Escoffier, F. F. (1977). *Hydraulics and Stability of Tidal Inlets*. Retrieved from <http://www.dtic.mil/docs/citations/ADA045523>
- FitzGerald, D. M. (2011). Sediment bypassing at mixed energy tidal inlets. *Coastal Engineering Proceedings*(18). doi:10.9753/icce.v18.%p
- FitzGerald, D. M., Kraus, N. C., & Hands, E. B. (2000). *Natural mechanisms of sediment bypassing at tidal inlets*. Retrieved from <http://www.dtic.mil/docs/citations/ADA588774>
- Gao, S., & Collins, M. (1994). Tidal inlet stability in response to hydrodynamic and sediment dynamic conditions. *Coastal engineering*, *23*(1-2), 61-80.
- Garel, E., Sousa, C., Ferreira, Ó., & Morales, J. (2014). Decadal morphological response of an ebb-tidal delta and down-drift beach to artificial breaching and inlet stabilisation. *Geomorphology*, *216*, 13-25.
- Gary D., E., & Erofeeva Y., S. (2002). Efficient inverse modeling of barotropic ocean tides. *Atmospheric and Oceanic Technology*, *19.2*, 183-204.
- Khalil, M. T., & Shaltout, K. H. (2006). *Lake Bardawil and Zaranik protected area*.
- Klein, M. (1986). Morphological changes of the artificial inlets of the Bardawil Lagoon. *Estuarine, Coastal and Shelf Science*, *22*(4), 487-493.
- Kraus, N. C., Larson, M., & Wise, R. A. (1998). *Depth of closure in beach-fill design*. Retrieved from Lake Bardawil. (2015). Retrieved 20/09/2018, from Google Earth
- Lanters, M. (2016). *A Hydrological Design of Lake Bardawil*. Delft University of Technology, Netherlands.
- Linersund, J., & Mårtensson, E. (2008). Hydrodynamic modelling and estimation of exchange rates for Bardawil Lagoon, Egypt. In: Lund: Lund University.
- Luijendijk, A. P., Ranasinghe, R., de Schipper, M. A., Huisman, B. A., Swinkels, C. M., Walstra, D. J., & Stive, M. J. (2017). The initial morphological response of the Sand Engine: A process-based modelling study. *Coastal engineering*, *119*, 1-14.
- Mangor, K. (2018). Coastal Hydrodynamics And Transport Processes. In *Coastal Wiki*.
- Nassar, K., Mahmood, W. E., Masria, A., Fath, H., & Nadaoka, K. (2018). Numerical simulation of shoreline responses in the vicinity of the western artificial inlet of the Bardawil Lagoon, Sinai Peninsula, Egypt. *Applied Ocean Research*, *74*, 87-101.

- Piere, d. G. (2016). *Geological description of the Bardawil Lake and deposits*.
- Roelvink, J., & Walstra, D.-J. (2004). Keeping it simple by using complex models. *Advances in hydro-science and engineering*, 6, 1-11.
- Tran, T. T. (2011). Morphodynamics of seasonally closed coastal inlets at the central coast of Vietnam.
- Trouw, K., Zimmermann, N., Mathys, M., Delgado, R., & Roelvink, D. (2012). Numerical modelling of hydrodynamics and sediment transport in the surf zone: A sensitivity study with different types of numerical models. *Coastal Engineering Proceedings*, 1(33)(sediment.23.). doi:<https://doi.org/10.9753/icce.v33.sediment.23>
- Umgiesser, G., Helsby, R., Amos, C. L., & Ferrarin, C. (2015). Tidal Prism Variation in Venice Lagoon and Inlet Response over the Last 70 Years. In M. Maanan & M. Robin (Eds.), *Sediment Fluxes in Coastal Areas* (pp. 151-165). Dordrecht: Springer Netherlands.
- van de Kreeke, J., & Brouwer, R. L. (2017). *Tidal inlets: hydrodynamics and morphodynamics*: Cambridge University Press.
- Yang, Z., & Wang, T. (2013). Tidal residual eddies and their effect on water exchange in Puget Sound. *Ocean Dynamics*, 63(8), 995-1009. doi:10.1007/s10236-013-0635-z

Appendices

Appendix A – Background

A-P relationship:

The equilibrium inlet cross-sectional area is defined in relation to the tidal prism. This empirical relationship between the inlet cross-sectional area and the tidal prism is first defined by LeConte (1905) and its further examined by O'Brien (1931), O'Brien(1969) and Jarrett(1976) (Bosboom & Stive, 2015). Its general form is written as:

$$A_{eq} = CP^q$$

In which:

A_{eq} (m²): The minimum equilibrium cross-section of the entrance channel

P (m³): Tidal prism

q (-), C (m^{2-3q}) : Coefficients

The C, q coefficients are determined with observational data and according to this formula, Escoffier (1977) introduced the values defined by Jarrett(1976) as follows:

Table A-1: Combination of the coefficients C and q defined with the O'Brien relationship by Jarrett (1976)(Escoffier, 1977).

Coast	Inlet	C (m ^{2-3q})	q (-)
Atlantic, gulf, Pacific coasts	All	5.74 x 10 ⁻⁵	0.95
	One or no jetty	1.04 x 10 ⁻⁵	1.03
	Two jetties	3.76 x 10 ⁻⁴	0.86
Atlantic coast	All	7.75 x 10 ⁻⁶	1.05
	One or no jetty	5.37 x 10 ⁻⁶	1.07
	Two jetties	5.77 x 10 ⁻⁵	0.95
Gulf coast	All	5.02 x 10 ⁻⁴	0.84
	One or no jetty	3.51 x 10 ⁻⁴	0.86
	Two jetties	-----	-----
Pacific coast	All	1.19 x 10 ⁻⁴	0.91
	One or no jetty	1.91 x 10 ⁻⁶	1.10
	Two jetties	5.28 x 10 ⁻⁶	0.85

All the combinations of C and q are valid for the inlets which have the same sediment characteristics, same wave and tidal conditions and similar geometry (Bosboom & Stive, 2015). However, these characteristics are not presented or not known in several inlets, thus the adaptation and consideration of these coefficients should always be taken with care. This indicates that the determination of the equilibrium inlet cross-sectional area might not be the exact while using this empirical equilibrium relationship in combination to high lack of data, as it is the case in Lake Bardawil.

Small basin approximation

The geometry of the basin/lagoon plays significant role for the response of the tidal flow within these systems. The tidal flow can have either progressive character or a standing motion can be observed (Bosboom & Stive, 2015). The main parameter that determines the small basin approximation is the length of the basin¹ compare the length of a particular tidal wave. The criterion states that if the basin length is much smaller than the tidal length then the water level in the basin follows the water level outside such as a pumping mode system. This phenomenon is clearly observed when the flood delta covers the whole basin. The equation is given as follows:

$$l_b < \frac{L}{20}$$

In which:

l_b : basin length (m)

L : Tidal length of a particular component (m)

To clearly indicate that in lake Bardawil this approximation is not valid, the tidal length of the main tidal component (M_2) is examined. Since the tidal wave is characterized as a long wave, the propagation velocity can be found as:

$$c = \sqrt{gh}$$

In which:

g : gravitational acceleration $9.81 \left(\frac{m}{s^2}\right)$

h : Average water depth (m)

The average water depth in lake Bardawil is considered to be 1.2 m. Accordingly, the tidal wave length is calculated as the multiplication of the propagation velocity with the wave period. The M_2 tidal component has approximately 12.42 hrs wave period, which in seconds is about 45 000s. The tidal wave length is found then to be equal of 154 km.

$$L_{M_2} = T \cdot \sqrt{gh} = 45\,000 \cdot 3.43 = 153.4 \text{ km}$$

The basin length varies from the west side to the east side with the maximum length to be approximately equal to 20.5 km. This length is mainly observed at the east side of the lake. Considering this value, the ratio between the basin length and tidal length equal to 0.13 which is larger than the $1/20$. This indicates that the small basin approximation is not valid for lake Bardawil. However, the

¹ Length of the basin is characterized as the dimension where the tidal wave propagates.

basin length at the west side of the lake is almost the half than the eastern side. Taking that into account the ratio is approximately about 0.065 which is still larger than the 1/20.

Depth of closure:

The concept of depth of closure (DoC) is important for various coastal engineering designs. Different definitions have been addressed for that. The precise definition of the DoC for a beach fill design as presented by Kraus, Larson, and Wise (1998) to be the following:

“The depth of closure for a given or characteristic time interval is the most landward seaward point of which there is not significant changes in bottom elevation and no significant net transport between the nearshore and the offshore.”

The DoC is defined with beach profile surveys. However, in case no available beach profile surveys are presented, the primary calculation of DoC is defined according to Hallermeier who depicted the follow expression:

$$D_c = 2.28 \cdot H_s - 68.5 \cdot \left(\frac{H_s^2}{g \cdot T^2} \right)$$

In which:

D_c (m): Depth of closure

H_s (m): Significant wave height at a nearshore location

T (s): Wave period of the specific wave height

g ($\frac{m}{s^2}$): Gravitational acceleration

The main parameter in this equation is the significant wave height. The significant wave height here represents the largest significant wave height which is exceeded in a sequence of 12 hours for a given wave record and it is determined at a nearshore location. The right part of the equation is a correction for the steepness of the specific wave height (Kraus et al., 1998).

To predict the nearshore wave height conditions in lake Bardawil a wave ray model is used. The nearshore transformation was done by using the Argoss wave model. The nearshore point chosen to be located at a distance of about 8 km from the eastern shoreline of the west inlet where the soft engineering measure is placed. This point located in 31° 12' 18" N and 32° 56' 42" E. A timeseries of the nearshore wave conditions with a time interval of 3 hours in the area are retrieved and are analysed to determine the highest significant wave height that is exceeded in a sequence of 12 hours. The highest significant wave height is found to be equal of 2.66 m with a wave period of T=12 s. This wave height is used to calculate the DoC. The DoC is found equal to 5.60 m.

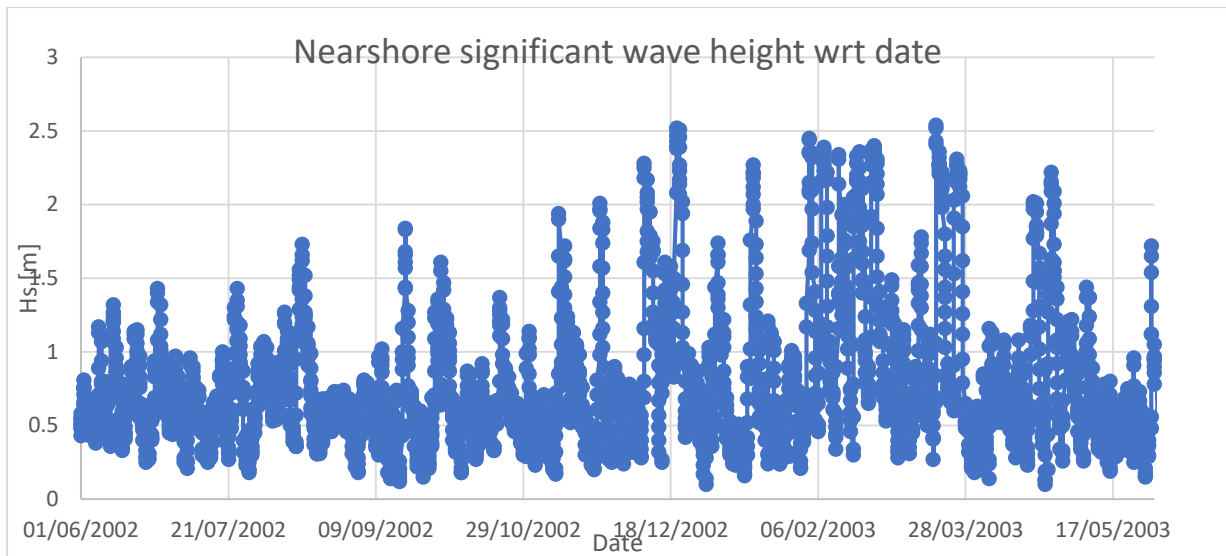


Figure A-1: Nearshore significant wave height time series. The highest 12-hour wave height was used for the determination of DoC.

Sand engine design:

Since 19th century, human interventions along the coasts increased substantially pursuing coastal safety. To prevent structural erosion due to sea level rise, tidal effects, wave conditions, hard structures were widely used. However, over the last decades, the need to find more ecologically sustainable solution, led to the execution of soft structures such as nourishments.

During March 2011 to November 2011, in the Dutch coast between Hoek van Holland and Scheveningen (Den Hague) a large (mega-scale) nourishment has been implemented. After ongoing investigations this mega nourishment presents positive results in respect to the lifetime of the structure and shoreline erosion. This is beneficial for the reduction of maintenance dredging operations along the coasts (de Schipper et al., 2014) which are exposed to large structural erosion levels.

The design of the Sand Engine pilot project was based on the climatic and hydrodynamic conditions presented in the Dutch coast, the sediment budget that was needed annually (de Schipper et al., 2014) and the requirements of multi stakeholders about several aspects such as nature development (Luijendijk et al., 2017). This led to a design of a peninsula with a width of about 1 km seaward directed and alongshore size of about 2 km. The nourishment consists of about 20 million m³ of sediment and its highest point is +7.3 m above sea level, well above the mean storm level (de Schipper et al., 2014). The cross-shore slope from the most seaward point to the toe of nourishment is 1:50 m and this point reach a depth contour equal to -8 m. The total surface area is 1.28 km² and consist sediment of D₅₀=278 μm which is related to the sediment properties of the surrounding area (Luijendijk et al., 2017).

To understand the response of the Sand Engine under the influence of the prevailing conditions in the area, a process-based model was used. It is found that the wave energy in the tip of the soft structure is an important factor for the redistribution of the sediment along the coast with the highest to account for large duration of storm conditions. On the other hand though, the high frequency of smaller waves leads to important erosion levels and should always be considered (Luijendijk et al., 2017). This implies that the higher capture of the energy based on the position of the nourishment indicates more redistribution of sediment along the coast.

Appendix B - Climate

Salinity and evaporation rates:

Lake Bardawil is considered as hypersaline lake due to the limited water exchange with the Mediterranean Sea. The salinity levels depend on the local climatic conditions and the evaporation rate (Ellah & Hussein, 2009). Lowest values of salinity present during winter period (Khalil & Shaltout, 2006), when the evaporation rate is less and strong wind forces exist (Ellah & Hussein, 2009) while the opposite happens during dry season. These values can be observed in the Figure B-1 and Figure B-2. The salinity levels in the western side of the lake Bardawil, in the west side of Boughaz 1 inlet, do not fluctuate through the years and almost constant value of 55‰ is observed. The salinity levels are considered higher compared the Mediterranean Sea. Subsequently, the high evaporation rates in lake Bardawil show significant values compared the nearby areas. The evaporation rate exceeds the value of 6 mm/day when the temperature is over 23 Celsius, which can be considered high enough than the other locations. However, these values may give inaccurate results since the meteorological stations are situated within the cities.

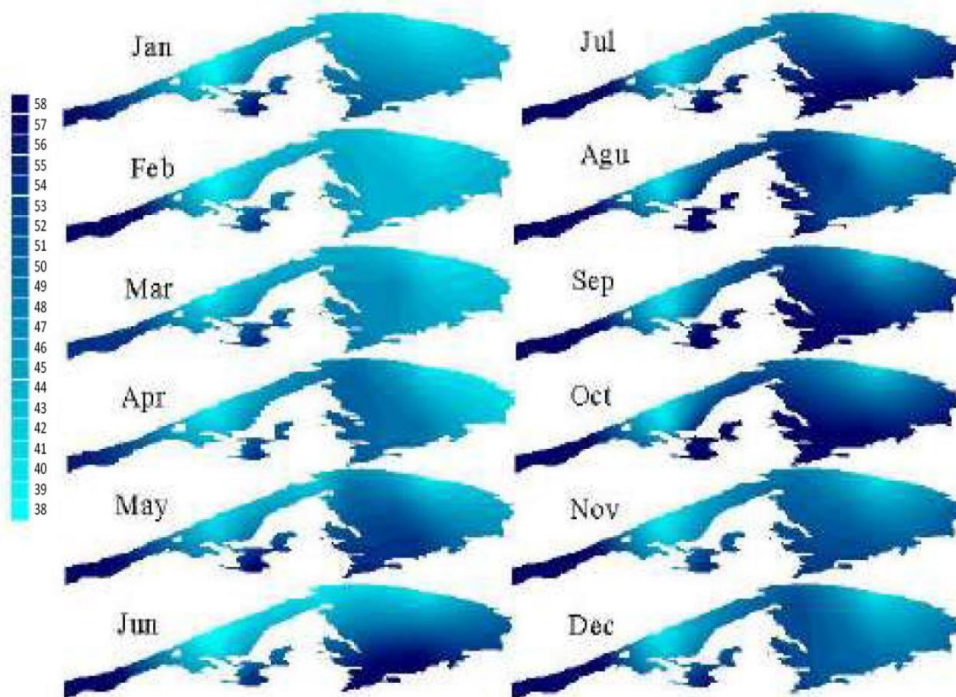


Figure B-1: Monthly salinity levels measured in ‰ (El-Bana et al., 2002; Lanfers, 2016)

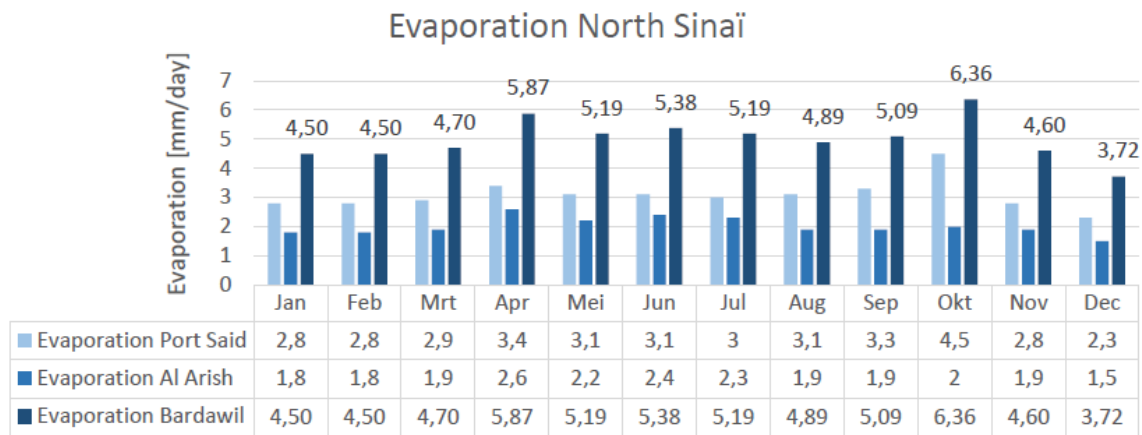
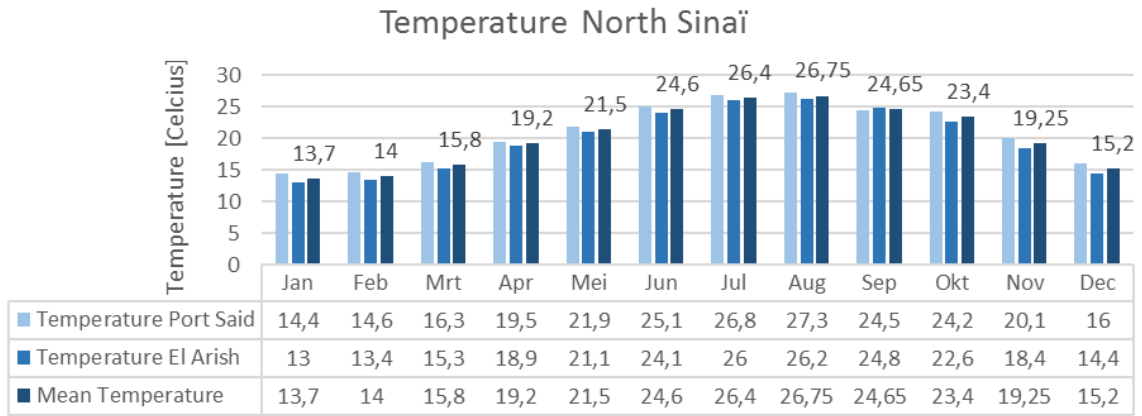


Figure B-2: Temperature (Celsius) and evaporation(mm/day) in North Sinai

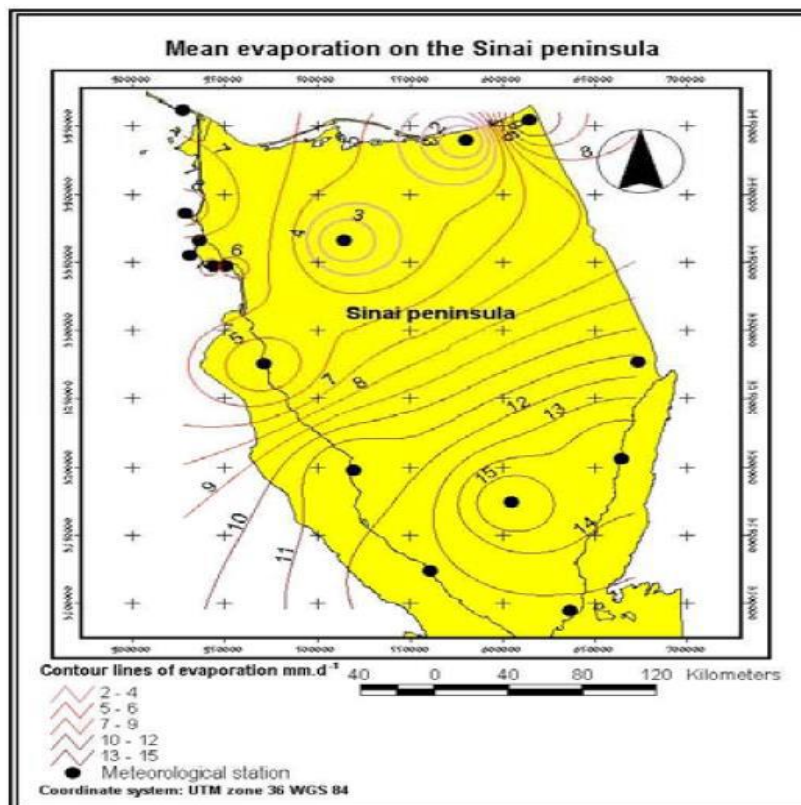


Figure B-3: Mean evaporation (mm/day) on Sinai Peninsula.

Wave climate:

Wave analysis:

For the prediction of the wave climate near Lake Bardawil, the Argoss wave model is used. An offshore model point (31 degrees 15'N, 32 45' E) which is located 20 km away from Boughaz 1 inlet was chosen, see Figure B-6. This model point was considered the most representative one for Boughaz 1 inlet since all the wave directions can be captured for this area. A model time series of 26 years (1992-2017) was analysed to define representative wave values for the full year. These waves are analysed a scatter plots have been constructed for that.

Seasonal variations were also examined, and similar predictions were observed as the full year analysis whilst the storm wave analysis was not considered since limited time of the year the waves are higher than 4 m (Klein, 1986). This is also indicated with the probability of occurrence of the highest waves during the whole year in the scatter plots below.

Offshore location 31° 15'N, 32° 45'E Size of offshore area for satellite data 200x200 km
Offshore model point 31° 15'N, 32° 45'E

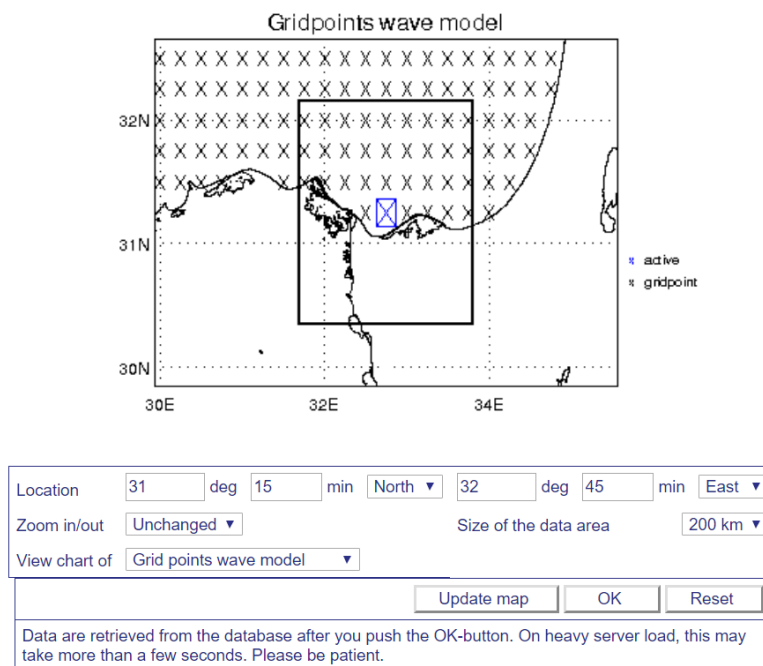


Figure B-6: Offshore wave model point location

Percentage of occurrence	Direction	N	NNE	NE	ENE	E	ESE	SE	SSE	S	SSW	SW	WSW	W	WNW	NW	NNW	Total
		Hs (m)																
0	0.2	0.15	0.16	0	0	0.01	0.01	0	0	0.01	0	0	0	0	0.15	0.18	0.16	0.96
0.2	0.4	1.11	1.01	0.51	0.19	0.07	0.06	0.04	0.04	0.02	0.02	0.02	0.03	0.06	1.82	3.17	1.42	9.59
0.4	0.6	1.78	1.72	0.89	0.35	0.16	0.11	0.08	0.06	0.03	0.03	0.05	0.09	0.23	4.97	7.96	2.26	20.74
0.6	0.8	1.47	1.78	0.85	0.32	0.11	0.05	0.04	0.02	0.04	0.04	0.08	0.16	0.35	6.64	8.8	1.51	22.25
0.8	1	0.81	1.23	0.51	0.13	0.06	0.01	0.01	0.01	0.01	0.02	0.04	0.18	0.39	6.07	5.91	0.78	16.17
1	1.2	0.44	0.77	0.32	0	0.02	0	0	0	0	0	0.03	0.09	0.36	4.28	3.47	0.43	10.27
1.2	1.4	0.23	0.43	0.13	0	0.01	0	0	0	0	0	0.01	0.06	0.32	2.8	1.91	0.22	6.15
1.4	1.6	0.11	0.28	0	0	0	0	0	0	0	0	0.01	0.05	0.29	1.9	1.21	0	4.02
1.6	1.8	0.06	0.17	0	0	0	0	0	0	0	0	0.01	0.04	0.2	1.39	0.72	0.07	2.73
1.8	2	0.04	0.09	0	0	0	0	0	0	0	0	0	0.05	0.16	0.97	0.48	0.04	1.84
2	2.2	0.03	0.06	0	0	0	0	0	0	0	0	0	0.04	0.13	0.7	0.32	0.03	1.31
2.2	2.4	0.02	0.03	0	0	0	0	0	0	0	0	0	0.02	0.12	0.48	0.24	0	0.92
2.4	2.6	0	0	0	0	0	0	0	0	0	0	0	0	0	0.39	0.16	0	0.7
2.6	2.8	0	0	0	0	0	0	0	0	0	0	0	0	0.08	0.31	0.14	0	0.57
total		6.26	7.77	3.43	1.12	0.44	0.24	0.17	0.13	0.11	0.11	0.25	0.85	2.97	33.95	35.09	7.08	100

Percentage of occurrence	Direction	N	NNE	NE	ENE	E	ESE	SE	SSE	S	SSW	SW	WSW	W	WNW	NW	NNW	Total
		Tp (s)																
2	3	0.14	0.15	0.17	0.11	0.09	0.05	0.04	0.02	0.02	0.02	0.04	0.03	0.04	0.07	0.11	0.08	1.18
3	4	1.58	1.66	1.36	0.51	0.19	0.12	0	0	0.06	0.07	0.13	0.25	0.28	0.57	1.69	1.38	9.85
4	5	2.12	2.88	1.17	0.28	0.11	0.02	0	0	0	0	0.04	0.14	0.3	2.65	6.06	2.21	17.98
5	6	1.42	2.18	0.57	0.15	0.05	0.01	0	0	0	0	0.01	0.15	0.43	8.19	12.31	1.61	27.08
6	7	0.64	0.74	0.1	0.02	0	0	0	0	0	0	0	0.11	0.67	11.92	10.44	1.06	25.7
7	8	0.14	0.11	0.01	0.02	0	0	0	0	0	0	0.01	0.05	0.39	4.31	2.5	0.39	7.93
8	9	0.08	0.04	0	0	0	0	0	0	0	0	0	0.06	0.52	3.86	1.59	0.22	6.37
9	10	0.06	0.01	0	0	0	0	0	0	0	0	0	0	0.23	1.92	0.3	0.11	2.63
10	11	0.03	0	0	0	0	0	0	0	0	0	0	0	0.07	0.37	0.05	0.02	0.54
		6.22	7.77	3.38	1.09	0.44	0.2	0.04	0.02	0.08	0.09	0.23	0.79	2.93	33.89	35.08	7.08	100

Table B-1: Scatter plot of significant wave height (m) relative direction and peak period (s) relative to direction.

Wave climate reduction:

To minimize the computational effort limited wave conditions are required in the model input. The input reduction method is applied to indicate representative wave conditions in the area. A maximum run time of a regular model is about 10 to 12 hours assuming an hour simulation time for one wave condition. Subsequently, the representative wave conditions should be less or equal to 10-12. The reduction of the wave conditions can be based on different targets such as the longshore transport, cross shore transport, stirring, sedimentation erosion patterns, sediment transport vectors and Brute forcing conditions. Furthermore, there are different input reduction techniques. One of them is the bin method which is considered the most preferred one as it can be coded as well.

A statistical representation of the entire wave climate in lake Bardawil is found with a tool provided by Deltares and the Korean Institute of Science and Technology (KIOSK). This open earth tool gives the opportunity to limit the wave raw data to representative wave conditions based on different wave input reduction techniques. The input reduction technique used in that case is the energy flux method with the weighting factor to be the wave energy. This is a binning method which was found to give promising results as the sediment transport bins method (de Queiroz, 2017). The energy flux method divides the wave data into equal bins with the same energy flux. The energy is calculated with:

$$E_f = \left(\frac{\rho \cdot g \cdot H^2}{8} \right) \cdot c_g$$

In which:

$$E_f: \text{Energy flux } \left(\frac{W}{m^2} \right)$$

$$\rho: \text{Water density } \left(\frac{Kg}{m^3} \right)$$

$$g: \text{gravitational acceleration } \left(\frac{m}{s^2} \right)$$

$$H: \text{wave height (m)}$$

$$c_g: \text{group celerity } \left(\frac{m}{s} \right)$$

For each bin the wave condition is calculated with the mean energy flux and the wave height and direction with the inverse function of that. The wave period is calculated as the average value within each bin (de Queiroz, 2017). This method was chosen since not up to date longshore sediment transport phenomena presented in the area. The timeseries of the wave heights and accordingly the wave period and directional spread of the wave conditions were plotted and as can be seen in the figure below, is shown a bimodal form.

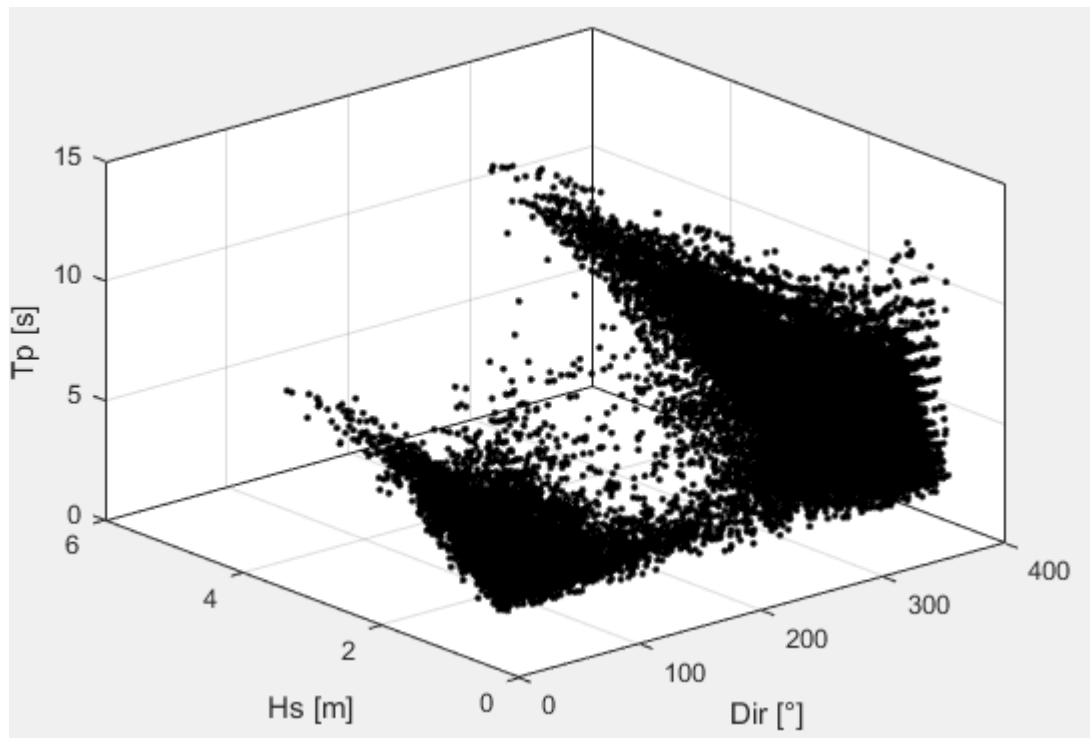


Figure B-7: Distribution of the wave height, $H_s(m)$, direction $Dir (^{\circ})$ and peak period $T_p(s)$.

According to the literature, the most frequent wave period in the area is below 8s for 98.2% of a year period whilst 80.5% of the time the wave period is 2-6 sec (Nassar et al., 2018). Taking that into account, waves with higher or lower values from the range 2-6 s were removed from the wave data timeseries to get the most frequent waves in the area. Furthermore, Nassar et al. (2018), indicate that for 62-65% of the measurements show the predominant alongshore current direction is directed eastwards from NW waves. Since the longshore transport is an important factor for the feasibility study of the selected design, the NW waves are considered to be the most important ones and thus focus on these waves have been made. Lastly, four wave conditions are selected for examining the brute forcing in the area.

Considering the assumptions, the binning method described above is performed. Longshore transport is higher when the angle of approach to the shore normal angle is at highest to 45° (Bosboom & Stive, 2015). The resulting conditions are illustrated in the Table B-2.

Wave conditions	H_s (m)	T_p (s)	$Dir (^{\circ})$	Percentage of occurrence (%)	Realistic period within the year	Morphac for a 30 days simulation period
1	0.69	5.30	316	50.13	183	6.1
2	0.83	5.90	296	34.58	126.2	4.2
3	1.47	6.70	314	8.63	31.4	1.05
4	1.76	6.70	292	6.66	24.3	0.77

Table B-2: Wave conditions defined from the input reduction method.

Bathymetry:

The figure below illustrates the depth map file used in the model to construct the nearshore depth contours.

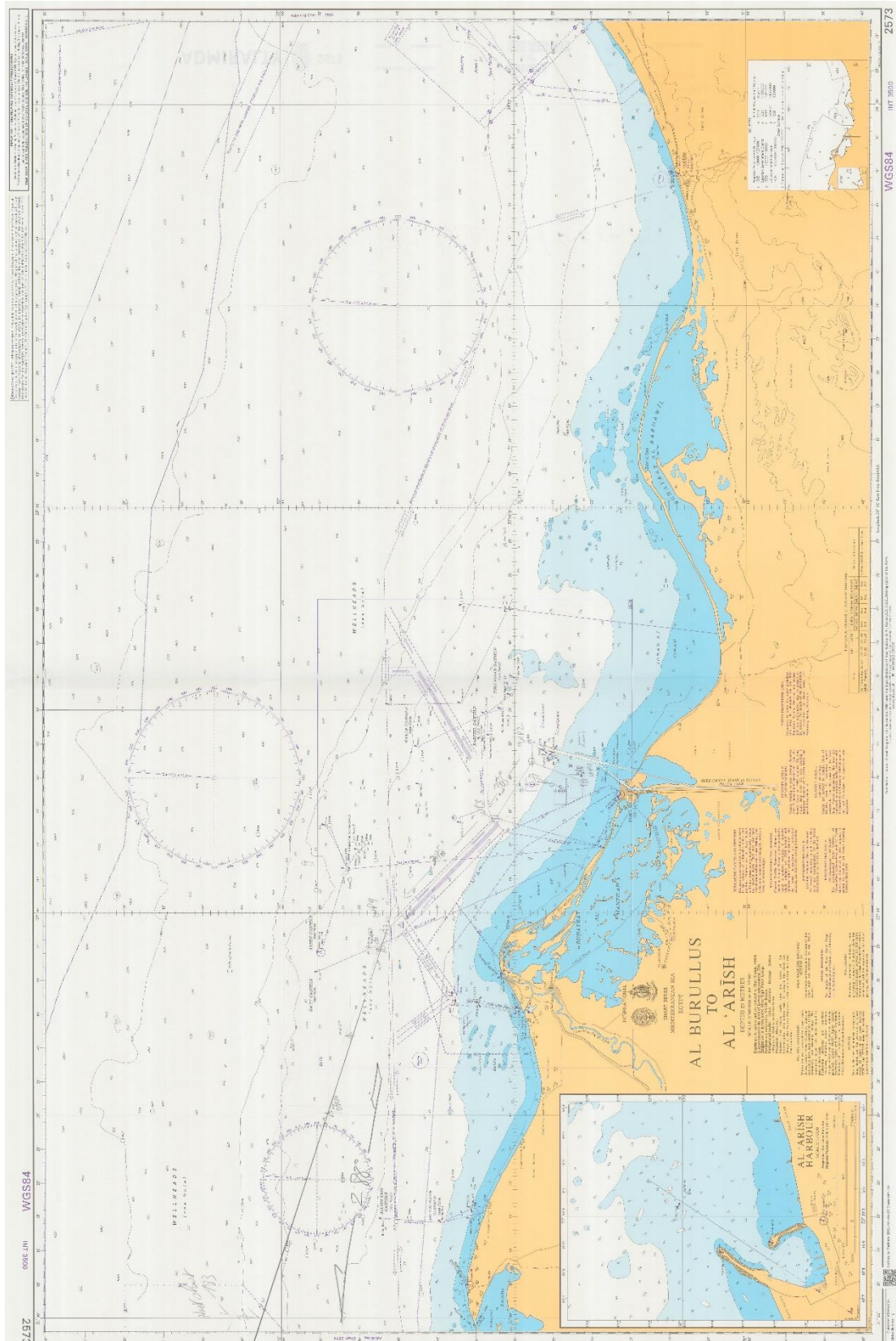


Figure B-8: Depth map used for the nearshore bathymetry.

Appendix C - Validation

Model accuracy:

The model accuracy and stability are highly based on the value of the CFL number (DELTA RES—FLOW MANUAL). The CFL number should be at maximum equal to 10 while in some cases larger values are accepted. The CFL number is highly depended on the calculation time step and the bathymetry model area as follows:

$$CFL = \frac{\Delta t \sqrt{g \cdot H}}{\{\Delta x, \Delta y\}}$$

Where:

- Δt (s): Time step
- g (m/s²): Gravitational acceleration
- H (m): (total) Water depth
- $\Delta x, \Delta y$: Horizontal grid cell sizes

The accuracy and stability of the model area is examined with two different CFL numbers and thus two different time steps. Time steps equal to 4.5 s and 6 s are chosen with maximum CFL numbers equal to 8.17 and 10.90 respectively. The choice to examine a CFL number which is above the threshold criterion is based on the computational demand of the model. Since the model area is very large and high-resolution level exists in the area the computational time increases substantially. Thus, it is important to be able reproduce high level of accuracy and stability within less computational time. The model runs are examined with respect to the offshore water level conditions, depth averaged velocities and tidal prism within the system. An illustration of the model results is given in Table C-1, Figure C-2: Depth-averaged velocity magnitude within the inlet, at 10 m depth. Blue: Marker x, time step 6s. Red: Marker o, time step 4.5 s. and Figure C-1: Water level variations for both models runs. Blue: Marker x, time step 6s. Red: Marker o, time step 4.5 s..

Table C-1: Model accuracy validation with two different time steps.

	Conditions	
Time step (s)	4.5	6
Courant number (CFL)	8.17	10.9
Water level range (m)		
Spring tide	0.40	0.40
Neap tide	0.17	0.17
Tidal prism (10 ⁶ m ³)		
Mean tidal prism	74.1	74.1
Depth-averaged velocity (m/s)		
Maximum velocity, 10 m depth	0.85	0.85

Table C-1, indicates the computed results with the two different time steps. Both CFL and accordingly time step conditions show the same model results which indicates that a CFL number more than 10, as the threshold criterion, is still able to reproduce accurately the model results. Since, the computational time is an important criterion for the simulation runs, a time step of 6 s is considered reasonable for the analyses of the model area. The same is indicated with the following figures.

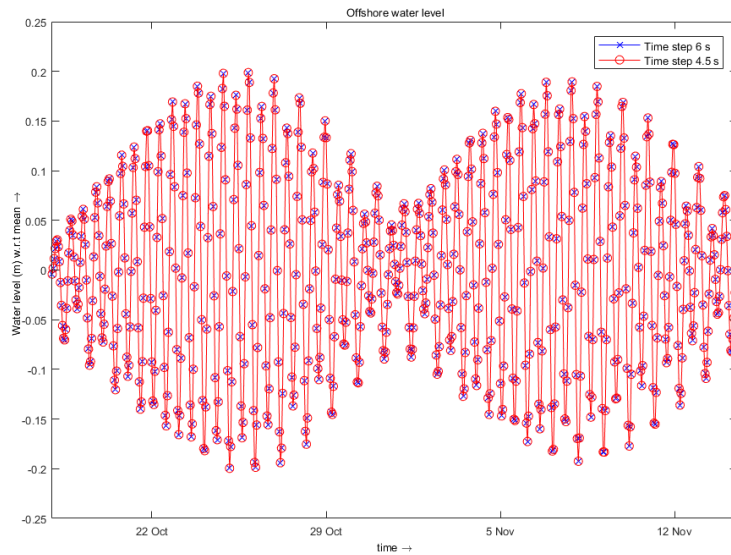


Figure C-1: Water level variations for both models runs. Blue: Marker x, time step 6s. Red: Marker o, time step 4.5 s.

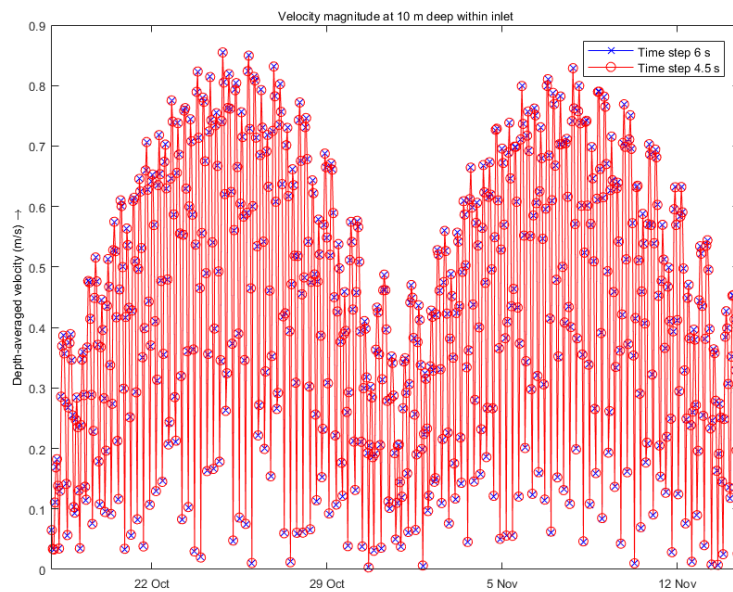


Figure C-2: Depth-averaged velocity magnitude within the inlet, at 10 m depth. Blue: Marker x, time step 6s. Red: Marker o, time step 4.5 s.

Appendix D – Overview of Results

Cross sectional area:

The results associated to the cross-sectional inlet design are summarized here. The table indicates all the results of all designs adapted with the cross-sectional area examination.

Table D-1: Tidal prism results for all the designs of the cross-sectional area design.

Design element	Total average tidal prism 10^6 m^3	Spring tidal prism	Neap tidal prism	Average discharge per tidal cycle 10^6 m^3	
Cross sectional area		$10^6 \text{ m}^3/\text{tidal cycle}$	$10^6 \text{ m}^3/\text{tidal cycle}$	West Inlet	East Inlet
Initial state	59.3	72.1	44.1	26.13	33.17
1	59.4	72.5	44.1	26.4	33.2
2	71.9	89.0	51.8	39.6	33.62
3	59.8	72.9	44.4	26.9	33.20
4	60.4	73.7	44.8	27.5	33.30
5	61.1	74.7	45.3	28.2	33.33
6	70.9	87.4	51.4	38.4	33.60
7	60.6	74.0	45.0	27.7	33.32
8	60.0	73.2	44.5	27.1	33.30
9	70.0	87.0	51.1	37.9	33.60

Residual eddies in inlet nourishment:

The shape and width of both the western barrier and the inlet nourishment concentrate the tidal flow within the inlet. This is also obtained with the eddy formation seen in the figures below. The ebb currents showed to be larger when the inlet nourishment is applied. Furthermore, reshaping the western barrier there is smoother transition of the tidal flow through the inlet.

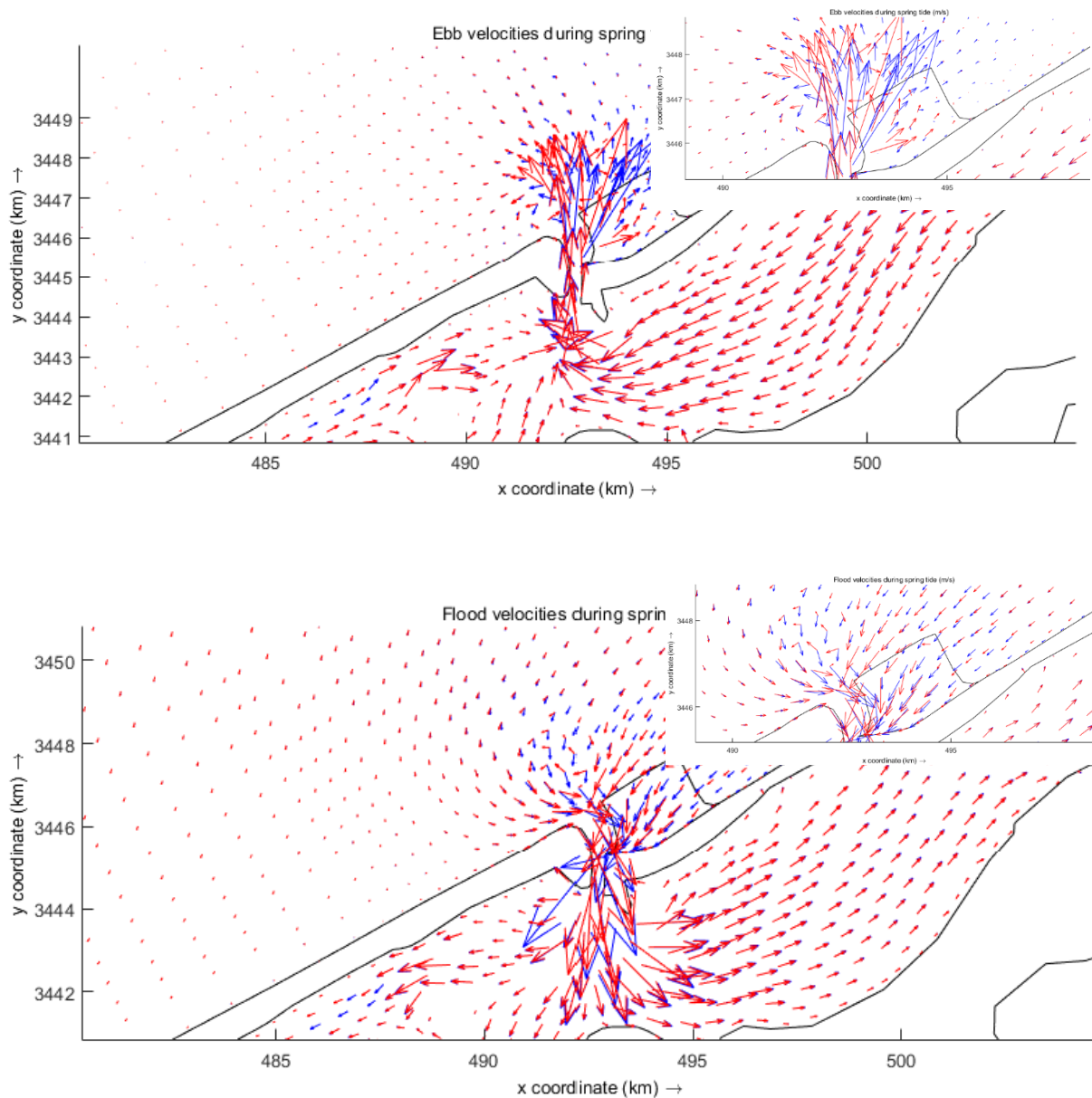


Figure D-1: Residual eddies found while implementing the inlet nourishment design during ebb and flood currents. The blue colour indicates the initial state, thus without the inlet nourishment and the red colour indicates the examination of the inlet nourishment design.

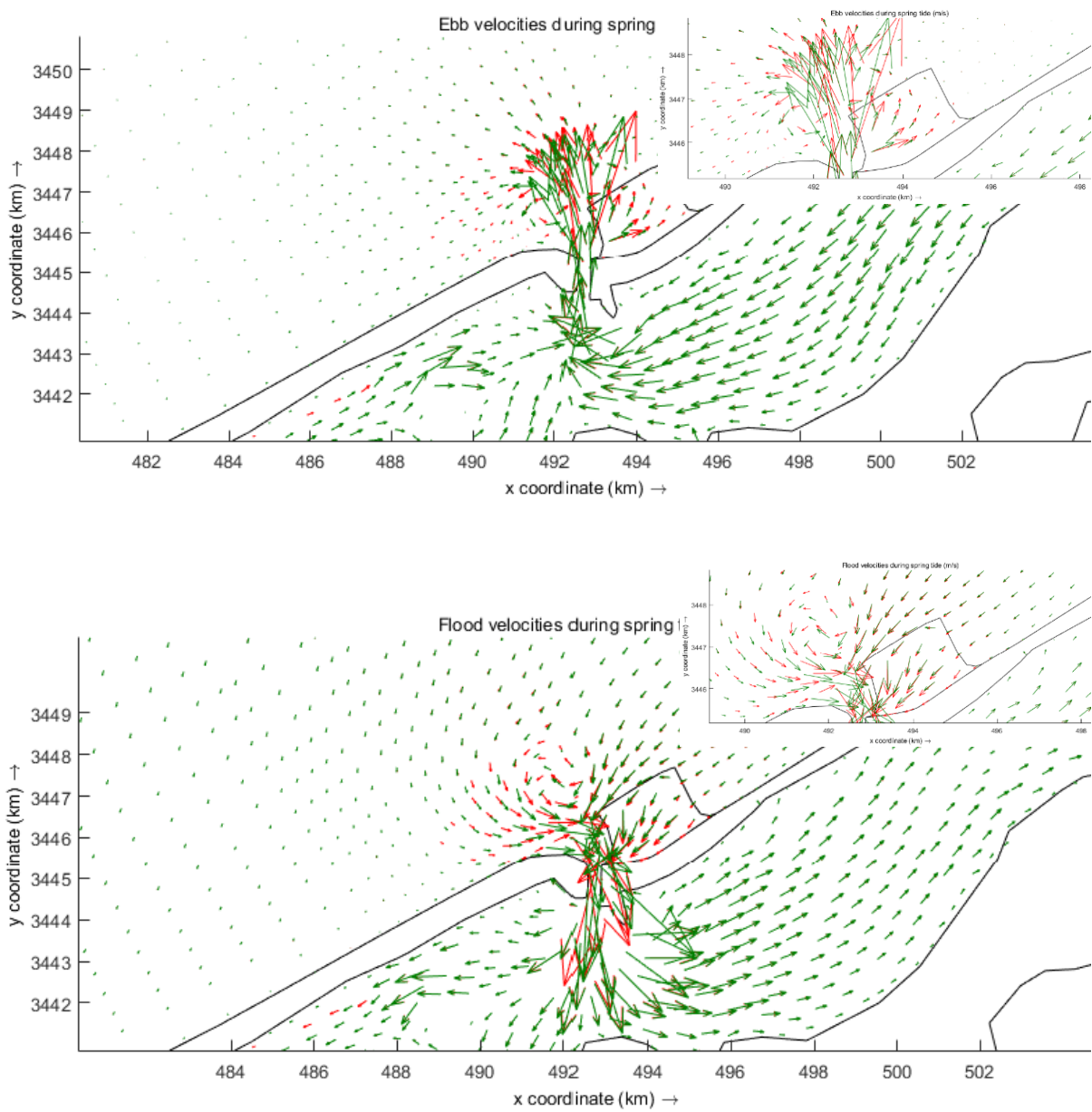


Figure D-2: Residual eddies found while implementing the new inlet nourishment design and reshaping the western barrier. The red colour indicates the old inlet nourishment design while the green colour the new design.

Hydrodynamics and morphology:

The tidal prism values during spring and neap for all the simulations done with the Delft3D software are firstly provided, as well as the sensitivity analysis results are given in Table D-4. Then all the morphological responses found for all the simulations are given with the inlet cross-section and the inlet nourishment cross section designs and a table of the sensitivity analysis to that. Some remarks are also given.

Table D-2: Tidal prism calculations during spring tide. The colour differences illustrate the two different grain sizes. With light blue: 180 μm while with light orange: 330 μm .

Models	Simulations	Spring tidal prism (10^6 m^3)			Percentage (%)	
		Lake Bardawil	Boughaz 1	Boughaz 2	Boughaz 1	Boughaz 2
Delft3D	1	89	53.8	37	59.3	40.7
	2	91.1	53.9	39.1	58.0	42.0
	3	89.6	53.9	37.6	58.9	41.1
	4	91.1	53.7	39.2	57.8	42.2
	5	91.1	53.7	39.2	57.8	42.2
	6	87.3	53.1	35.9	59.7	40.3
	7	89.7	53.4	38	58.4	41.6
	8	89.1	53.5	37.4	58.9	41.1
	9	89.2	53.6	37.4	58.9	41.1
	10	83	52.8	31.6	62.6	37.4
	11	87.6	53.3	36	59.7	40.3

Table D-3: Tidal prism calculations during neap tide. The colour differences illustrate the two different grain sizes. With light blue: 180 μm while with light orange: 330 μm .

Models	Simulations	Neap tidal prism (10^6 m^3)			Percentage (%)	
		Lake Bardawil	West	East	West	East
Delft3D	1.0	60.6	33.1	27.5	54.6	45.4
	2.0	62.9	33.3	29.6	52.9	47.1
	3.0	61.3	33.1	28.2	54.0	46.0
	4.0	63.0	33.1	30.0	52.5	47.5
	5.0	62.8	33.2	29.8	52.7	47.3
	6.0	56.8	32.2	24.6	56.7	43.3
	7.0	60.9	32.8	28.2	53.8	46.2
	8.0	60.7	32.8	27.8	54.1	45.9
	9.0	60.8	33.0	27.9	54.2	45.8
	10.0	61.3	31.9	20.8	60.5	39.5
	11.0	58.0	32.5	25.5	56.0	44.0

Table D-4: All the combinations and associated results of the tidal prism while applying sensitivity analysis.

Simulations	Lake Bardawil							Boughaz 1							Boughaz 2						
	Initial tidal prism (10 ⁶ m ³)	Relative difference between initial and calibrated tidal prism in the lake (10 ⁶ m ³)						Initial tidal prism (10 ⁶ m ³)	Relative difference between initial and calibrated tidal prism in the lake (10 ⁶ m ³)						Initial tidal prism (10 ⁶ m ³)	Relative difference between initial and calibrated tidal prism in the lake (10 ⁶ m ³)					
		Calibration factors							Calibration factors							Calibration factors					
		Erosion of adjacent dry cells		Current related transport factor		Wave related transport factor			Erosion of adjacent dry cells		Current related transport factor		Wave related transport factor			Erosion of adjacent dry cells		Current related transport factor		Wave related transport factor	
0.5	1.0	10	20	0.1	0.25	0.5	1.0	10	20	0.1	0.25	0.5	1.0	10	20	0.1	0.25				
2	76.9	0.0	0.0	1.7	2.9		-	43.7	0.0	0.0	0.4	0.7	-	-	33.9	0.0	0.0	1.4	2.4		-
3	74.9	0.0	0.0	2.9	4.8			43.5	0.0	0.0	0.6	1.0	-	-	32.1	0.0	0.0	2.4	4.0		-
7	75	0.0	0.0	1.4	2.2	1.4	1.1	43.1	0.0	0.0	0.2	0.4	0.0	0.0	32.6	0.0	0.0	1.2	1.8	1.4	1.1
11	71.5	0.0	0.0	3.0	3.8	2.2	2.0	42.9	0.0	0.0	0.3	0.6	0.0	0.1	29.3	0.0	0.0	2.6	3.2	2.1	1.9
Simulations	Lake Bardawil							Boughaz 1							Boughaz 2						
	Initial tidal prism (10 ⁶ m ³)	Relative difference between initial and calibrated (%)						Initial tidal prism (10 ⁶ m ³)	Relative difference between initial and calibrated (%)						Initial tidal prism (10 ⁶ m ³)	Relative difference between initial and calibrated (%)					
		Calibration factors							Calibration factors							Calibration factors					
		Erosion of adjacent dry cells		Current related transport factor		Wave related transport factor			Erosion of adjacent dry cells		Current related transport factor		Wave related transport factor			Erosion of adjacent dry cells		Current related transport factor		Wave related transport factor	
0.5	1.0	10	20	0.1	0.25	0.5	1.0	10	20	0.1	0.25	0.5	1.0	10	20	0.1	0.25				
2	76.9	0.0	0.0	2.2	3.8		-	43.7	0.0	0.0	0.9	1.6		-	33.9	0.0	0.0	4.1	6.9		-
3	74.9	0.0	0.0	3.9	6.5		-	43.5	0.0	0.0	1.4	2.2		-	32.1	0.0	0.0	7.5	12.5		-
7	75	0.0	0.0	1.9	2.9	1.9	1.5	43.1	0.0	0.0	0.5	0.9	0.0	0.0	32.6	0.0	0.0	3.7	5.6	4.3	3.4
11	71.5	0.0	0.0	4.2	5.3	3.1	2.8	42.9	0.0	0.0	0.7	1.4	0.0	0.2	29.3	0.0	0.0	8.9	10.9	7.2	6.5

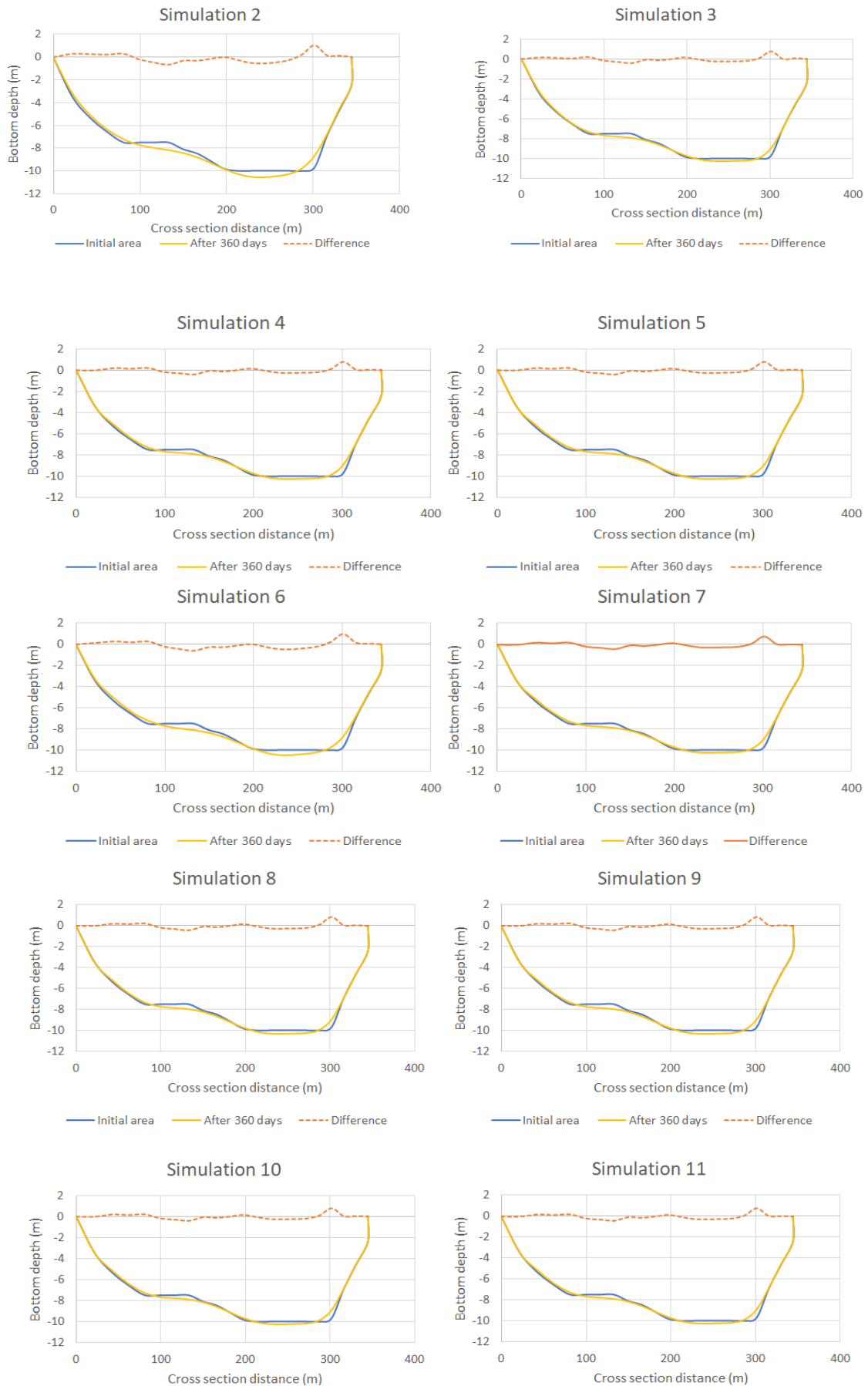


Figure D-3: Morphological changes of the inlet cross sectional area for all the simulations. The same behavior is observed for all the simulations.

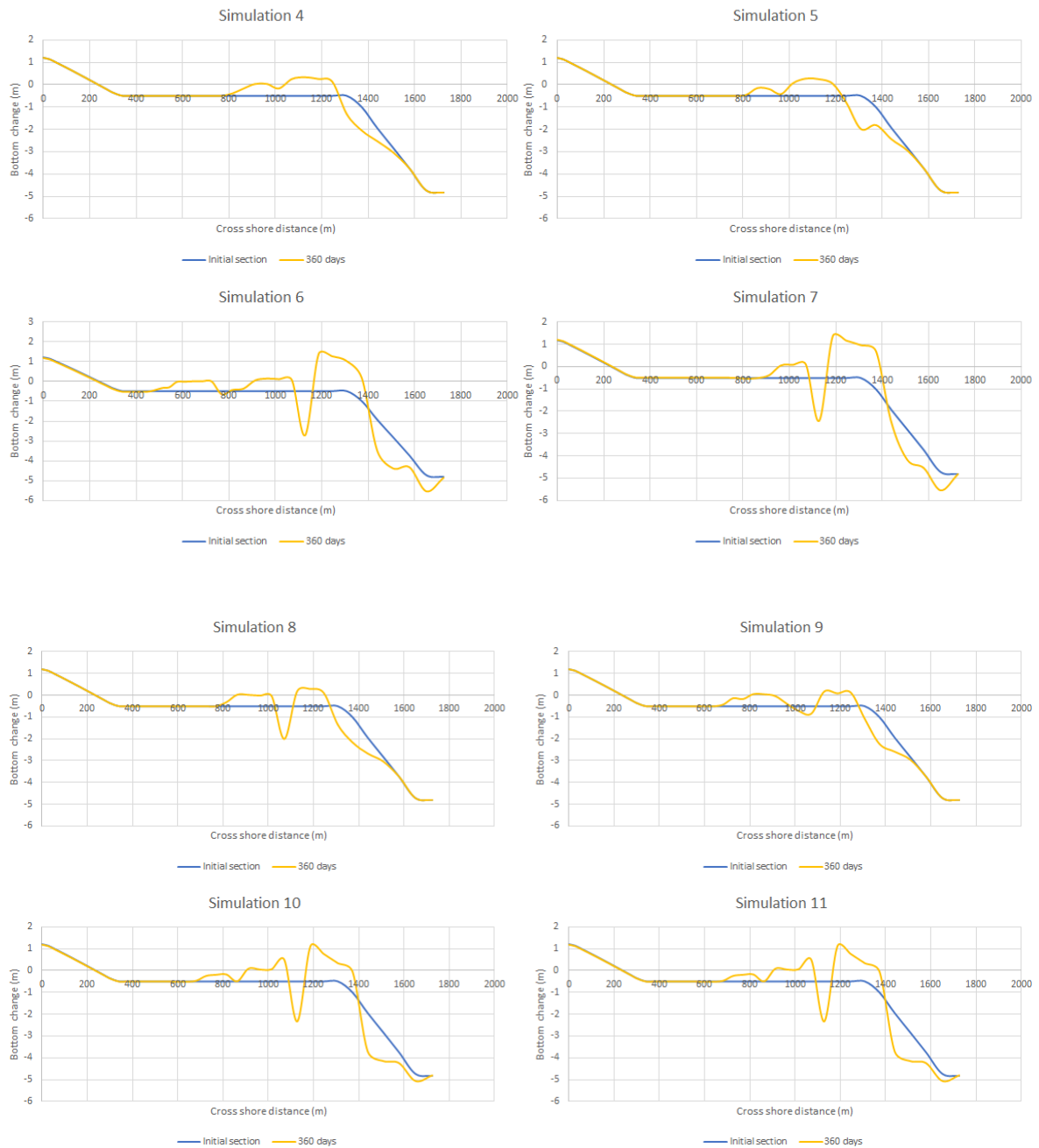


Figure D-6: Morphological changes of the inlet nourishment design for all the simulations.

As it is observed from Figure D-3: Morphological changes of the inlet cross sectional area for all the simulations. The same behavior is observed for all the simulations.

Figure D-4: Morphological changes of the inlet nourishment design for all the simulations. Figure D-5 and Figure D-6: Morphological changes of the inlet nourishment design for all the simulations., the inlet is eroded similarly for every simulation, which this indicates that the waves do not affect the response of the inlet. These cross sections are derived in the middle of the inlet length where the wave exposure is zero. The deepest part is eroded while accretion is seen in the edges of the cross section. On the other hand, the inlet nourishment shows morphological variations for every simulation. The high wave energy conditions, provide larger onshore transport than the smaller waves. Erosion is obvious at the tip of the structure, while the DoC concept seems to be valid for all the simulations.

The gully observed between 1000 – 1200 m from the land is due to the large current concentration at that point. However, no clear conclusions can be given for that since several factors included in the model affecting the morphological behaviour of the system, see Table D-5.

Table D-5: Morphological changes based on sensitivity analysis.

Calibration factors	Inlet		Approach channel						Inlet nourishment		Basin	
	Inlet gorge		Marginal flood channel		Ebb channel		Marginal flood channel		Engine		Flood delta	
	Min	Max	Min	Max	Min	Max	Min	Max	Min	Max	Min	Max
Erosion of adjacent dry cells	0.0	0.0	0.0	0.0	0.0	0.0	0.0	0.0	0.0	0.0	0.0	0.0
Current related transport factor	2.1	5.5	0.0	3.2	-0.2	-0.5	-0.8	-1.6	0.0	2.6	-0.4	-0.9
Wave related transport factor	0.3	1.3	0.5	0.8	0.0	-0.1	-0.2	-0.8	0.1	0.6	-0.1	-0.2

Figure D-7: Bottom depth changes of the inlet nourishment with different values of the wave related transport factor.

Figure D-8 indicates the bottom depth variation of the inlet nourishment design with different values of the wave related transport factor. Since Delft3D is not capable to provide accurately the onshore transport, it is important to understand if the response defined throughout all the simulations is similar by modifying the wave calibration factor which is related to that. By minimizing the value of this factor, it seems that erosion is observed within the offshore slope as found with the default value of this factor. However, differences are distinguished with the gully created with the default and 0.25 values compare the 0.1 value. This indicates the sensitivity to analyse in detail the morphological response of this design element. However, in a broader view, there is an onshore sediment transport with the related wave conditions. Furthermore, the DoC concept is validated which specifies that the inlet nourishment design is correctly attained but further research is needed to understand its morphological behaviour.

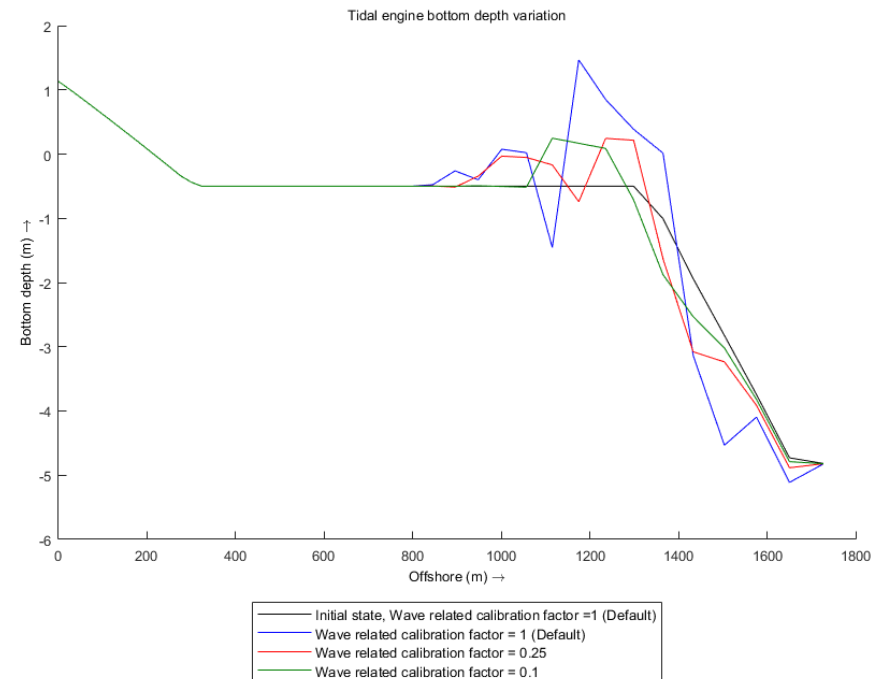


Figure D-7: Bottom depth changes of the inlet nourishment with different values of the wave related transport factor.